A novel conception of piezoelectricity physical nature is proposed and dicussed. Some peculiarities of piezoelectric crystals (so cold polar-neutral crystals) would be described by a assumption of their intrinsic (latent) polarity. Its components show a critical law $P \sim (\theta - T)^n$ and vanish at the phase transition temperature θ. The critical parameter equals to $n = 1$ if all components of intrinsic polarity are flatness arranged (two-dimensional case, 2D). For spatial (3D) arrangement of the latent polarity components this exponent is $n = 2$. These differ essentially from 1D ferroelectric spontaneous polarization that shows P(T) critical law with the $n = 0.5$. For technical application, it means that under the anisotropy of boundary conditions any high-gap III-V semiconductor-piezoelectric shows a behavior of pyroelectric crystal. Such crystals might be used as far infrared sensor or as a piezoelectric sensor integrated with amplifier in one III-V crystal.

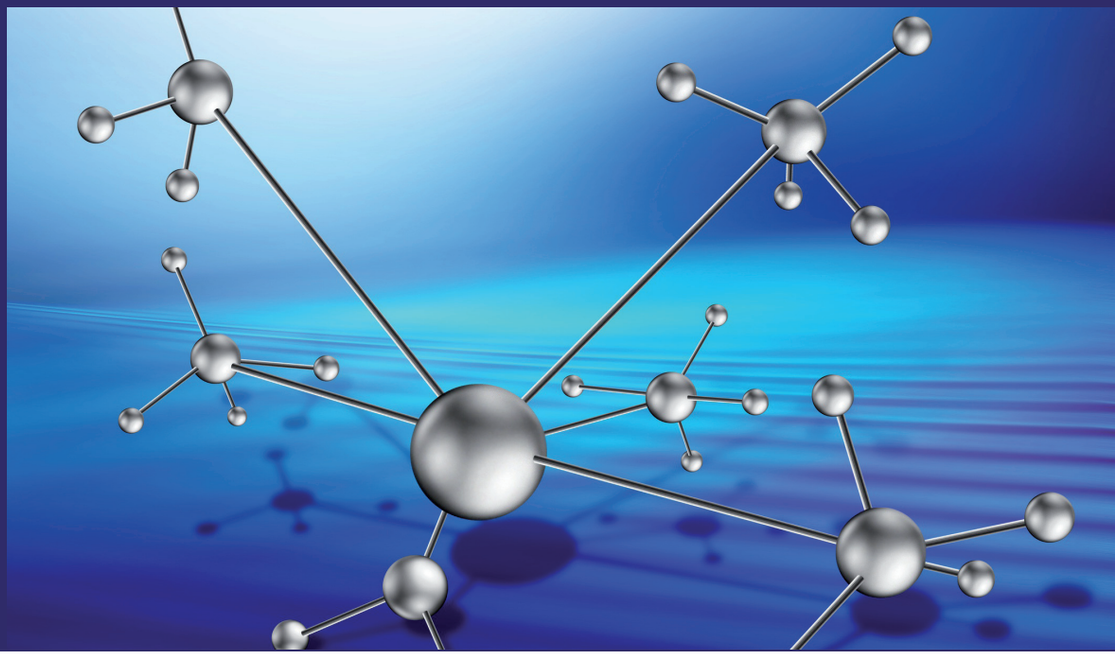

Yuriy Poplavko

Poplavko Yuriy Mikhailovich, Doctor of Physical and Mathematical Sciences, Professor of Microelectronics of National Technical University of Ukraine "KPI". The founder of scientific direction "Dielectric Spectroscopy of Ferroelectrics", the author of over 200 scientific articles. Gave lectures in universities of European countries, USA, Japan, etc.

978-3-659-54290-9

Yuriy Poplavko

Polar Crystals

Physical Nature and New Effects

LAP LAMBERT Academic Publishing

Yuriy Poplavko

Polar Crystals

Yuriy Poplavko

Polar Crystals

Physical Nature and New Effects

LAP LAMBERT Academic Publishing

Impressum / Imprint
Bibliografische Information der Deutschen Nationalbibliothek: Die Deutsche Nationalbibliothek verzeichnet diese Publikation in der Deutschen Nationalbibliografie; detaillierte bibliografische Daten sind im Internet über http://dnb.d-nb.de abrufbar.

Bibliographic information published by the Deutsche Nationalbibliothek: The Deutsche Nationalbibliothek lists this publication in the Deutsche Nationalbibliografie; detailed bibliographic data are available in the Internet at http://dnb.d-nb.de.

Coverbild / Cover image: www.ingimage.com

Verlag / Publisher:
LAP LAMBERT Academic Publishing
ist ein Imprint der / is a trademark of
OmniScriptum GmbH & Co. KG
Heinrich-Böcking-Str. 6-8, 66121 Saarbrücken, Deutschland / Germany
Email: info@lap-publishing.com

Herstellung: siehe letzte Seite /
Printed at: see last page
ISBN: 978-3-659-54290-9

Contents

Introduction

Polar crystals are substances with mixed ionic-covalent bonds. Just this characteristic causes low symmetry of polar crystals, and most of them belong to the non-centrally symmetric groups of crystals. On the contrary, the purely ionic bonded crystals as well as the purely covalent bonded crystals are non-polar. They belong to the centrally symmetric classes of crystals. In most cases of the ionic crystals a full symmetry exists, and usually there is no special orientation in the atomic bonding. In the same way, in the simple covalent crystals formal charges of all atoms remain unchanged, however, the atomic bonds have common electron pair. That is why they usually are centre-symmetric ones.

The primary cause of the polarity in crystals is the asymmetry in the electron density distribution along the atomic bonds. This is conditioned by the differences in the electro-negativity of atoms. Sometimes the distinction of electro-negativity in different atoms might be large (on Poling' scale). Atom with higher electro-negativity strongly attracts the electron-pair bond, so his true charge becomes more negative. Atom with a lower electro-negativity acquires, respectively, the increased positive charge. Together these atoms form a polar bond.

Consequently, in the polar crystals a system of built-in polar moments exists. In a three-dimensional crystal the structure and symmetry of polar bonds can be rather complicated but its distinctive feature is the absence of central symmetry. It has an influence on many physical properties of polar crystals: on the electrical, mechanical, thermal and chemical features. Moreover, the polar bonds cause essential mutual relations between these features. As a consequence of this interdependence, the electromechanical, electrothermal and other interrelations appear.

For example, a mechanical influence to a polar crystal may lead to an electrical response (i.e., the piezoelectric effect). The point is that reciprocal displacement of the atoms that are constrained by polar bonds generates electricity on the crystal surface (polarization). On the contrary, if the atomic bonds are non-polar, no electrical response is possible to any mechanical or thermal perturbation.

Non-centrally symmetric arrangement of electrical charges in the polar crystals can be characterized by different structural patterns, such as imaginary dipole, sextuple, or octopole.

The simplest case is the dipole structural pattern, which corresponds to the spontaneous polarization P_s in crystal. It might be represented by a polar vector "built into the crystal structure" that is, in other words, a polar tensor of the first rank.

This internal polarization results in the vector response to any external scalar action on the crystal, in particular, in the volumetric piezoelectric effect in the case of all-round (hydrostatic) pressure, and in the pyroelectric effect in the case of uniform heating or cooling.

The crystals with spontaneous polarization (i.e., with dipole-type polarity) belong to pyroelectrics. However, many others polar crystals are not pyroelectrics, but piezoelectrics.

Respectively, in the piezoelectrics the imaginary sextuple or octopole electrical moments (correspondingly, tensors of the second or the third rank) also possess internal polarity but it is a latent (totally compensated) polarity. Therefore, an arbitrary scalar action (hydrostatic pressure or uniform heating) can not “awake" in such a crystal any vectorial response. Only tensorial external actions, such as mechanical stress X_{ij} (second rank tensor) or temperature gradient (vector grad T), are capable of provoking the hidden polarity to a vectorial response (that is, to induce voltage or electrical current).

Electrical, elastic, and thermal properties of polar crystals are interrelated. Moreover, even in the case of investigation of only electrical effects (for instance, polarization), the parameters depend on the mechanical and thermal boundary conditions. For instance, the permittivity of a mechanically free crystal (ε^X) differs from the permittivity of a clamped crystal (ε^x), at that $\varepsilon^X > \varepsilon^x$. Likewise, if a polar crystal is exposed to alternating electrical field in the adiabatic conditions (when there is no time to exchange energy between crystal and environment) the permittivity ε^S is less than the ε^T obtained under isothermal conditions.

Mechanical properties of a piezoelectric, such as its elastic stiffness c (or its elastic compliance s), are dependent on the electrical condition of the crystal (close-circuited, $E = 0$, or open-circuited, $D = 0$), and sometimes the c^E differs from the c^D in several times. Similarly, adiabatic elastic parameters c^S or s^S differ from the isothermal c^T or s^T. In the same way, when seemingly "purely thermal" experiment is provided, for example, measuring the specific heat capacity C, one can see significant differences between C^E and C^D, that is to say, when the electrodes deposited on the test sample are close-circuited ($E = 0$) or open-circuited ($D = 0$). Similarly, different specific heat capacity is observed for mechanically free ($X = 0$) and mechanically clamped ($x = 0$) crystals: $C^X \neq C^x$.

1. Internal polarity manifestation

Electrical polarization is a separation of electrical charges that is accompanied by the deformation of the crystal (strain). Therefore polarization is not just electrical but also electromechanical phenomenon. In the case of the piezoelectric effect an external mechanical stress applied to the crystal does not produce, but only manifests the existing internal polarity of the crystal (hidden polarity).

Electromechanical coupling becomes apparent, especially, in the elastic waves excitation by the electrical field. Two types of elastic bulk waves can exist in a homogeneous elastic medium: longitudinal waves, in which the displacement of particles occurs in the direction of wave propagation, and transverse waves, in which the particle displacement takes place in a plane perpendicular to the direction of wave propagation.

Longitudinal and transverse waves are three-dimensional oscillations in the elastic medium. Bulk waves are used in various piezoelectronic devices: in the mode of standing waves in the resonant devices as well as in the mode of travelling waves in the case of surface acoustic waves. Some examples of bulk wave application are shown in Fig. 1.1 for simple piezoelectric elements made of polarized ferroelectric ceramics.

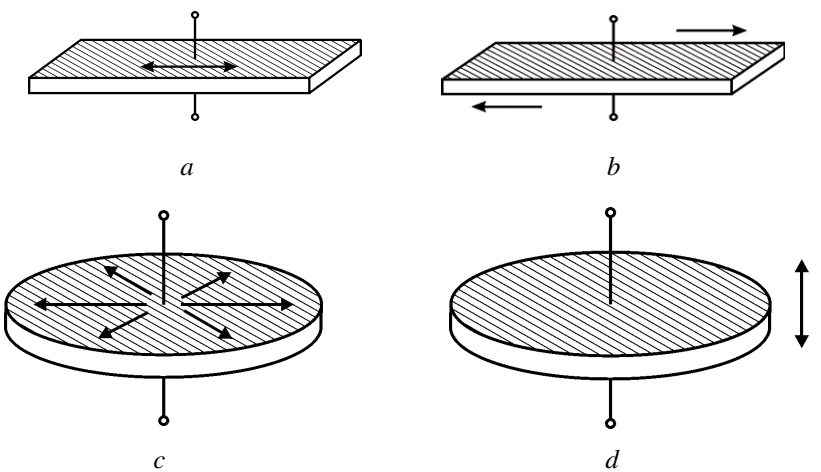

Fig. 1.1. Different types of vibrations in the bulk piezoelectric elements (shading shows electrodes, arrows show direction of deformations): *a* – piezoelectric plate polarized in thickness with transverse vibrations; *b* – piezoelectric plate polarized in thickness with shear deformation; *c* – piezoelectric disk element polarized in its thickness with radial deformations, *d* – piezoelectric disk element polarized in thickness and having thickness deformation

In addition to bulk waves, in the elastic media surface acoustic waves (SAW), widely used in the acousto-electronics, may exist. These waves propagate along the free surface of solids or along the boundaries between solids and other environments, Fig. 1.2.

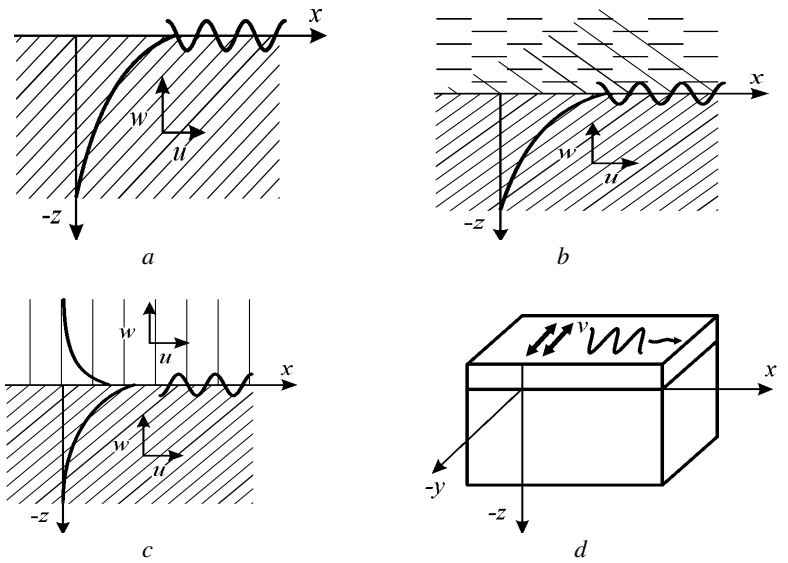

Fig. 1.2. Surface wave schematic representation: *a* – Rayleigh waves on the free solid; *b* – Rayleigh waves on the boundary between solids and liquids; *c* – Stoneley waves at the boundary between two solids; *d* – Love waves at a boundary "solid half-space - solid layer"

Surface waves exist in two types, namely, those with vertical polarization, i.e., when the vector of the oscillatory particles displacement in the medium is located in a plane perpendicular to the boundary, and those with horizontal polarization, i.e., when the particles displacement vector is parallel to the boundary but perpendicular to the direction of wave propagation.

The most common surface waves are as follows, see also Fig. 1.2:

- Rayleigh waves, propagating along the boundaries between the elastic half-space and the vacuum (or rather a rarefied gas medium);
- decaying waves of Rayleigh type on the boundary between solid and liquid;
- Stoneley waves propagating along the plane interface of two solid media;
- Love surface waves with horizontal polarization, which may spread to the layered structure of the "elastic layer on an elastic half-space".

1.1. Simplified description of piezoelectric effect

Piezoelectric is capable to convert the mechanical energy into the electrical energy, or, conversely, the electrical energy into the mechanical one. The first of these effects is called as a direct piezoelectric effect while the second is denoted as an inverse effect.

In the case of direct piezoelectric effect under the influence of mechanical stress X (or caused by mechanical stresses elastic deformation of x), non centre-symmetric dielectrics (i.e., piezoelectrics) generates electrical polarization, Fig. 1.3 (*b, c*). Since the electrical conductivity of a piezoelectric (as it is a dielectric) is very small, the polarization is expressed in the form of mechanically induced electrical charges that appear on the surface of the deformed piezoelectric. The density of these charges is described by the induced polarization P while the direction of the polarization vector is selected from the sign "–" to the sign "+", as it is shown in Fig. 1.3, (*b, c*). Polarization is proportional to the electrical induction D, Fig. 1.3 (*g*).

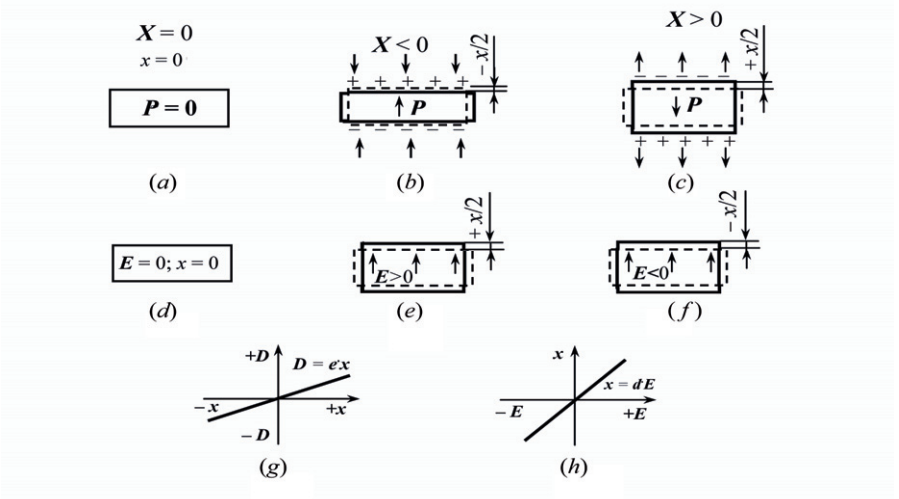

Fig. 1.3. Explanation of direct (*a, b, c, g*) and inverse (*d, e, f, h*) piezoelectric effects

If mechanical stress is absent ($X = 0$), no free charges on the surface of piezoelectric appear, and therefore it is electrically neutral, Fig. 1.3 (*a*). Piezoelectric shows its polarization as a result of positive (stretching) deformation when $x > 0$ or negative (compression) deformation $x < 0$. While changing the sign of mechanical stress (such as compression is changing to stretching, Fig. 1.3 (*b*) and (*c*), the sign of mechanically induced electrical polarization P supersedes. In the case of direct piezoelectric effect the value of polarization is directly proportional to the strain:

$$P = ex,$$

where parameter e is piezoelectric strain constant.

The inverse piezoelectric effect occurs when electrical field deforms the non-centrally symmetric crystal, Fig. 1.3 (*i, f*). The sign of electrically induced strain varies with the sign of the electrical effect, Fig. 1 (*h*). The crystal' deformation value depends linearly on the magnitude of the field:

$$x = dE,$$

where d is piezoelectric modulus.

A very simplified explanation of the direct piezoelectric effect in the α-quartz (SiO_2) is presented in Fig. 1.4. Generally accepted model of the hexagonal quartz structure is a hexagon with positive silicon and negative oxygen ions that form a non-centrally symmetric structure.

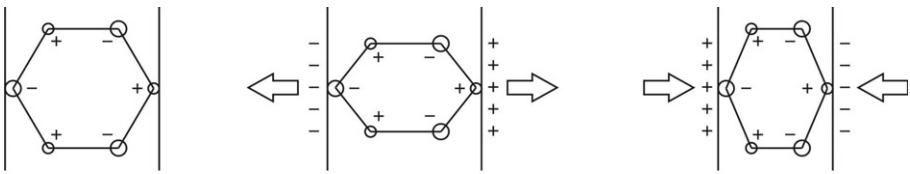

Fig. 1.4. Simplified model of piezoelectric effect in quartz

Some manners of hexagon deformation can produce electrical polarization. If deformation is absent, no polarization is observed, Fig. 1.4 (*a*). Stretching the model cell in the horizontal direction induces charges and electrical field, Fig. 1.4 (*b*), this is a direct longitudinal piezoelectric effect. At that, the "–"-charge dominates on the left side of cell while the "+"-charge appears on the right side of cell. Upper and lower parts of cell generates no charge – they remain neutral (no transverse effect).

The similar result might be achieved by the cell compression in the vertical direction, Fig. 1.4 (b) but in the vertical direction no longitudinal effect is seen on the upper and lower parts of cell. However, after the vertical compression a transverse piezoelectric effect is apparent, again on the left and on the right parts of cell. The point is that horizontal direction of the selected cell is a polar direction, while the vertical direction is non polar. Figure 1.4 (*c*) demonstrates that the change in the sign of mechanical impact gives rise to a change in the piezoelectric polarity as it should be in the case of linear effects.

Therefore, the simple one-dimensional model shown in Fig. 1.4 describes a longitudinal piezoelectric modulus, at which the electrical response has the same direction as the mechanical influence. In this case the highest possible piezoelectric

modulus d_{max} is observed. In various directions in the quartz crystal modulus d has another value, and piezoelectric response distribution is rather complicated, Fig. 1.5.

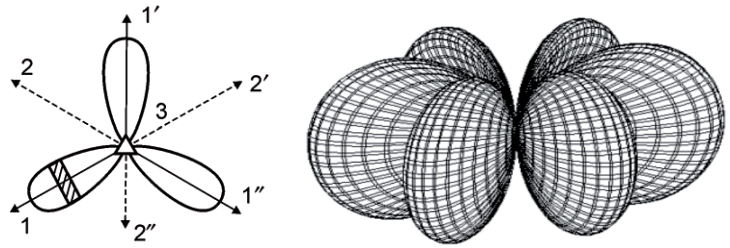

a *b*

Fig. 1.5. Longitudinal piezoelectric modulus of quartz: *a* – planar distribution, Curie cut is shown by the dashed lines, *b* – spatial distribution of modulus (guide surface – indicatrix)

From the Fig. 1.4 one can see that any piezoelectric effect in quartz is absent in the vertical axis – in the Fig. 1.5 (*a*) it is denoted as *2*. Similarly, this effect cannot be observed along the non-polar axes *2′* and *2″*, equivalent to *2*. The third rank axis *3* is also non-polar in the quartz. However, the maximums of piezoelectric effect are observed along three the polar axes *1, 1′* and *1″*. Any cut of crystal made perpendicularly to this direction is called a Curie cut. The planes slanting to the Curie cut have a decreased piezoelectric activity, and its distribution in plane is described as $d = d_{max}\cos 3\varphi$ where φ is the plane angle.

Piezoelectric modulus spatial distribution in the polar coordinates is $d = d_{max}\sin^3\theta\cdot\cos 3\varphi$ where θ is azimuth angle. This spatial pattern shown in Fig. 1.5 (*b*) looks like six almond surfaces joined in the center. In the *Z*-direction as well as in the three *Y*-directions the piezoelectric effect in quartz does not occur. Through the radius vector from the center of the figure to the distribution surface can determine the magnitude of the piezoelectric effect in any cut of the quartz. It is obvious that maximums of the effect occur along any of the three *X*-axes.

Main feature of piezoelectric effect is its linearity, and this important fact enables to distinguish the inverse piezoelectric effect from the electrostriction. In any dielectric the external electrical field produces deformation that is characterized by the quadratic dependence on the field:

$$x = RE^2,$$

where R is the constant of electrostriction, Fig. 1.6 (*a*). It is seen that the strain in the case of electrostriction does not change its sign with the change of electrical field polarity.

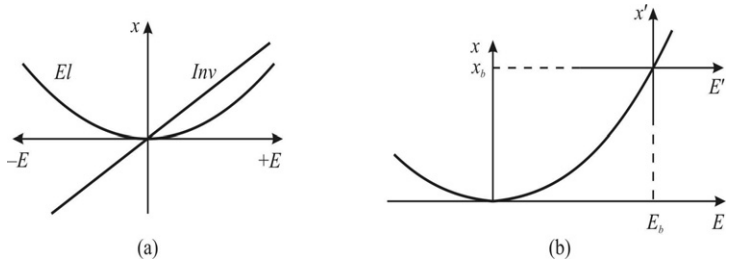

Fig. 1.6. Comparison of inverse piezoelectric effect (*Inv*) and electrostriction (*El*):
a – parabolic and linear field dependences of strain;
b – under bias field E_b quasi-linear dependence $x'(E')$ imitates piezoelectric effect

Except the quadratic type of $x(E)$ dependence, the electrostriction is different from the piezoelectric effect also by the fact that electrostriction has no retroactive mechano-electrical effect. As to linear piezoelectric effect, one can see both the direct and the inverse effects.

However, the linear electromechanical effect (which is a peculiar property of polar structures) can be interpreted as linearized electrostriction, Fig. 1.6 (*b*). Suppose that external direct electrical field (bias field E_b) is applied to usual centre symmetric crystal (that is non-piezoelectric at $E = 0$). The applied field changes the original symmetry due to its electrical polarization: due to electrostriction the strain x_b that corresponds to the field E_b. Under the external direct field the crystal structure turns into a polar structure (non-centrally symmetric). So a resemblance of linear electromechanical response should be observed: on the wing of electrostriction parabola at the presence of the bias field the alternating electric influence E' generates practically linear mechanical response: $x' \approx d'E'$ where d' is electrically induced piezoelectric modulus. (Calculations show that $d' \approx 2Q\varepsilon_0^2\varepsilon^2 E'$ where $\varepsilon_0\varepsilon$ is the electrical permittivity and Q is the electrostriction parameter).

In compliance with the electrically induced (artificial) piezoelectric effect (possible in any solid dielectric), one can imagine that the usual piezoelectric effect also might be explained as linearized electrostriction, as in the Fig. 1.6 (*b*). In this case no external field exists, but the internal (spontaneous) distribution of electrical charges can be roughly characterized by a "bias effective internal crystal field, E_b". This field is large, and therefore the external electrical field can only lead to a slight increase of spontaneous mutual displacement of the ions or to reduce it, but does not change the overall direction of internal polarization. This model is in line with the conception that the fundamental reason of crystal internal polarity is the asymmetry

in the electron density distribution along polar bond between atoms that have quite different electro-negativity.

1.2. Simplified mechanism of pyroelectric effect

Piezoelectrics are closely connected with pyroelectrics. In all pyroelectrics both piezoelectric effects (the direct and the inverse ones) are observed, but only in a pyroelectric it is possible to observe a very important for practical applications volumetric piezoelectric effect, that is, an electrical response to hydrostatic pressure.

Pyroelectric effect can be explained using a simplified model of one-dimensional polar crystal (Fig. 1.7). This model of pyroelectricity comes to a simple molecule consisting of a pair of ions separated by a distance a that is smaller than the distance b between the adjoining polar unit cells. This asymmetry is explained by the large difference in the electro-negativity of positive and negative ions.

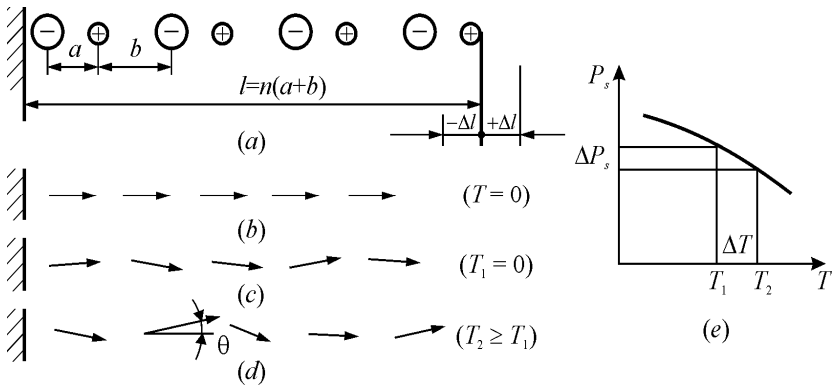

Fig. 1.7. One-dimensional model of a pyroelectric crystal: *a* – polar chain of two-ions molecules; *b* – dipole moments orientation without thermal motion ($T = 0$); *c* and *d* – different degrees of thermal disordering and thermal expansion of a dipoles chain; *e* – spontaneous polarization dependence on temperature

Polar crystal has its own electrical moment P_s that summarizes many elemental moments p_0. The unit cells are marked in Fig. 1.7 as molecule dipoles. They can be distinguished, for the simplest example, in the spontaneously polarized low-temperature pyroelectric crystal HCl, as well as in the wide-gap semiconductors of CdS type ($A^{II}B^{VI}$ crystals) belonging to the pyroelectrics 6*mm* point symmetry class.

In this one-dimensional model one can observe not only pyroelectric but also a piezoelectric effect, which, in fact, contributes to the pyroelectricity. Indeed, the mechanical stretching or compression of the dipole chain leads to a change in the

specific electrical moment: $P \sim \Delta l/l$. Thus, not only from the general considerations, but also from the simple model it follows that any pyroelectric should have piezoelectric properties (but the opposite conclusion would be false).

Diatomic polar molecules in the Fig. 1.7 (*b*) are replaced by the arrows that represent single dipole moments. In the idealized case (at absolute temperature $T = 0$) all dipoles are strictly oriented. As the temperature increases, the thermal chaotic motion, firstly, results in the partial disordering of dipoles, and, secondly, leads to a thermal expansion of the crystal. In the mechanically free crystal both these mechanisms give rise to reduction of spontaneous polarization P_s with increasing temperature, Fig. 1.7 (*e*). The first mechanism (polar units disordering) is observable in any polar crystal, but the second mechanism (crystal thermal expansion) is possible to observe in the mechanically free crystal only.

The temperature change of P_s in the linear ("hard") pyroelectrics, such as tourmaline or lithium sulfate crystals, is mostly due to the thermal expansion of the crystal. This type of pyroelectricity is produced by the piezoelectric conversion of thermal strain, and it is referred to as a *secondary* pyroelectric effect. The temperature change of P_s in the non-linear ("soft") pyroelectrics, which include most of the ferroelectrics, is caused mainly by the thermal disordering of the dipole structure. Temperature alteration in the dipole orientation leads to a *primary* pyroelectric effect.

Due to fast temperature change in the ferroelectric spontaneous polarization (large dP_s/dT) near the Curie point, only these materials are mostly used as pyroelectric sensors. In the model shown in Fig. 1.7 elementary electrical dipole moment alteration is $dp = p_0(1 - \cos\theta)$. Since the angle θ is small, it can be considered proportional to the intensity of the thermal motion: $\theta \sim kT$. Therefore, the change in the polarization is $\Delta P = \gamma^{(1)}\Delta T$ where $\gamma^{(1)}$ is a primary pyroelectric coefficient.

For secondary pyrolectric effect the proportionality in the ΔP and ΔT is, firstly, a result of thermal expansion linear law: $\Delta l = \alpha\Delta T$, where Δl is linear deformation and α is the coefficient of thermal expansion, and, secondly, a result of the linear dependency of the direct piezoelectric effect: $\Delta P = e\Delta l/l$, where e is the piezoelectric strain constant. From these two formulas it is possible to obtain linear equation for secondary pyroelectric effect: $\Delta P = \gamma^{(2)}\Delta T$, where $\gamma^{(2)}$ is secondary pyroelectric coefficient.

Consequently, taking into account the contributions from both mechanisms of pyroelectricity, one can obtain for the thermally induced polarization

$$P = (\gamma^{(1)} + \gamma^{(2)})\Delta T.$$

As the temperature T is a scalar while the polarization is a vector, the pyrolectric coefficient γ is a vector. But it is a particular, "material", vector, which differs from the "power" type vectors (such as field intensity vectors E, D, or P).

The first rank material tensor (i.e., the material vector) describes the distribution of pyroelectric electrical response in the crystal. The appropriate indicatory surface (indicatrix) is shown in the Fig. 1.8 and consists of two spheres.

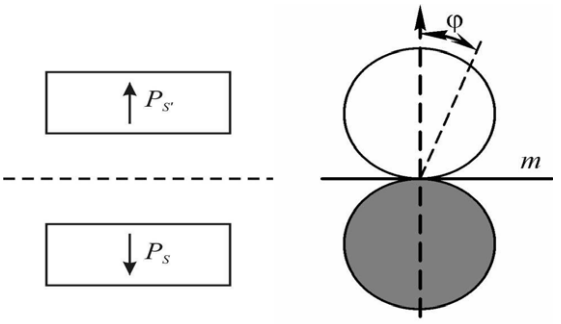

Fig. 1.8. Spontaneous polarization orientation and the correspondent indicatory surface (indicatrix) for the pyroelectric coefficient; black area shows the negative part of pyroelectric coefficient

These spheres are located above and below the symmetry plane *m,* and they are characterized by the equation $\gamma(\varphi) = \gamma_{max}\cos\varphi$. It is evident that pyroelectric coefficient spatial distribution corresponds to the spontaneous polarization orientation in the polar crystal: $P = P_{max}\cos\theta$. The upper sphere is the indicatory surface for upper orientation of P_s while the bottom sphere only means the change in the sign of γ_i if spontaneous polarization has the opposite direction.

Material vector γ reaches its maximum in the ordinate direction that coincides with spontaneous polarization direction. So the γ_{max} might be measured in the crystal cut perpendicular to the main polar axis. Angle φ is the angle between the ordinate axis and the slanting crystal cut where the pyroelectric effect is studied. By the radius vector from the center (see Fig. 1.8) it is possible to determine the size of pyroelectric effect in any slanting cut of the crystal. It is obvious that the pyroelectric effect is absent perpendicularly to the ordinate axis.

Next section discusses the boundary conditions in which polar crystals are studied or applied.

1.3. Boundary conditions for polar crystals investigations

Internal polarity of the crystal allows converting mechanical energy into electrical energy (i.e., the direct piezoelectric effect) or, opposite, converting electrical energy into mechanical one (i.e., the inverse piezoelectric effect). Also, these crystals are capable of electro-thermal and thermo-electric conversions (i.e. the electrocaloric and pyroelectric effects respectively). All these effects are described by different linear relationships – depending on the combination of various boundary conditions, under which the polar crystals are used or investigated.

In the following paragraphs we consider the idealized electrical, mechanical and thermal boundary conditions that are relevant for polar crystals.

Electrical boundary conditions:

$\boldsymbol{E = 0}$, the polar crystal is electrically free, which means that the crystal's entire surface is the equipotential. Since the electrical induction is $D = \varepsilon_0 E + P$, so in the electrically free crystal $D = P$. In the case of static procedure of piezoelectricity study, the condition $E = 0$ can be realized by considering an entirely metallized crystal. In practice, this condition is ensured by shorting the electrodes deposited on the piezoelectric. Under dynamic testing, when mechanically or thermally induced polarization is variable in time, the condition $E = 0$ leads to the electrical current, i.e. the crystal is the source of current.

$\boldsymbol{D = 0}$, the polar crystal is electrically disconnected, $D = \varepsilon_0 E + P = 0$. In a static case, the implementation of this condition for research requires extremely low conductivity of piezoelectric: only in this case the piezoelectric polarization P is compensated by mechanically induced electrical field: $\varepsilon_0 E = -P$. In the case of dynamic excitation of the polar crystal the condition $D = 0$ is ensured, for example, in the acoustic waves that have longitudinal polarization.

Mechanical boundary conditions:

$\boldsymbol{X = 0}$, mechanically free condition of polar crystal, in which all components of the stress tensor are equal to zero. In the static studies this condition can be realized by providing a total freedom for crystal deformation. In the dynamic condition $X = 0$ is performed with the same caution and, in addition, polar crystal should be investigated at the frequencies below the mechanical resonance.

$\boldsymbol{x} = 0$, the piezoelectric is mechanically clamped. Theoretically, to provide this condition in the static experiment the crystal must be surrounded by "infinitely rigid"

shell and is "rigidly stuck" to it. Such studies are either impossible or impractical. In practice, the mechanical clamping is realized by introducing a dynamic method at the high frequency range studies, i.e., the frequencies much higher than the frequency of the electromechanical resonances of the crystal. In this case, the own inertia prevents crystal deformation, and so the condition $x = 0$ is satisfied.

Thermal boundary conditions:

***T* = const**, isothermal condition with invariable temperature, when crystal has enough time to exchange energy with the environment during the measurements. It is this approximation that one uses in thermodynamics as a convenient case for theoretical investigations. In practice, one has to do with a quasi stationary condition or a very slow change in time.

***S* = const**, adiabatic condition with constant entropy, when the crystal cannot exchange energy with the environment during measurements. For example, this is measurements at a relatively high frequency.

These boundary conditions are just idealized models of reality, and the approach to their implementation depends on the research goals set, e.g., a study of the electro-mechanical or electro-thermal properties of a crystal. In practice, the polar crystals are used in some intermediate conditions: they are partially clamped – partially free, neither entirely short-circuited nor entirely open-circuited but loaded to a certain impedance value. However, the above-named idealized boundary conditions should be assumed as a basis for piezoelectric or pyroelectric effects study.

1.4. Relations diagram for elastic, electrical and thermal effects

Elastic, thermal and electrical properties of polar crystals are interdependent. Relations diagram looks like two triangles connected by their vertices, Fig. 1.9. The nine lines connecting the vertices represent the nine linear effects that can be observed in the polar crystals.

Three lines of this diagram, connecting a vertex of the inner to a vertex of the outer triangle, represent separately thermal, electrical and mechanical interaction. In particular, the line connecting the bottom-right vertices symbolize the equation $\Delta Q = C\Delta T$, which describes the relationship of basic thermal parameters of the crystal. ΔQ and ΔT are the change in heat and temperature while C is specific heat. The line connecting the top vertices of the triangles indicates electrical parameters of the crystal in the case of electrically induced polarization: $P_i = \varepsilon_0 \chi_{ij} E_j$. The line

joining the bottom-left vertices of the diagram symbolizes mechanical properties of the crystal (Hooke's law): $X_{kl} = c_{klmn}x_{mn}$, where X_{kl} and x_{mn} are stress and strain tensors while c_{klmn} is elastic stiffness tensor.

The six edges of the two triangles in the diagram represent linear effects, reflecting the connection of thermal, elastic and electrical properties in polar crystal. In particular, the lower (horizontal) edges indicate thermoelastic effects, for instance, $x_{mn} = \lambda_{mn}\Delta T$, where λ_{mn} is thermoelastic tensor for mechanically clamped crystal.

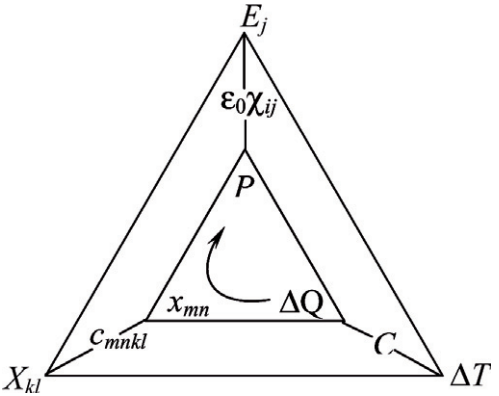

Fig. 1.9. Relations diagram of polar crystal electrical, mechanical and thermal properties (after W. Cady)

In the case of mechanically free crystal the strain is absent and $x_{mn} = \alpha_{mn}\Delta T$, where α_{mn} is thermal expansion tensor. Depending on the process implementation, i.e., adiabatic ($\Delta Q = 0$) or isothermal ($\Delta T = 0$), as well as depending on mechanical conditions of the crystal, i.e., which might be free ($X_{kl} = 0$, allowing strains) or clamped ($x_{mn} = 0$, disallowing strains), the thermoelastic effects can be described by different linear equations. Moreover, two opposite directions of these effects are possible: the primary influence may be a thermal one (a change in heat or temperature) while the response is mechanical (change in strain or stress). Alternatively, the primary influence may be mechanical excitation of the crystal, and the reaction may be a change in temperature or heat. For example, stretching the crystal results in cooling, while the compression results in heating. As a result, eight linear equations can describe the thermo-elastic effects – the interrelations between ΔQ, ΔT, X_{kl} and x_{mn}.

The left-hand side of the diagram (Fig. 1.9) corresponds to the electromechanical phenomena. If the initial perturbation of the equilibrium condition is mechanical deformation x_{mn} (crystal is free) or mechanical stress X_{mn} (crystal is

clamped), the open-circuited electrical response to this influence will be an electrical field: $E_i = h_{imn}x_{mn}$ or $E_i = g_{ikl}X_{kl}$ respectively. In the case of closed-circuited conditions the electrical response is the occurrence of polarization: $P_j = e_{jmn}x_{mn}$ or $P_j = d_{jkl}X_{kl}$. Thus, depending on the boundary conditions, the direct piezoelectric effect is described by four linear relationships. The inverse piezoelectric effect reflects a similar situation for two mechanical boundary conditions (free or clamped crystal) as well as two electrical conditions (open circuit and closed circuit). So the left part of diagram symbolizes eight linear equations which describe the linear electromechanical effects – the interrelations between E_i and P_j, on one hand, and X_{kl} and x_{mn} on the other hand, for the direct as well as the inverse piezoelectric effects.

The right-hand side of the diagram (Fig. 1.9) describes eight electro-thermal effects in a polar crystal. Pyroelectric effect occurs when the disturbance factor is the thermal influence while the response has electrical nature. Depending on the thermal conditions (i.e., adiabatic with $\Delta Q = 0$ or isothermal with $\Delta T = 0$) as well as electrical conditions (i.e., open circuit and closed circuit) four possible equations describe the pyroelectric effect: $P_i = \gamma_i \Delta T$, $P_i = \gamma'_i \Delta Q$, $E_j = \gamma''_j \Delta T$ and $E_j = \gamma_j''' \Delta Q$, where various pyroelectric coefficients correspond to different boundary conditions.

Electrocaloric effect is obviously the reverse of the pyroelectric one, and it also may be described in four different linear relationships – depending on the boundary conditions. One important consequence of electrical, thermal and elastic effects relationship in polar crystals is the appearance of secondary effects. The path for one of them is denoted in the diagram by an arc with an arrow. In this example we indicate that one can observe a secondary pyroelectric effect that occurs under certain boundary conditions: a free-crystal thermal expansion leads to electrical polarization through the piezoelectric effect.

Another consequence of this relationship is the dependence of thermal, electrical or mechanical processes passing in the polar crystals on the boundary conditions. For example, in an open circuit pyroelectric the specific heat C^E differs from the specific heat C^P in a closed circuit crystal. In the same manner, there is a difference in the specific heat of mechanically free (C^X) and mechanically clamped (C^x) crystals. Similarly, the elastic stiffness in the Hooke's law for polar crystals depends on the electrical conditions: open-circuited elastic stiffness (c^P_{klmn}) differs from closed-circuited (c^E_{klmn}). When the Hooke's law is studied in a polar crystal, the observed elastic stiffness depends on isothermal (c^T_{klmn}) or adiabatic (c^S_{klmn}) conditions.

1.5. Peculiarities in dielectric properties of polar crystals

It is well known that fundamental permittivity ε is conditioned by the some intrinsic (microscopic) processes of polarization (ionic, electronic, dipole). In the polar crystals (piezoelectrics and pyroelectrics) at low frequencies to the value of ε one has to add the "piezoelectric contribution" ε_{EM}, given by the electromechanical response from test sample deformation as a whole. At the very low frequencies in pyroelectrics it is possible to observe also the "electro-thermal contribution" ε_{ET}, when the tested sample can exchange thermal energy with the environment during its polarization.

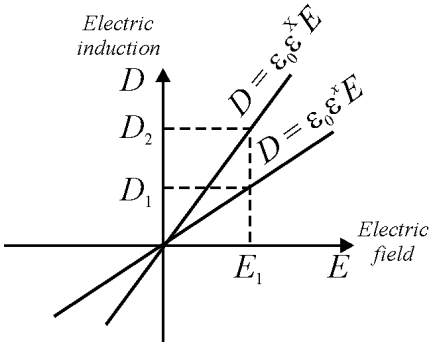

Fig. 1.10. Electrical induction D depending on the electrical field E for free ($X = 0$) and clamped ($x = 0$) piezoelectric

The nature of piezoelectric contribution to the permittivity is explained in Fig. 1.10. If crystal cannot change its dimensions in the electrical field E_1 (crystal is clamped) the electrical induction is D_1 that represents intrinsic polarization mechanisms. However, if the crystal is free for piezoelectric deformation the induction in the same electrical field E_1 will be larger (D_2) due to electro-elastic contribution.

In a piezoelectric that is free for deformation, it is necessary to take into account the piezoelectric effect: $P = -ex$, where e is piezoelectric strain constant and x is mechanical strain:

$$D = \varepsilon_0 \varepsilon E + ex.$$

Therefore, piezoelectric reaction looks like an additional mechanism for the electrical polarization, because it emulates the corresponding contribution to the dielectric constant. If the piezoelectric is free, then $\varepsilon = \varepsilon^X$, and if it is mechanically clamped, then $\varepsilon = \varepsilon^x$. From the previous equation one can obtain:

$$\varepsilon^X = \varepsilon^x + e^2 / \varepsilon_0 .$$

When dielectric properties of crystal are studied at low frequencies (below possible electromechanical resonances) then the permittivity ε^X is observed, and the piezoelectric reaction e^2/ε_0 contributes to the dielectric constant. At the very high frequencies, much above electromechanical resonances, then the permittivity ε^x is observed. In the second case the point is that own mechanical inertia of test sample makes impossible electromechanical reaction ($x = 0$).

A comparison of free and clamped dielectric constants of piezoelectric active crystals is shown in Fig. 1.11 for the most well-known and well-studied ferroelectrics.

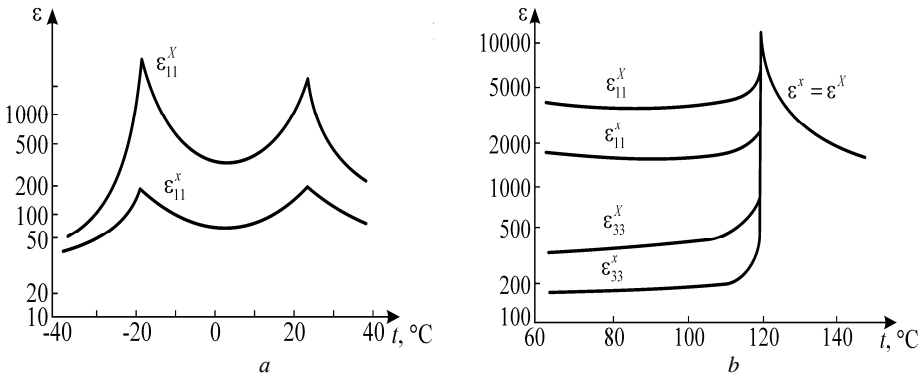

Fig.1.11. Temperature dependence of the dielectric permittivity for free (at the frequency of 10^3 Hz) and clamped (at 10^{10} Hz) crystals: *a* – Rochelle salt, *b* – barium titanate

In the Rochelle salt crystal the piezoelectric effect is typical in the entire temperature range, so in all studied temperature range, Fig. 1.11 (*a*) the permittivity of free and clamped crystal differ greatly everywhere. In the vicinity of ferroelectric Curie points the effect of clamping is very large: $\varepsilon^X/\varepsilon^x \approx 50$.

In the barium titanate when the temperature is above the Curie point, in the cubic (centrally symmetric) phase, the piezoelectric effect is absent, and $\varepsilon^X = \varepsilon^x = \varepsilon$. But below the Curie point (T_C = 120° C) in a single-domain crystal of $BaTiO_3$ near the room temperature the ratio $\varepsilon^X/\varepsilon^x$ has a magnitude about two, while in the polarized $BaTiO_3$ piezoelectric ceramics $\varepsilon^X/\varepsilon^x < 2$.

The transition from the increased permittivity ε^X obtained for a free crystal (at low frequencies) to the reduced permittivity ε^x inherent for a clamped crystal (at very high frequencies) is accompanied by many electromechanical resonances, as it is shown in Fig. 1.12. As an outstanding example, the KH_2PO_4 (KDP) crystal is selected because in this case a record ratio of $\varepsilon^X/\varepsilon^x \approx 100$ is observed.

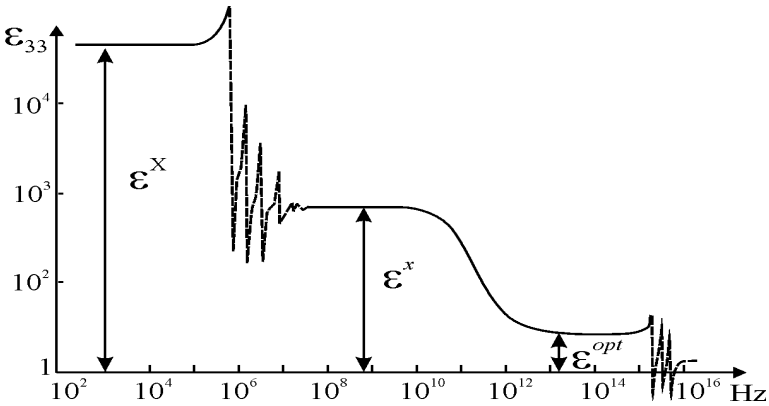

Fig. 1.12. Dielectric spectrum of KDP crystal near its Curie point: in the frequency range of $10^5 \ldots 10^8$ Hz a series of piezoelectric resonances is observed

Another possible influence on the polar crystal permittivity is the "electro-thermal contribution" ε_{ET}, which is also known as electro-caloric contribution. In fact, this is the difference $\varepsilon^T - \varepsilon^S = \varepsilon_{ET}$ between the permittivity ε^T measured under isothermal conditions, when T = const and the dielectric has enough time to exchange energy with the environment, and the permittivity ε^S measured in the adiabatic conditions, at the constant entropy S = const, i.e. when the heat exchange is impossible.

The electro-caloric contribution to permittivity can be essential when ε is large and its dependence $\varepsilon(T)$ is significant, for example, near the ferroelectric phase transition.

When we employ thermodynamics, it is possible to calculate the $\varepsilon^T - \varepsilon^S$ difference:

$$\frac{\varepsilon^T - \varepsilon^S}{\left(\varepsilon^T - 1\right)\left(\varepsilon^S - 1\right)} = \frac{\varepsilon_0 T}{C_P}\left(\frac{\partial E}{\partial T}\right)_P^2,$$

where C_P is the specific heat at the condition P = const. It easy to see that $\varepsilon^T > \varepsilon^S$; sometimes their difference can reach 10...50% (for example, just below the ferroelectric phase transition).

1.6. Peculiarities in elastic properties of polar crystals

When piezoelectric mechanical properties are studied, one can observe a significant difference in the elastic compliance of short-circuited (s^E) and open-

circuited (s^D) polar crystals. Under the influence of outside stress, Fig. 1.13 (*a*), the strain is linearly increased, Fig. 1.13 (*b*), in accordance with the Hooke's law. However, if the piezoelectric is short-circuited, elastic compliance will be bigger than in the case of the open-circuited crystal. The reason is that the piezoelectric voltage generated by a strain in the case of open-circuited crystal increases its harshness (resistance to deformation).

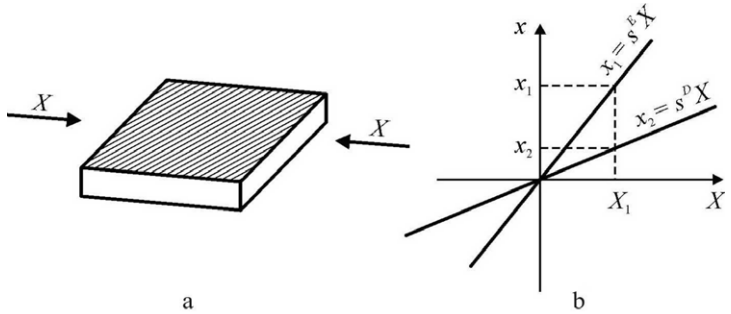

Fig. 1.13. Difference in the elastic compliance in the piezoelectric: *a* – mechanical action on the piezoelectric plate; *b* – Hooke's law in open-circuited (s^D) and in short-circuited (s^E) polar crystal

Experimental example of this effect is shown on Fig. 1.14. In the polar phase of barium titanate (below its ferroelectric phase transition) one can see a difference between the elastic compliance of open-circuited and short-circuited crystal.

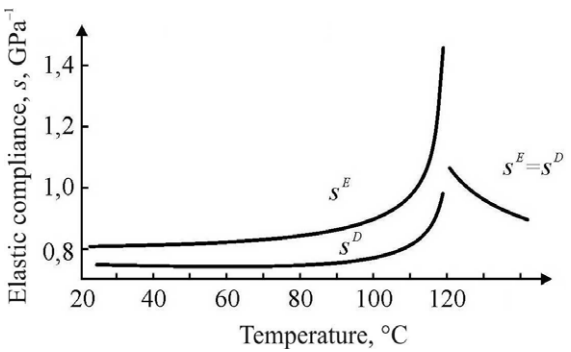

Fig. 1.14. Effect of electrical conditions on the barium titanate elastic compliance at different temperatures: s^D – open-circuited and s^E – short-circuited crystal

Above the ferroelectric phase transition the barium titanate has a cubic, centrally-symmetrical structure and, therefore, the piezoelectric effect is absent. That is why, in the paraelectric phase $s^E = s^D$. But below the phase transition barium titanate moves into a tetragonal polar phase, which is characterized by the piezoelectric effect, and so the elastic compliance for various mechanical conditions

becomes quite different: $s^E > s^D$. Most impressive, the compliance s^D is reduced at the Curie point.

In the same way, experiments show an essential difference in the elastic stiffness in the Rochelle Salt. The largest difference one can see at the Curie points. These data were obtained by the sound velocity measurements, and at the Curie points the sound velocity drops by a factor of 8.

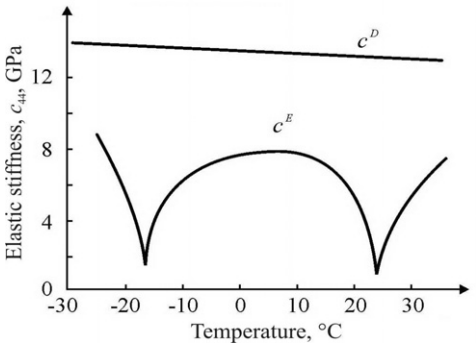

Fig. 1.15. Effect of electrical conditions on Rochelle Salt elastic stiffness in the polar direction: c^D – open-circuited crystal ($D = 0$) and c^E – short-circuited ($E = 0$) crystal

There are many other examples how the electrical conditions influence the mechanical and thermal properties of polar crystals. In turn, the mechanical boundary conditions also may strongly affect the electrical as well as the thermal properties. In this way, the polar crystals differ from a great number non-polar crystals and non-crystalline dielectrics.

Conclusions to part 1

Electrical polarization is separation of electrical charges, and this is accompanied by the deformation of the crystal (strain). Therefore polarization is not only an electrical but also an electro-mechanical phenomenon. In the case of the piezoelectric effect the external mechanical stress which is applied to the crystal does not produce, but only exposes the existing internal polarity of the crystal (its hidden polarity). In the same way, by the pyroelectric effect a connection between the internal polarity and thermal motions in polar crystal is revealed.

2. Internal polarity nature

Piezoelectric effect is possible to obtain in the crystals of 20 non-central classes of point symmetries (as well as in 2 types of textures). As to these 20 classes of crystals, 10 of them belong to the pyroelectrics; the other 10 non-central classes would be referred to as "actual" piezoelectrics. In this book basically these crystals are considered, and the question is how to explain piezoelectricity microscopically in the case of non-centrally symmetric but non pyroelectric crystal.

2.1. Simple model of crystal polarity

There is a strong affinity between piezoelectricity and pyroelectricity, and it can be supposed that both of these effects are the result of internal multiple electrical moment M_{ijk} that exists in any polar crystal. Generally, this moment is the third rank tensor but in some separate cases it appears as a first rank tensor (vector) or as a second rank tensor. For example, one-dimensional (1D) "dipole-type" moment $M_i = P_S$ is a spontaneous polarization vector for pyroelectric or ferroelectric. However, some "actual" piezoelectrics are described by the second rank intrinsic (latent) electrical moment M_{ij} that is specific for the 2D arrangement of M_{ij} components, while the properties of many other piezoelectrics can be described by the third rank electrical moment M_{ijk} that corresponds to the 3D polarity.

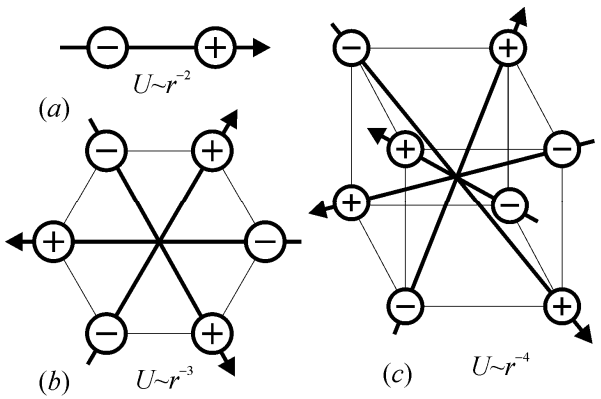

Fig. 2.1. Simplified representation of intrinsic polarity in the non centrally symmetric crystals: *a* – dipole moment; *b* – sextuple moment, *c* – octopole moment

Simplified model of high rank polar moments is shown in Fig. 2.1. In polar pyroelectric classes of crystals the dominating motive is polar dipole moment, Fig. 2.1 (*a*), and it should be mentioned that the energy of dipole-to-dipole interaction

comparatively weakly decreases with the distance: as ~ r^{-2}. This 1D internal polar correlation is capable for a long time withstand to unavoidable disorienting thermal fluctuations (that consists of 3D perturbations in the crystal). That is why ordinary pyroelectric keeps its spontaneous polarization at high temperatures up to the crystal melting. However, if the 3D thermal disordering begins to overcome the internal ordering in a polar 1D system (as it is the case in the ferroelectrics), its collapse becomes very fast (critical), giving rise to the phase transition into a non-polar phase.

Two-dimensional polar sextuple moment, shown in Fig. 2.1 (*b*), corresponds to dominating arrangement of internal polarity typical in some piezoelectrics of lower symmetry. In the case of 2D internal correlation the interaction energy of sextuple moments decreases with distance faster in comparison to the case of 1D interaction, namely as ~ r^{-3}. That is why a second rank intrinsic (latent) electrical moment M_{ij} can be destroyed by the chaotic 3D thermal fluctuations more gradually (than in the case of 1D). Nevertheless, M_{ij} also vanishes only at the critical temperature, and a 2D polar crystal can have a phase transition to a non-polar state.

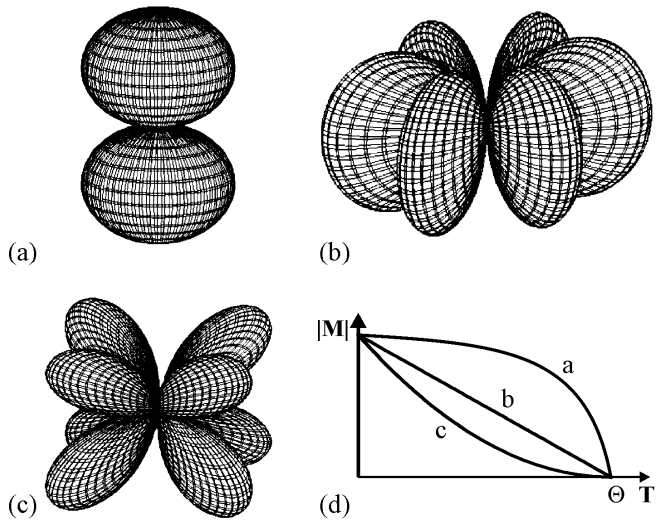

Fig. 2.2. Piezoelectric M_{ijk} modulus that vanishes at the temperature θ by critical law $(\theta - T)^n$ (*d*). Exponent $n = 0.5$ is Landau critical index that is specific for $M_i = P_S$ dipole system; exponent $n = 1$ is typical for the M_{ij} sextuple, while $n = 2$ corresponds to the M_{ijk} octopole

When a piezoelectric has cubic symmetry, Fig. 2.1 (*c*), three-dimensional polar octopole moment dominates, and octopole-to-octopole interaction energy decreases with distance very quickly, namely, as ~ r^{-4}. That is why 3D thermal fluctuations can

more rapidly destroy the interaction of polar octopole moments, so 3D latent polar moment M_{ijk} decreases faster than 2D or 1D polar moments.

The comparison of all three cases is shown on Fig. 2.2 (*d*), where θ is the phase transition temperature. The three-dimensional figures represent: (a) – the first rank material tensor which is the material vector $M_i = P_S$ (i.e., the pyroelectric coefficient); (b) – a spatial distribution of second rank material tensor (which corresponds to the quartz piezoelectric modulus); (c) – possible representation of the third rank material tensor (for example, GaAs piezoelectric module). Spatial distribution of octopole moment is shown on Fig. 2.2 (c), and it is described by the equation $P_{111} = P_{max}\sin\theta\cdot\sin 2\theta\cdot\cos 2\varphi$.

The polar moment temperature dependence shown on Fig. 2.2 (d) can be used in electronics for thermal sensors. In a similar way, all these polar moments depend on pressure, and this is possible to exploit in mechanical sensors. Eventually, these characteristics can be used to take account the noises that arise due to the chaotic fluctuations of polarisation.

Sextuple moment is a plane-situated non-centrally symmetric three-dipole configuration, while the octopole moment is a spatially situated four dipoles with non centre symmetric arrangement, Fig. 2.1 (b,c). It should be emphasized that the latent polar structure in the pyroelectrics is non-compensated, whereas it is totally self-compensated in the so-called "true piezoelectrics" (for the sextuple, as well as for the octopole moments).

Table 2.1.

Polar responses in dielectrics (classification)

Induced by stress		*Induced by temperature*
PIEZOELECTRICITY	New effects in 20 "piezoelectric" classes of polar crystals	PYROELECTRICITY
Conventional piezoelectric effect in 20 polar classes ("piezoelectric" classes)	Artificial pyroelectric effect in 20 classed	Conventional pyroelectric effect in 10 polar classes ("pyroelectric" classes)
Volumetric piezoelectric effect in 10 "pyroelectric" classes of polar crystals	Artificial volumetric piezoelectric effect in 20 classes	Tertiary pyroelectric effect in 20 classes of polar crystals
Electric field induced piezoelectricity in all 32 classes		Electric field induced pyroelectricity in all 32 classes

But this self-compensation is total only if the crystal is in a stress-free state. Non-isotropic partial clamping can destroy the self-compensation of the intrinsic polarity. This decompensation allows observing in such crystals vectorial responses to scalar influences, Table 2.1. It is necessary to note that in the piezoelectric materials a tertiary pyroelectric effect is also possible (actinoelectricity). It is caused by the temperature gradient due to non-uniform heating.

The ***partial clamping*** of piezoelectric crystal is proposed here as a way to artificially obtain the responses of vectorial type, γ_i (or ξ_i), in non-pyroelectric crystals. Thus it is possible to observe new effects (shown in Table 2.1) in any piezoelectric crystal. Among them, there are such important piezoelectrics as quartz and the semi-insulating $A^{III}B^{V}$ crystals (such as gallium arsenide), which are very promising materials in the microelectronics and micromachining. Under the conditions of partial clamping, it is possible to eliminate the symmetry of their response, effectively "converting" these common microelectronics crystals into artificial pyroelectrics.

This opens new possibilities for sensor devices. In addition to sensor applications, it is shown that any device based on the $A^{III}B^{V}$ semiconductor which have erroneous orientation of crystal generates polarization-noises induced by external vibrations or internal thermal fluctuations.

2.2. Relationship between pyroelectricity and piezoelectricity

The relationship between piezoelectricity and pyroelectricity is obvious from some artificially induced effects. For instance, the external electrical field (bias field E_b) can induce artificial piezoelectric effect as well as artificial pyroelectric effect, Table 2.1.

Nevertheless, the understanding of the nature of pyroelectric spontaneous polarization and, all the more so, of the piezoelectric intrinsic polarity is, in many respects, still incomplete. It will suffice to mention that even the crystal of single chemical element – the carbon – can take, occasionally, the form of pyroelectric wurtzite (class 6*mm*) in addition to its principal form of *m*3*m* cubic structure (the diamond). Among various piezoelectrics several crystals of single chemical element exist as well. Examples are the crystals of Te and Se which belong to the piezoelectric structure of quartz-type (32 class of point symmetry). Undoubtedly, in the mentioned examples of single-element crystals only the dissymmetry of

electronic atomic shells can be responsible for the intrinsic crystal polarity. However, in this work only the crystals with mixed ionic-covalent bonds are discussed.

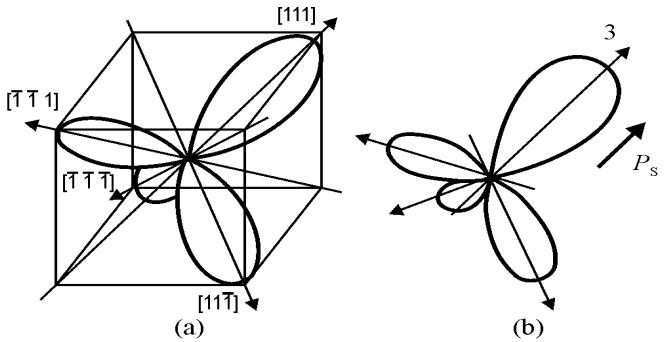

Fig. 2.3. The spatial distribution of the positive part of piezoelectric responsiveness in 3D polar crystal: *a* – total compensation of polar activity; *b* – the appearance of a dipole component, equivalent to the spontaneous polarization P_S

The second example of pyroelectricity and piezoelectricity relationship is the polymorphism of $\bar{4}3m$ (piezoelectric) and $6mm$ (pyroelectric) structures. Zinc sulphide crystal is the best example of piezoelectric and pyroelectric affinity. Interatomic interactions provide some relatively stable configuration of 4ZnS type (zinc blende) from which both sphalerite and wurtzite structures can be built.

In the former case (the sphalerite), the piezoelectric polar structure of ZnS can be well-determined by the octopole electrical moment, and this model can be suitably represented by the four 3-fold polar axes of type [111] which intersect at the angle 109.5°, as it is shown in Fig. 2.2 (c). Such latent three-dimensional (3D) polar structure is absolutely self-compensated if the crystal is stress-free, Fig. 2.3 (a).

The second principle structure of ZnS is a pyroelectric wurtzite that includes not only octopole-type polar axes arrangement but also a dipole (1D) component, Fig. 2.3 (*b*). In spite of the symmetry difference, the dissimilarity in the atomic displacements of these two principle forms of zinc blende is so small that they can alternate each other in one crystal.

There is a rich of experimental evidence of the spontaneous polarization existence ($P_S = M_i$) in the pyroelectrics and ferroelectrics, so this is commonly known. That is why we give below detailed arguments of the existence of "latent" polarity only for the case of the piezoelectric crystals.

1. During the crystallization process, the density of piezoelectric crystal decreases in comparison to its melt. For example, a growing GaAs crystal can swim

in its melt (as the ice in the water). It may be deduced that the formation of polar bonds expands a non-centrally symmetric material.

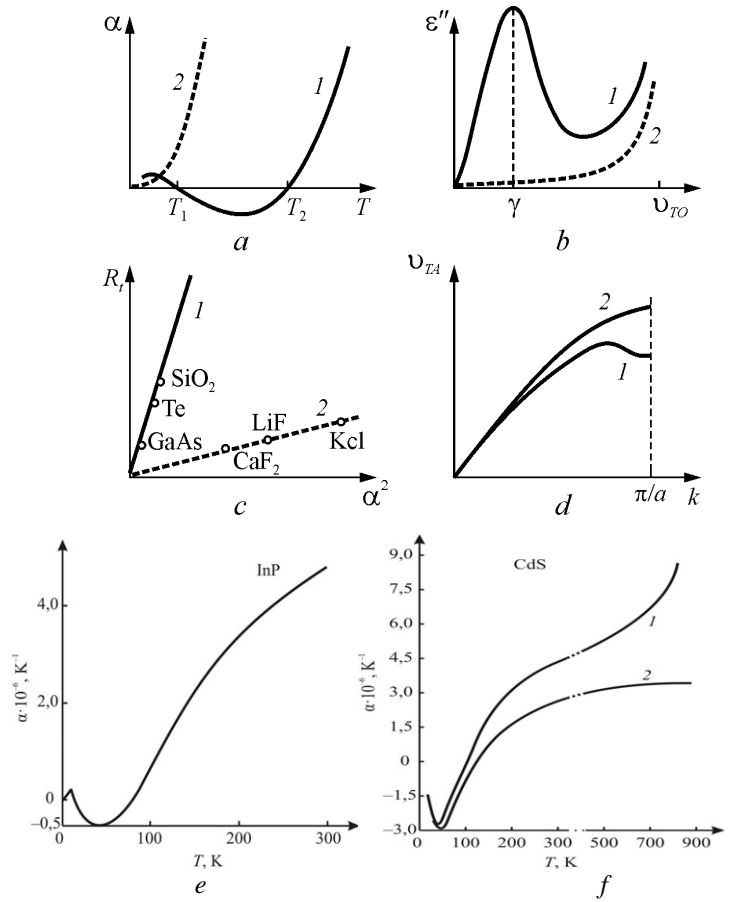

Fig. 2.4. Thermal physics and lattice dynamics properties of piezoelectric crystals in comparison with common centrally symmetric crystals: *a* – thermal expansion coefficient α temperature dependence for polar crystal (1) and for non-polar (2) crystals: in the range between T_1 and T_2 parameter α in polar crystals have negative value, which indicates some polar ordering in their structure; *b* – sub-millimetre waves (terahertz frequency range) losses have a maximum in polar crystals; *c* – thermal resistivity coefficient R_t dependence on the α^2 typical for polar crystals (*1*) and for non-polar crystals (2): increased R_t in the polar crystals is due to stronger phonon scattering; *d* – acoustic branch in Brillouin zone for polar crystal (*1*) in comparison with non-polar crystal (2) *e, f* – experimental temperature dependence linear thermal expansion coefficients for cubic piezoelectric InP and hexagonal pyroelectric CdS (curve 1 shows $\alpha_\perp$ and curve *2* is $\alpha_\parallel$

2. The temperature dependence function of the thermal expansion coefficient α of the piezoelectrics passes through a zero in the temperature interval of 10 – 100 K,

Fig. 2.4 (*a, e, f*), instead of showing a classical dependence $\alpha \sim T^3$. It can be attributed to the assumption that the polar bonds in a piezoelectric at low temperatures become more ordered. Appropriate experimental data are shown in Fig. 2.4, *e*, *f* as for piezoelectric so for pyroelectric.

3. The heat diffusion resistance in the non-centrally symmetric crystals far exceeds the one for centrally symmetric crystals, Fig. 2.4 (*c*). Increased thermal resistance in the piezoelectrics is conditioned by the peculiarities of phonon dissipation process in these crystals (acoustical and optical phonons relation).

4. Fundamental (lattice) microwave dielectric absorption ε'' of non-centrally symmetric crystals is vastly superior to the absorption of centrally symmetric crystals. Here ε'' is a dielectric loss coefficient, that is, the imaginary part of complex dielectric permittivity $\varepsilon^* = \varepsilon' - i\varepsilon''$. In the piezoelectrics the microwave dielectric losses show an additional maximum of a quasi-Debye type absorption, due to the bonding between optical and acoustical phonons. Theoretical prediction of the loss maximum at the frequency γ is shown in Fig. 2.4 (*b*). Experimental evidence shown in the Fig. 2.5 is a comparison of microwave properties of two semiconductors.

One is a non-polar crystal, silicon, Fig. 2.5 (*a*), that is characterized by pure covalent bonds, and its losses are caused exclusively by the conductivity (σ), so loss factor decreases with frequency but increases with temperature:

$$\varepsilon''(\omega,T) \approx \frac{\sigma_0 \exp\left[a(T-T_0)\right]}{\varepsilon_0 \omega},$$

where σ_0 is conductivity at certain temperature T_0, ε_0 is electrical constant, and a is peculiar parameter for a given semiconductor.

The other is polar crystal, such as semi-insulating gallium arsenide, Fig. 2.5 (*b*), in which the influence of conductivity at microwaves is negligible but the loss factor increases with frequency correspondingly with Debye formula:

$$\varepsilon''(\omega,T) \approx \frac{\omega}{\omega_D} \exp\left(-\frac{U}{k_B T}\right),$$

where ω_D is Debye frequency, k_B is Boltzmann constant, U is relaxation potential barrier. Therefore, losses increase as with frequency so with the temperature increase.

5. The above mentioned special features of piezoelectrics correlate with their acoustic phonon spectrum near the Brillouin zone boundary, where transverse

acoustic mode has an anomaly, as an example, for GaAs and quartz crystals, Fig. 2.4 (*d*). This is an evidence of the short-range interaction between the nearest atoms which could be described by the multiple electrical moments.

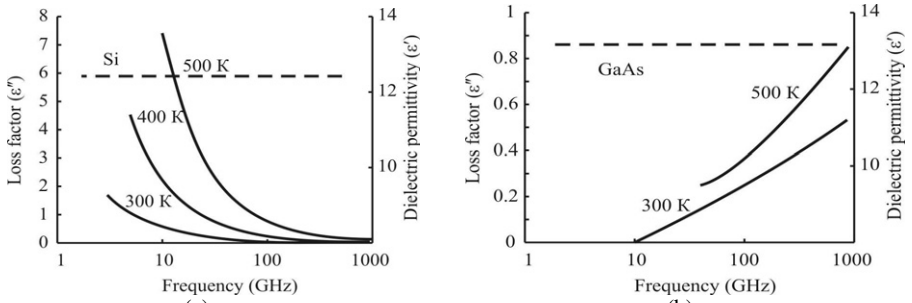

Fig. 2.5. The frequency dependence of permittivity ε′ (dashed line) and loss factor ε″ (solid line) for silicon and for semi-insulating gallium arsenide (*s/i*-GaAs) at different temperatures

There are many other qualitative evidences of non-central crystals latent polarity. Above discussed peculiarities, piezoelectric exhibit the unipolarity in his chemical properties. For instance, the etching of quartz occurs more rapidly at the "positive" ends of polar *X*-axis while the etching is very slow at the "negative" ends of *X*-axis. Therefore, the etch figures for quartz plates are very different for "+" and "–" surfaces. In just the same way, in the cubic polar GaAs crystal one can see a considerable distinction in chemical properties between two surfaces of the (111)-plate that should be taken into account while electrodes deposition.

2.3. Partial clamping effect influence upon 2D latent polarity crystal

The novelty of studied effect needs more detailed explanation based on the conception of classic pyroelectric response. Conventional pyroelectric effect is the variation of spontaneous polarization dP_i in the polar crystal during the uniform change of its temperature dT, Fig. 2.6.

Pyroelectric coefficient in a free-stress crystal is $\gamma_i = dP_i/dT$ (vector is marked by one index, such as *i, j* = 1, 2, 3). Pyroelectric effect is divided onto a primary part $\gamma_i^{(1)}$ and a secondary part $\gamma_i^{(2)}$, and constitutes a sum: $\gamma_i = \gamma_i^{(1)} + \gamma_i^{(2)}$.

Primary effect is pyroelectricity of a clamped (free-strain) crystal that means crystal` study in the condition when all components of strain are absent: $x_m = 0$ (second rank tensors are marked here by indexes *m, n* = 1, 2, … 6).

Secondary pyroelectric coefficient can be measured as a difference between the pyroelectric effects in the free and clamped crystals, and this coefficient can be

calculated from the equation of piezoelectric response: $P_i = e_{im} x_m$, where e_{im} are components of piezoelectric module (third rank tensor), and x_m is component of strain.

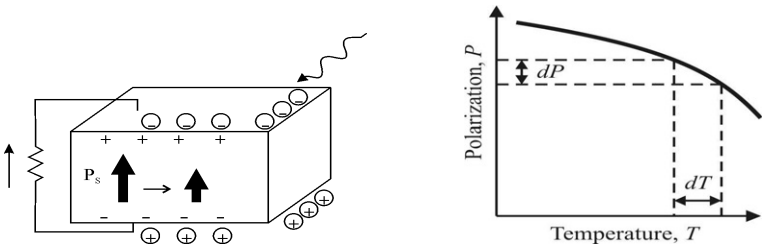

Fig. 2.6. Pyroelectric effect in pyroelectrics the ferroelectrics

Under the thermal influence, this piezoelectric effect is excited by the thermal deformation of crystal: $x_m = \alpha_m dT$, where α_m is the component of thermal expansion coefficient (second rank tensor). As a result:

$$\gamma_i^{(2)} = e_{im}\alpha_m$$

In the "hard pyroelectrics" (such as tourmaline, zinc blend, and many others) the part of secondary pyroelectricity usually exceeds the part of primary effect: $\gamma^{(2)} > \gamma^{(1)}$ (see Section 1.3). On the contrary, in the ferroelectrics (that might be called as "soft pyroelectrics") a primary pyroelectric effect dominates: $\gamma^{(1)} > \gamma^{(2)}$. In this case spontaneous polarization decreases as $P_S \sim (\theta - T)^{0.5}$ where θ is Curie-Weiss temperature.

Usually at the free-stress condition the actual piezoelectric is $\gamma_i^{(2)} = 0$ as well as $\gamma_i^{(1)} = 0$, so no pyroelectric response is possible. In the same way, in the case of free-strain condition, one can also see in the piezoelectric no pyroelectric response: $\gamma_i = 0$. However, at the ***partial clamping*** conditions an actual piezoelectric is liable to a "secondary type" of pyroelectric effect because the sum $e_{im}\alpha_m \neq 0$. In the Table 2.1 it is refereed as "artificial pyroelectric effect".

From the 10 classes of actual piezoelectrics, the quartz is the simplest example for explanation of internal polarity nature. Trigonal α-quartz, that belongs to 32 class of symmetry, is electrically active only in the [100]-direction, and the correspondent (100)-plate of quartz is known as a "Curie cut", Fig. 1.3 (*a*). This cut might be prepared perpendicularly to any one of two-fold polar axes: *1*, *1´* or *1˝*. The figure 1.3 (*a*) represents the distribution of intrinsic polar activity in the (001)-plane that is perpendicular to the "antipolar" axis 3 of the quartz crystal.

In the standard crystallographic set up of quartz crystal, the matrix of piezoelectric coefficients e_{im} consists of one longitudinal (e_{11}), one transverse (e_{12}) and three share components of piezoelectric strain modulus (e_{14}, e_{25} and e_{26}):

$$e_{im} = \begin{bmatrix} e_{11} & e_{12} & 0 & e_{14} & 0 & 0 \\ 0 & 0 & 0 & 0 & e_{25} & e_{26} \\ 0 & 0 & 0 & 0 & 0 & 0 \end{bmatrix}$$

The transverse component e_{12} equals to the longitudinal one but has an opposite sign: $e_{12} = -e_{11}$. Only one of share piezoelectric modules (e_{14}) is independent, other share components are $e_{25} = -e_{14}$, and $e_{26} = 2e_{11}$. So the only two components of matrix (2) are independent.

Before proceeding further, let us show that any homogeneous influence (uniform change of temperature or hydrodynamic pressing) cannot induce any electrical response in the plate specimens of quartz taken from a Curie cut, Fig. 1.3 (*a*). First of all, no share strain can be produced in a sample if the external influence is of scalar type. So the only longitudinal or transverse electrical response should be taken into account.

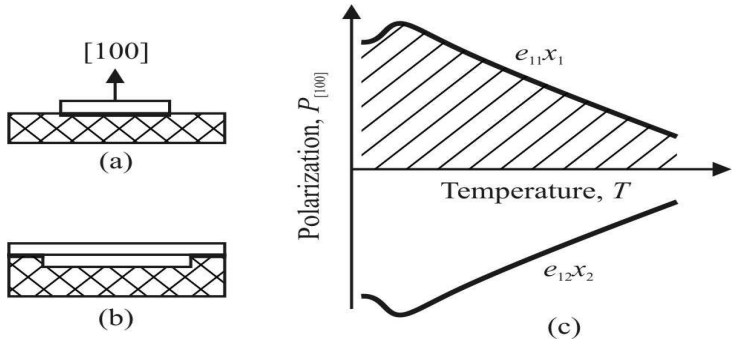

Fig. 2.7. Partially clamped quartz samples: *a* – tangential strain in thin plate is forbidden by its soldering to the substrate; *b* – membrane` variant of clamping; *c* – thermally excited polarization through the piezoelectric effect

That is why, in a stress-free quartz sample of any form, the longitudinal piezoelectric effect (e_{11}) and the transverse one ($e_{12} = -e_{11}$) will compensate each other. This is illustrated in Fig. 2.7 (c), which describes the thermal treatment of a quartz plate: one part of piezoelectric polarization ($e_{11}x_1$) that is mechanically induced by the thermal deformation x_1 equals to the other part ($e_{12}x_2$) but with the opposite sign.

However, so far as rather complicated tensor properties of non-central crystals are discussed, it makes sense to give an additional proof that electrical response in a piezoelectric is compensated in the case of scalar impact. This is shown in Fig. 2.7, *c*. Mechanically induced (by the direct piezoelectric effect) electrical polarization component P_1 is given by

$$P_1 = e_{1m}x_m = e_{11}x_1 + e_{12}x_2 + e_{13}x_3 + e_{14}x_4 + e_{15}x_5 + e_{16}x_6 = e_{11}x_1 + e_{12}x_2.$$

The sum depends on the mechanical boundary conditions of the crystal:

(*i*) In the strain-free crystal (which is totally clamped) the mechanically induced polarization is impossible: $P_1 = 0$ due to $x_m = 0$.

(*ii*) It is essential to demonstrate that in the stress-free quartz crystal the polar response is absent as well ($P_1 = 0$). The point is that in the quartz many components of piezoelectric module are zero: it is seen from the matrix (1) that $e_{13} = e_{15} = e_{16} = 0$. Moreover, in Eq. (3) the shared strain $x_4 = 0$ because any shared strain should be absent if the external action is uniform.

It is important to prove also that in the stress-free quartz crystal the strains x_1 and x_2 in the (100)-plane are equal: $x_1 = x_2$. In fact, in the case of uniform thermal action ($x_m = \alpha_m dT$) these strains are equal due to the parity of the corresponding components of quartz thermal expansion coefficient: $\alpha_1 = \alpha_2$ (however, $\alpha_1 \neq \alpha_3$). In the case of uniform stretching (or expansion), again, the strains $x_1 = x_2$ due to the equality of the corresponding quartz elastic stiffness components: $c_{11} = c_{22}$. The strains can be calculated from the equation $x_m = c_{mn}dp$, where dp is uniform (hydrodynamic) stress.

(*iii*) However, in quartz crystal we have $P_1 \neq 0$ when it is partially clamped, and hence it is this condition that we propose to exploit when internal (latent) polarity of quartz should be examined. Equally, we propose to use partially clamped quartz (and other piezoelectrics) in the temperature and pressure sensors.

Thus, the excitation in the piezoelectric by any homogeneous (be it thermal or elastic) deformation does not lead to polarization, since the piezoelectric contributions from the strains $e_{11}x_1$ and $e_{12}x_2$ to the polarization $P_{[100]}$ compensate each other, Fig. 2.7 (*c*).

The fundamental idea of this work is that an artificial limitation (by the mechanical boundary conditions) of one of mentioned strains (x_1 or x_2) should transform the plate of piezoelectric quartz into the artificially created “pyroelectric”.

Suppose that one of two types of deformations can not be realized in a piezoelectric plate. For example, it is possible to suppress the tangential strain ($x_2 = 0$ and $x_3 = 0$) if the piezoelectric plate is firmly fixed on a massive incompressible substrate with a zero coefficient of thermal expansion, such as fused silica, in which $\alpha \approx 0$, Fig. 2.7 (*a*). In this case, homogeneous heating or cooling (as well as hydrostatic compression) will lead to the appearance of the polar response: $P_{[100]} = e_{11}x_1$. Similarly, the inhibition on the normal strain ($x_1 = 0$) with the possibility of tangential strain would cause the response of the opposite polarity: $P_{[100]} = e_{12}x_2$ but experimental realization of the second case is difficult.

In practice, it is easier to limit the plane strain x_2 if Curie cut plate is soldered onto fused silica. That is why the only thickness strain x_1 can be realized, and just in the direction of polar axis "1" which is transformed from a "neutral polar" axis into a "peculiar" polar axis.

Therefore, a substantial reduction of one type of deformations transforms the piezoelectric into the artificial pyroelectric. This effect is defined as the change of polarization of partially clamped piezoelectric at the uniform change of its temperature. Partial clamping is provided with non-uniform mechanical boundary conditions which limit some thermal strains of the non-central crystal, and it becomes uniformly but anisotropically stressed.

2.4. 2D latent polarity temperature dependence

This artificial thermo-piezoelectric effect is characterized by the coefficient γ^* that is equivalent to the pyroelectric coefficient. It depends on electrical, elastic and thermal properties of the non-central crystal, as well as on the way of its deformation is inhibited:

$$\gamma^* = d_{im}\lambda^*_m, \qquad (2.1)$$

where d_{im} is piezoelectric modulus and λ^*_m is effective thermo-elastic coefficient for a partially clamped crystal.

The spatial distributions of the sensitivity for artificial pyroelectric effect in the crystals of quartz-symmetry, such as berlinite ($AlPO_4$), cinnabar (HgS), tellurium (Te), etc. are similar to quartz. It is possible to discover pyroelectric coefficients in these crystals, even in slanting plates. The spatial distribution of $\gamma^*(\theta,\varphi)$ that characterizes artificial pyroelectric coefficient in the quartz type crystals can be presented in the polar coordinates as: $\gamma^*(\theta,\varphi) = \gamma^*_{max}\sin^3\theta\cdot\cos 3\varphi$, where θ is azimuth angle and φ is plane angle. This spatial pattern is equivalent to longitudinal

piezoelectric modulus distribution that was shown in Fig. 1.3 (*b*). Through the radius vector from the center of that figure it is possible to determine the magnitude of the artificial effect in any cut of the quartz-type crystals. It is obvious that the maxima of the effect occur along any of the three *X*-axes.

A solution of thermodynamic equations of non-centrally symmetric (but not pyroelectric) crystal is used in order to get effective pyroelectric coefficient $\gamma^* = dP_i/dT$. It is assumed that the crystal is short-circuited ($E = 0$), and exact solution is given below:

$$dx_n = s_{nm}\, dX_m + \alpha_m\, dT;$$
$$dP_i = d_{im}\, dX_m \qquad (2.2)$$

where the s_{nm} are the components of elastic compliance tensor. Solving Equations (2.2) for the trigonal crystal class (which includes the quartz crystal) leads to the following expression:

$$\gamma^*_{100} = \frac{d_{11}(\alpha_1 s_{33} - \alpha_3 s_{13})}{s_{11}s_{33} - s_{13}^2}. \qquad (2.3)$$

For the quartz crystal one can obtain $\gamma^*_{100} = 2.6$ μC/m^{2}K, for other crystals of the 32 symmetry class this parameter is larger: $\gamma^*_{100} = 5.7$ μC/m^{2}K for berlinite, 8.7 μC/m^{2}K for cinnabar, and 10 μC/m^{2}K for tellurium crystal. This parameter is not negligible, because the first historically known pyroelectric, tourmaline, has pyroelectric coefficient $\gamma = 4$ μC/m^{2}K, while in the well-studied wurtzite crystal ZnS the usual pyroelectric response is characterized by the $\gamma = 0.3$ μC/m^{2}K.

The artificial pyroelectric effect in the quartz as well as in other piezoelectrics was experimentally investigated using a quasi-static technique, and the pyroelectric coefficient was determined from the time it takes the pyroelectric current to charge a standard capacitor. The corresponding electronics setup, which includes a Peltier heat-cool actuator, was provided for pyroelectric coefficient measurement in the periodical heating-cooling regime. The studied samples were in the form of piezoelectric plates of about 100 μm thickness and area of ~ 1 cm^2 with copper electrodes. These plates were soldered onto quartz glass substrates. Quasi-static conditions were ensured by low-frequency temperature oscillations, so the temperature gradient in the sample did not exceed 2% of the amplitude of temperature oscillation.

Temperature dependence of artificial pyroelectric response of partially clamped in the (100)-plane quartz crystal is shown in Fig. 2.8. Investigation shows

that artificial coefficient γ^*_{100} changes with temperature very slowly while the alteration of some other components of tensors that are present in Eq. (2.3) can be very complicated. In a wide temperature range the artificial "pyroelectric" coefficient is almost constant but there is a tendency of γ^*_1 to decrease at low temperatures, perhaps due to minimum of thermal expansion coefficient.

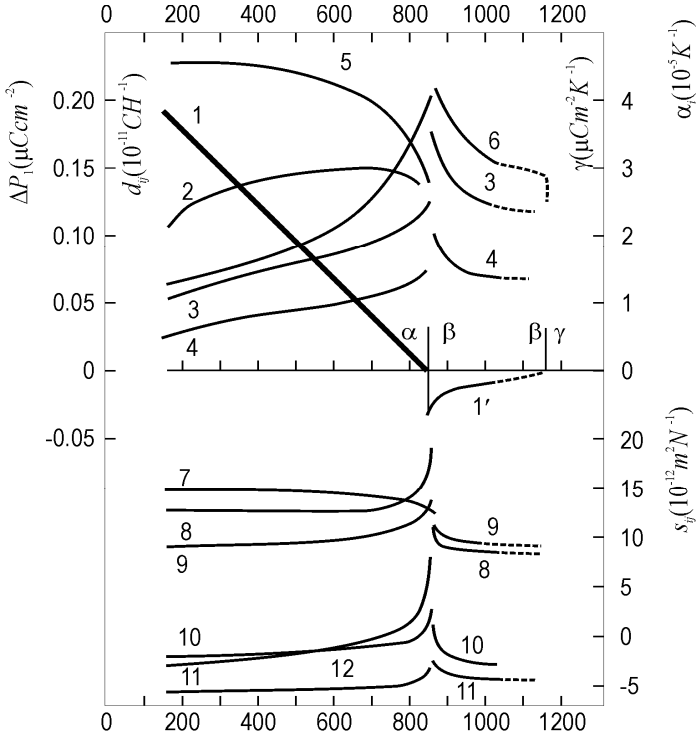

Fig. 2.8. Temperature dependence of latent (hidden) intrinsic polarity for quartz in comparison with other thermal and elastic parameters of this crystal:
1 $-\Delta P_1$ observed in a [100]-cut thin plate of quartz α-phase;
1`– ΔP_1 observed in a [110] oriented rod in high-temperature β-phase of quartz;
2 – artificial pyroelectric coefficient of the clamped [100]-cut of quartz α-phase;
3, 4 – thermal expansion coefficients α_1 (3) и α_3 (4) of quartz crystal;
5, 6 – piezoelectric modulus d_{11} (5) и d_{14} (6) of quartz α-phase;
7-12 – elastic compliance components: $0{,}5 \cdot s_{66}$ (7), s_{11} (8), s_{33} (9), s_{12} (10), s_{13} (11), s_{44} (12)

The most interesting result is that γ^*_1 vanishes in the vicinity of quartz $\alpha \rightarrow \beta$ phase transition at the temperature of $\theta_1 = 846$ K. It is also remarkable that the simplest temperature dependence is observed for the latent polarity component

$P_{[100]} = \Delta P_1$. Calculated from the γ^*_1 component of intrinsic polarization ($\Delta P_1 = \int \gamma^*_1 dT$) decreases with temperature linearly: $\Delta P_1 \sim (\theta - T)$.

The piezoelectrics of quartz symmetry type (SiO_2 and $AlPO_4$) have, in addition to the $\alpha \rightarrow \beta$ phase transition, a second high-temperature transition, and that one is between the β and γ phases. The temperature dependence of the artificial pyroelectric response (Fig. 2.8, curve *1'*) characterises quartz in the β-phase with the temperature dependence of octopole moment M_{ijk}. It is described by another component equation; $P_{13} \sim (\theta_2 - T)^2$ with $\theta_2 = 1143$ K. One can see from Fig. 2.8 (curve *1'*) that that component of octopole moment vanishes at the $\beta \rightarrow \gamma$ transition. The second high-temperature γ-phase of the quartz crystal is non-polar.

It is necessary to note that a study of the volumetric piezoelectric effect would also require a rigid substrate. However, only theoretical estimation on this effect is provided.

2.5. 3D latent polarity temperature dependence

Well known ferroelectrics of KH_2PO_4 (KDP) type in their paraelectric phase belong to the polar-neutral crystals, and at room temperature they are piezoelectrics. Figure 2.9 shows main properties of KDP crystal above its ferroelectric phase transition, where KDP is a piezoelectric of the 422 class of symmetry. In this case the latent polarity corresponds to the octopole model.

For internal polarity investigation in the crystals of the KDP type (or ADP = NH_3PO_4) the standard crystallographic orientation should be changed by turning the axis *1* and *2* around the axis *3* by an angle $\pi/4$. In this case the piezoelectric sample should be prepared as a long rectangular rod extending along one of new axes (*1'* or *2'*), with the electrodes deposited on the sample surface that is perpendicular to the axis *3'* = *3*.

The inhibition on the longitudinal deformation of this rod allows obtaining an artificial pyroelectric response with the following coefficient

$$\gamma^*_3 = \frac{2d_{36}\alpha_1}{2s_{11} + 2s_{12} + s_{66}}. \qquad (2.4)$$

Investigations show that in the paraelectric phase of KDP crystal the artificial pyroelectric coefficient equals $\gamma^*_3 = 6$ $\mu C/m^2K$, while in the ADP crystal $\gamma^*_3 = 15$ $\mu C/m^2K$. It is found that crystals of KDP type in their paraelectric phase also have

(similarly to quartz) a high-temperature phase transition where their polar-neutral 422 group changes its symmetry to the non-polar group, Fig. 2.10.

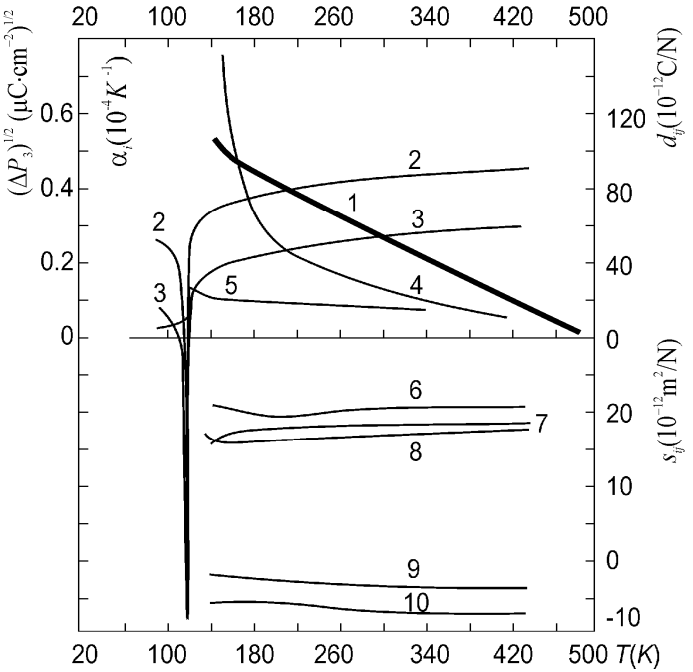

Fig. 2.9. Temperature dependence of latent (hidden) intrinsic polarity of KDP crystal in comparison with other thermal and elastic parameters of this crystal:
1 – ΔP_3 obtained by study KDP rod oriented in [110];
2, 3 – thermal expansion coefficients α_3 (2) and α_1 (3) of KDP crystal;
4, 5 – piezoelectric modulus d_{36} (4) and d_{14} (5) of KDP crystal;
6-12 – elastic compliance components: 0,5·s_{66} (7), s_{11} (8), s_{33} (9), s_{12} (10), s_{13} (11), s_{44} (12)

Microwave measurements show that along with a temperature increase the dielectric constant ε_1 of KDP drops at the temperature of θ = 483 K, while the internal polarity quite gradually vanishes by the law $P \sim (\theta - T)^2$ with the same θ. Respectively, the curve *1* on the Fig. 2.10, which represents the $P^{1/2}$, vanishes by a linear law, curve *2*.

The conception of latent octopole moment can be further applied for many other actual piezoelectrics. For instance, in the crystals of the 23 cubic class of symmetry the polar directions correspond to the 4 threefold axes and the artificial pyroelectric coefficient is given by the equality:

$$\gamma^*_{[111]} = \frac{2\sqrt{3}\alpha d_{14}}{4s_{11} + 8s_{12} + s_{44}}. \qquad (2.5)$$

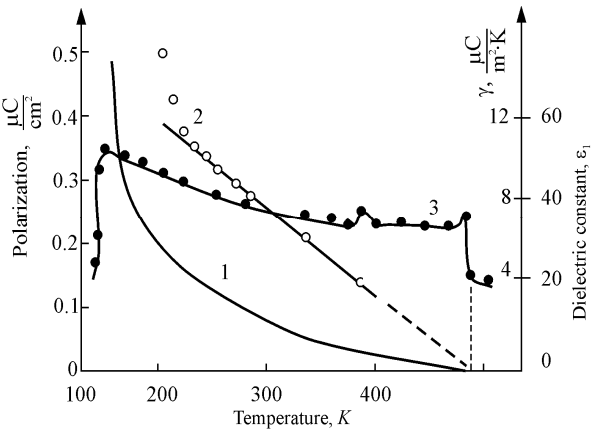

Fig. 2.10. Temperature investigation of partially clamped KDP crystal in the paraelectric phase: *1* – component of octopole moment $|M| \sim (\theta - T)^2$; *2* – artificial pyroelectric coefficient of partially clamped crystal; *3* – dielectric constant ε_1 at frequency 10 GHz

It is interesting to notice that parameter γ^*_{111} is rather large in the case of sillenite type crystals. Some of them, such as $Bi_{12}GeO_{20}$ and $Bi_{12}SiO_{20}$, are widely used in the electronics industry. Artificial coefficient for $Bi_{12}GeO_{20}$ is estimated as $\gamma^* \approx 25$ μC/m^2·K, however, among these classes of piezoelectric crystals it is possible to find artificial pyroelectric coefficients of up to 100 μC/m^2·K.

The most important fact is that the 43*m* (cubic) class is among the actual piezoelectrics, and the III-V semiconductors belong to that class. The dielectric properties of these semiconductors, including their piezoelectric activity, usually were beyond consideration because of the increased conductivity (due to the carrier screening effect). Nevertheless, the screening effect becomes negligible in the *s/i*-GaAs already above the frequency 1 kHz. Moreover, AlGaAs crystal is possible to use as a "dielectric" sensor even at the frequency 20 Hz. That is why, in this work, the charge generation process in the $A^{III}B^{V}$ crystals is ignored, whereas the "charge separation" (that is, the change of electrical polarization) is regarded as a main process.

Correspondingly, the lattice of $A^{III}B^{V}$ semiconductor is considered here as a dielectric, so only the electrical polarization is taken into account. This assumption is close to reality for *s/i*-GaAs and all the more so for its solid solutions with AlAs (all

the more for GaN crystal). Previously, the piezoelectric properties of $A^{III}B^{V}$ crystals have not been used in devices. Nevertheless, any crystal of the $A^{III}B^{V}$ type has a polar structure that might be used to convert the impact of external pressure or temperature into electrical signal (in the same manner as it works for a pyroelectric).

The crystals of the 43m class of point symmetries (such as GaAs) have a maximum of the piezoelectric activity in the direction of [111]-type axes. It should be noted that standard crystallographic representation for crystals of these type is based on the [100], [010] and [001] axes. In this case, the matrix of piezoelectric module has piezoelectric module components of only share type:

$$e_{im} = \begin{bmatrix} 0 & 0 & 0 & e_{14} & 0 & 0 \\ 0 & 0 & 0 & 0 & e_{25} & 0 \\ 0 & 0 & 0 & 0 & 0 & e_{36} \end{bmatrix}. \qquad (2.6)$$

This matrix represents a third rank tensor of the piezoelectric coefficients. In this installation, for the (100), (010) and (001) crystal plates all the longitudinal (e_{11}, e_{22}, e_{33}) as well as the transverse (e_{12}, e_{13}, e_{21}, e_{23}, e_{31}, e_{23}) modules are zero. Therefore, the [100]-oriented plates of $A^{III}B^{V}$ semiconductors, being the ones that are usually used in the industry and in the most experiments, are non-sensitive to any mechanical stress except the shear ones, which correspond to share modules $e_{14} = e_{25} = e_{36}$. It is obvious from the matrix (2.6) that no response is possible if the external influence on crystal is of scalar type.

In other words, being applied to the standard (100)-plates of $A^{III}B^{V}$ crystals, any partial clamping cannot invoke a polar response. Meanwhile, the crystal plates of (100) orientation are conceptually the sole chips being in use in GaAs type devices. It is not improbable that this is the main reason that the mentioned polar effects were out of consideration previously.

Figure 2.11 (*a, b*) shows a special orientation of $A^{III}B^{V}$ crystal that is required to invoke a polar response. The polar cut of $A^{III}B^{V}$ crystal has to be oriented in such a way that the [111]-axis is perpendicular to the plane. This (111)-plate is fixed upon an "ideally hard" substrate. In the case of volumetric piezoelectric effect investigation, the hard steel could be used as a rigid substrate. This excludes any plane component of strain ($x_1 = x_2 = 0$) so only the depth direction electrical response $P_3 = e_{33}x_3$ can be realized. It is obvious that the volumetric piezoelectric effect can be created artificially in such a composite structure.

In a similar fashion, the *s/i*-GaAs (or GaN) crystalline (111)-plate would be activated for the pyroelectric response, if the rigid substrate shown in Fig. 2.11 (*b*) would, in addition, have a thermal expansion coefficient $\alpha \sim 0$ (in our experiments, a fused silica was used).

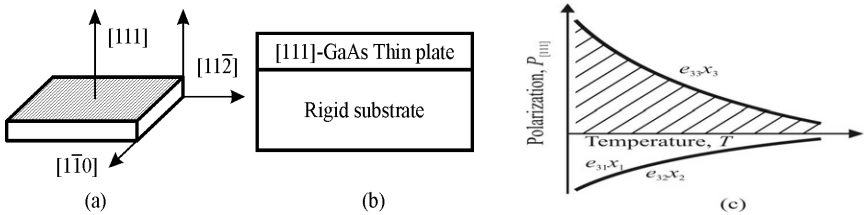

Fig. 2.11. Partial (plane) clamping realization: *a* – experimentally used orientation of *s/i*-GaAs [111]-cut; *b* – thin plate is soldered to rigid substrate, *c* – partial clamping can decompensate internal polarity change

Figure 2.11 (*c*) illustrates secondary pyroelectric effect when polarization is produced by the thermal strain $x_n(T)$ that is transformed to the electrical response through the piezoelectric effect in the cubic crystals of 43m class of point symmetry. One part of polarization ($P_3 = e_{33}x_3$) is induced by the longitudinal piezoelectric effect, while the other part ($P_3 = e_{31}x_1 + e_{32}x_2$) is induced by the transverse piezoelectric effect.

Under conditions of partial clamping it is possible to ensure that the sum $e_{in}\alpha_n \neq 0$. It is this effect that is proposed here to utilize in the sensor devices. The polar properties of some cubic crystals have a strong anisotropy. To obtain the maximum of piezoelectric response in the GaAs type crystal one must use a polar [111]-direction of the crystal. That is why the orientation of crystal should be such as it is shown on Fig. 2.11 (*a*).

In the new (nonstandard) crystallographic orientation, the new axis "*3*" is directed to the [111]-type of axes while another new axis "*1*" should be oriented perpendicularly to the plane passing through the "*3*" axis of a cube. The last new axis "*2*" is predetermined by the rectangular coordinate system. In other words, tested crystal plate should be cut perpendicularly to the [111] direction.

The correspondent matrix of piezoelectric module for the new crystal orientation is given by:

$$e_{im} = \begin{bmatrix} 0 & 0 & 0 & 0 & e_{15} & e_{16} \\ e_{21} & e_{22} & 0 & e_{24} & 0 & 0 \\ e_{31} & e_{32} & e_{33} & 0 & 0 & 0 \end{bmatrix},$$

where $e_{21} = -e_{22}$ and $e_{31} = e_{32} = -0.5\, e_{33}$. It can be seen that polar (111)-cut of GaAs type crystal shows longitudinal piezoelectric effect ($P_3 = e_{33}x_3$) as well as a transverse piezoelectric effect: $P_3 = e_{31}x_1 + e_{32}x_2$.

Of course, no homogeneous influence (i.e., uniform change of temperature or hydrodynamic contraction) can induce an electrical response in a free piezoelectric (111)-plate of the GaAs specimen. First of all, share stress or strain in the (111)-plate cannot be excited, because share components of piezoelectric module are absent in the third line of matrix and external influence is of a scalar type. Therefore, only the longitudinal and the transverse electrical responses should be taken into account.

In a stress-free sample of any form the longitudinal piezoelectric effect (e_{33}) and the two transverse effects (e_{31} and e_{32}) compensate each other: $e_{31} + e_{32} = -e_{33}$. It was illustrated in Fig. 2.11 (*c*), which describes the thermal treatment of GaAs (111)-plate: one component of piezoelectric polarization ($e_{33}x_3$, induced by thermal deformation x_3) equals to the other components ($e_{31}x_1 + e_{32}x_2$) but with the opposite sign (in this case, index "3" corresponds to the [111]-axis). The strain components in a stress-free cubic crystal are equal: $x_1 = x_2 = x_3$ because the excitation is homogeneous. That is why in the non-pyroelectric crystal the sum of transverse and longitudinal piezoelectric coefficients is zero:

$$e_{31} + e_{32} + e_{33} = 0 \qquad (e_{31} = e_{32} = -\frac{1}{2} e_{33}).$$

As a result, piezoelectric effect produced by the longitudinal strain component $x_3 = \alpha dT$ is compensated by the effect of two transverse strain components $x_1 = x_2 = \alpha dT$, therefore no polar response is possible. Consequently, stress-free polar (111)-plate of GaAs type crystals is not sensible to homogeneous excitations.

However, the artificial limitation of any of the mentioned strain components (x_3 or $x_1 + x_2$) should transform the piezoelectric (111)-plate of GaAs type crystal into an artificially created "pyroelectric". In practice, it is easier to limit the plane strain ($x_1 + x_2$) by a simple mechanical design. In this case, only the thickness strain x_3 can

be excited, and just in the direction of the polar axis "*3*" ([111]-direction) which is transformed into a "particular" polar axis.

New effects are impossible neither in the stress-free nor in the free-strain crystals, as both artificial effects are result of non-isotropic partial clamping. Only a partially clamped piezoelectric crystal manifests artificial pyroelectricity or volumetric piezoelectric effect.

Figure 2.12 shows temperature dependence of latent polarity components P_{111} for GaAs and GaP in comparison with quartz internal polarity component $P_{[100]}$.

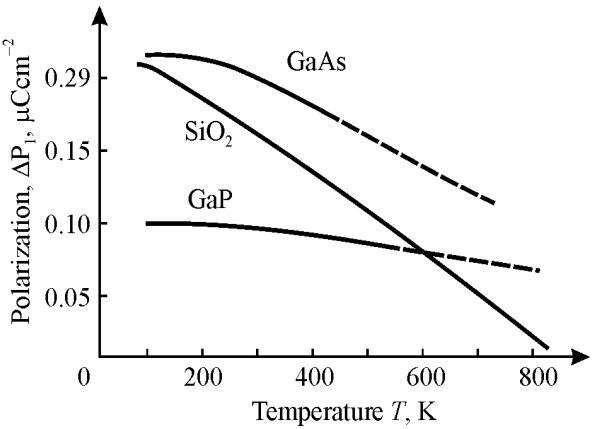

Fig. 2.12. Temperature dependencies of the dipole component ΔP_{111} for GaAs and GaP crystals, in comparison to the ΔP_{100} of SiO_2 (α-quartz) crystal

For all studied piezoelectrics the internal (latent) polarization decreases while the temperature is increased. In the quartz crystal this polarity vanishes at the temperature of $\alpha \rightarrow \beta$ transition. In is supposed that for $A^{III}B^{V}$ crystals the P_{111} latent polarity also vanishes but at the melting temperature. It is obvious that in the melt condition no firm polar bolding can be settled. However, while crystallisation, $A^{III}B^{V}$ crystals are widened due to polar bonds formation, while the density of crystal is less than the density of melt. While forming, the polar bonds swell up the crystal structure.

2.6. Possible applications of artificial pyroelectricity

To summarize, artificial pyroelectricity extends the possibility to obtain electrical response from external mechanical or thermal influence. To explain in more detail the "artificial" type of pyroelectric response in the piezoelectrics, it is

convenient to compare the new effect with "classic" pyroelectric response of pyroelectric and ferroelectric crystals, Fig. 2.13.

Following the generally accepted theory of pyroelectricity, the concept of spontaneous polarization P_S temperature change is usually used, Fig. 2.13 (*a*). Due to the thermal expansion and to the thermal disordering of polar structure the spontaneous polarization of a "hard pyroelectric" slowly decreases with the temperature. At the same time, the corresponding pyroelectric coefficient γ gradually increases with the growth of temperature.

In ferroelectrics (so-called "soft pyroelectrics") the spontaneous polarization decreases by the law $P_S \sim (\theta - T)^{0.5}$, where θ is the Curie-Weiss temperature and power "0.5" is Landau critical index, Fig. 2.13 (*b*). The pyroelectric coefficient γ sharply increases near the phase transition temperature θ, which is widely used in the pyroelecric sensors.

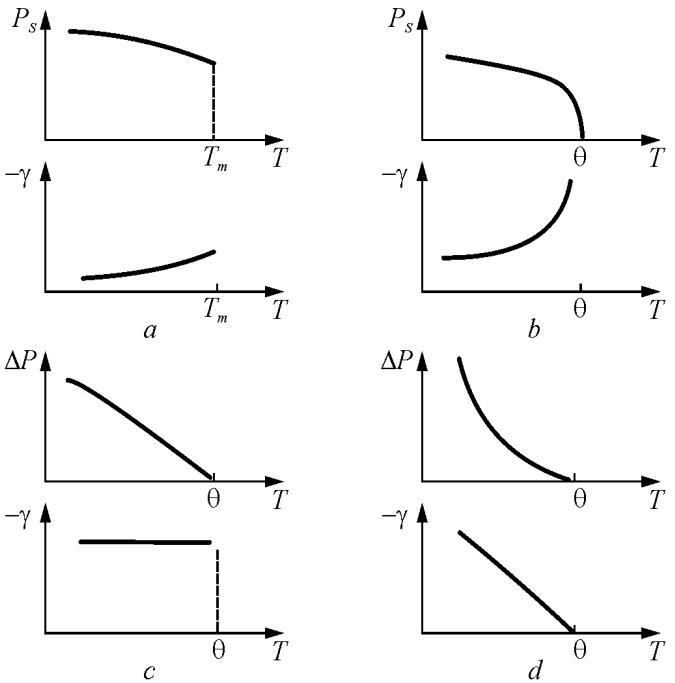

Fig. 2.13. Comparison of temperature dependence of pyroelectric polarization P_s and its derivative dP_s/dt that is the pyroelectric coefficient γ for various polar crystals: *a* – "hard pyroelectric"; *b* – ferroelectric; *c* – piezoelectric with 2D internal polarity; *d* – piezoelectric with 3D polarity

In the actual (polar-neutral) piezoelectric with 2D arranged polarity one can see a linear law of polarity temperature dependence: $\Delta P \sim (\theta - T)$, so critical index equals to "1", while pyroelectric coefficient γ is approximately constant. By the way, such a linear dependence of spontaneous polarization is typical for improper ferroelectrics as well, in which the strain is the ordering parameter. At last, the actual piezoelectric with 3D latent polarity demonstrates a decrease in both parameters ΔP and γ with temperature increase, with the critical index "2", Fig. 2.13 (*d*).

Among artificially created pyroelectrics there are semiconductors of $A^{III}B^{V}$ type, and this fact is possible to exploit, in order to combine in one crystal the pyroelectric sensors (or volumetric piezoelectric sensors) with the amplifiers and the read-out electronics.

Conclusions to part 2

An original opinion is proposed as to the physical nature of mechano-electrical response in the non central symmetric crystals. All of them are polar crystals, but their complicated polar structure is electrically non-compensated in the pyroelectrics (including ferroelectrics), yet, it is totally self-compensated in the actual piezoelectrics (if they are stress-free).

Uniform but non-isotropic partial clamping of the actual piezoelectric crystal can destroy its self-compensation, and allows obtain in these piezoelectrics an effective electrical response on any scalar influence. Such electrical response would be explained as a "dipole projection" of self-compensated internal polarity that is broken by partial clamping.

In the examined piezoelectrics it is shown that the temperature dependence of the high rank polar moment components M_{ijk} reminds the temperature decrease of spontaneous polarization of ferroelectrics $P_S(T)$. In particular, multiple components of $M(T)$ show a decay at phase transition temperature θ that follows a critical law $(\theta - T)^n$. It is shown that the exponent $n = 2$ if the multiple moment is represented by the 3D octopole, while $n = 1$ in the case of 2D sextuple; unlike the Landau critical index $n \approx 0.5$ that is specific for 1D spontaneous polarization.

3. Some theoretical aspects of polar crystals

Piezoelectricity is a scientific and technical direction of research, lying in the intersection of two classical research areas: first, the mechanics of solid deformable body and, second, the electrodynamics of continuous media.

The linear theory of elasticity, as a mathematical model of that describes the influence of external mechanical force (stress, X) on the solid's deformation (strain, x), was developed in the XIX century by Cauchy, Poisson and Green.

The differential equations of electrodynamics establish a link between the vectors of electrical field **E**, electrical induction **D**, magnetic field **H** and magnetic induction **B**. It is considered that any speeds are much lower than the speed of light in the dielectric. In this case, the magnetic effects can be ignored, and instead of electrodynamics equations the electrostatic case is applied, in which the vector fields satisfy the properties *rot* $\mathbf{E} = 0$ and *div* $\mathbf{D} = 0$. Based on this theory, piezoelectrics were described in the Section 1.1.

The connection between the electrical and the mechanical effects was described in a mathematical form by German scientist Voigt, who established the main piezoelectric quantitative relationships (in the years 1910-1920). Voigt developed a complete system of relations which summarized the accumulated knowledge of piezoelectricity in the previous period.

In the sequel, only homogeneous mechanical deformation and homogeneous electrical field will be described. For inhomogeneous deformations (except piezoelectric and electrostriction effects) there are others electromechanical phenomena, such as flexoelectricity (which is very important for liquid crystals). Under the influence of a temperature gradient the piezoelectric tertiary pyroelectric effect (actinoelectricity) occurs. However, the theories of flexoelectricity and actinoelectricity are not considered here.

3.1. Polar crystals dielectric properties

The most of polar crystals are dielectrics. Electrical charges in the dielectric structure are strongly constrained, so in the dielectrics the concentration of free charge carriers (causing electrical conductivity) are usually very small. In this regard, we assume (with some exceptions) that the conductivity is absent: $\sigma = 0$. Thus, the main property of dielectrics is a polarization that is usually induced by the applied external field. However, in the piezoelectrics polarization can be caused by the

mechanical impact, while in ferroelectrics and pyroelectrics the polarization can exist spontaneously, due to the intra-crystalline electrical non-symmetry.

Polarization that appears under the influence of an external electrical field is produced by electrical charge displacement from their equilibrium position, resulting in the induced electrical moment:

$$\mathbf{M} = \sum_{i=1}^{N} q_i x_i ,$$

where N is the number of charged particles in dielectric; q_i is electrical charge of i-th particle; $\boldsymbol{x}_i$ is charged particle displacement from the equilibrium position under the influence of electrical field. The unit of measurement for the electrical moment is the Coulomb-meter: [M] = C·m. The apparent density of the electrical moment is called polarization: $\mathbf{P} = \mathbf{M}/V$, where V is volume of polarized dielectric. The unit of measurement for polarization is: [P] = C/m^2, which corresponds to another definition of polarization as the density of the bound surface charge on the metallic electrode deposited onto polarized dielectric.

Polarization induced by electrical field E is:

$$P = \varepsilon_0 \chi E,$$

where χ is dielectric susceptibility (dimensionless parameter). For vacuum $\chi = 0$, for most dielectrics χ = 0,5...10, but in paraelectrics and ferroelectrics the dielectric susceptibility may be very large: $\chi = 10^2...10^5$. Parameter $\varepsilon_0 = 8{,}854 \cdot 10^{-12}$ F/m is called as electrical constant, which in the SI system has the dimensions of the ratio between P and E.

Besides polarization vector, to describe polarization an electrical induction vector D is introduced:

$$\mathbf{D} = \varepsilon_0 \mathbf{E} + \mathbf{P}.$$

Induction is defined in the same units as the polarization: [D] = C/m^2 and it is also characterized by a surface density of electrical charge on the metal electrodes. If the metallised insulator is considered as an electrical capacitor, then the induction describes the charge on the plates of this capacitor: $D = \rho_t$, while polarization P characterizes only the part of the total charge charges located at electrode: $P = \rho_t (1 - \varepsilon^{-1})$, Fig. 3.1.

Permittivity ε is introduced as the factor of proportionality between electrical induction and field intensity:

$$D = \varepsilon \varepsilon_0 E.$$

Dimensionless parameter ε is a relative permittivity that is connected with the susceptibility χ by a simple relation: $\varepsilon = 1 + \chi$.

The electrical field *E*, polarization *P* and electrical induction *D* are vectors. These vectors in the ordinary isotropic dielectrics are collinear. In most of polar dielectrics (that are anisotropic) the directions of vectors *D, E* and *P* are different, Fig. 3.1 (e), according to above written vectorial relation.

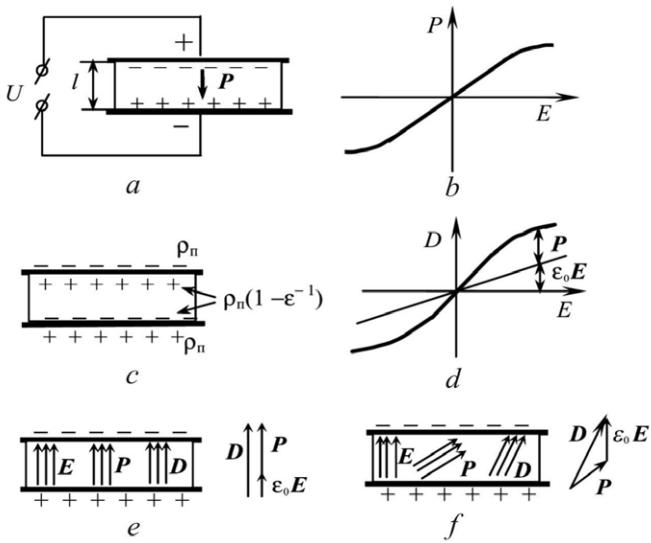

Fig. 3.1. Macroscopic description of the electrical polarization

Polar vectors **D, E** and **P** may be presented without the bold symbol of the vector, but with the lower subscripts *i, j* = 1, 2, 3. Converting one vector to another, it is possible to write, for example:

$$D_i = \varepsilon_0 \varepsilon_{ij} E_j.$$

Accordingly, it is possible to write polarization as $P_i = \varepsilon_0 \chi_{ij} E_j$. So for anisotropic media the first rank *power tensor* (vector) is denoted with one index: D_i or E_j. In the case of second rank *material tensor* two indexes should be used: ε_{ij} or χ_{ij}. One of these indexes is derived from the vectorial impact (in this case, the E_j), while the second is the vectorial response (D_i), whose direction does not always correspond to the direction of the impact, Fig. 3.1. Parameters ε_{ij} or χ_{ij} can be represented as a diagonally symmetrical matrix:

$$\varepsilon_{mn} = \begin{bmatrix} \varepsilon_{11} & \varepsilon_{12} & \varepsilon_{13} \\ \varepsilon_{21} & \varepsilon_{22} & \varepsilon_{23} \\ \varepsilon_{31} & \varepsilon_{32} & \varepsilon_{33} \end{bmatrix}.$$

In the isotropic dielectric only ε_{11}, ε_{22} і ε_{33} are nonzero and equal, so the permittivity can be written as a scalar quantity: $\varepsilon_{ij} = \varepsilon$. However, in the anisotropic dielectric the main (diagonal) components of the permittivity matrix can be represented by the ellipsoid. So permittivity of the anisotropic dielectric is not a definite number: it depends on the direction chosen in crystal:

$$\frac{x^2}{\varepsilon_{11}} + \frac{y^2}{\varepsilon_{22}} + \frac{z^2}{\varepsilon_{33}} = 1.$$

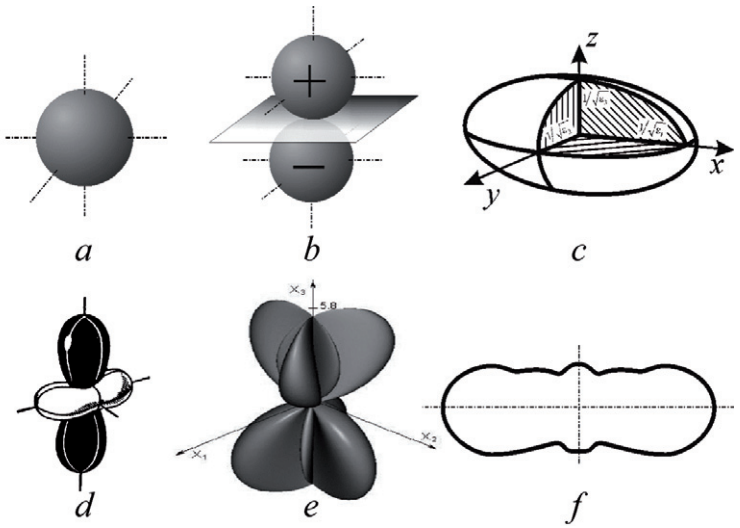

Fig. 3.2. Images for material tensors of different ranks: *a* – zero rank (scalar); *b* – first rank (pyroelectric coefficient), *c* – second rank (dielectric constant); *d* – second rank (coefficient of thermal expansion), *e* – third rank (piezoelectric module), *f* – projection of fourth rank tensor (elastic compliance)

The dielectric ellipsoid is shown in Fig. 3.2 (*c*), among the representations of the other material tensors, having different ranks. In the case of isotropic dielectrics $\varepsilon_{11} = \varepsilon_{22} = \varepsilon_{33}$, and the dielectric ellipsoid becomes a sphere, Fig. 3.2 (*a*). For the tetragonal, hexagonal and trigonal crystals, as well as for polarized ferroelectric ceramics two components are equal $\varepsilon_{11} = \varepsilon_{22}$, but they differ from ε_{33}, and the

dielectric ellipsoid becomes an ellipsoid of rotation.

Thus, the permittivity of anisotropic polar dielectrics is not a constant, but it is characterized by a certain surface in the space, namely – by the dielectric ellipsoid.

3.2. Mechanical properties of polar crystals

Stress tensor. The concept of mechanical stresses for structures of different dimensions is illustrated in Fig. 3.3.

First consider the one-dimensional structure. In Fig. 3.3 (*a*) a long homogeneous elastic rod (one-dimensional crystal) is shown that is subjected to the mechanical stress. Mechanical stress is not a single vector, it is denoted by a pair of vectors equal in magnitude and opposite in direction. So a mechanical stress (in contrast to a mechanical force, which is a vector, denoted **F**, with measurement unit $[F] = \mathrm{N}$) does not induce mechanical motion, so the stressed rod remains stationary. Stress tends to stretch the rod ($X > 0$), or to compress it ($X < 0$), and the unit of measurement of one-dimensional stress is $[X] = \mathrm{N/m^2}$.

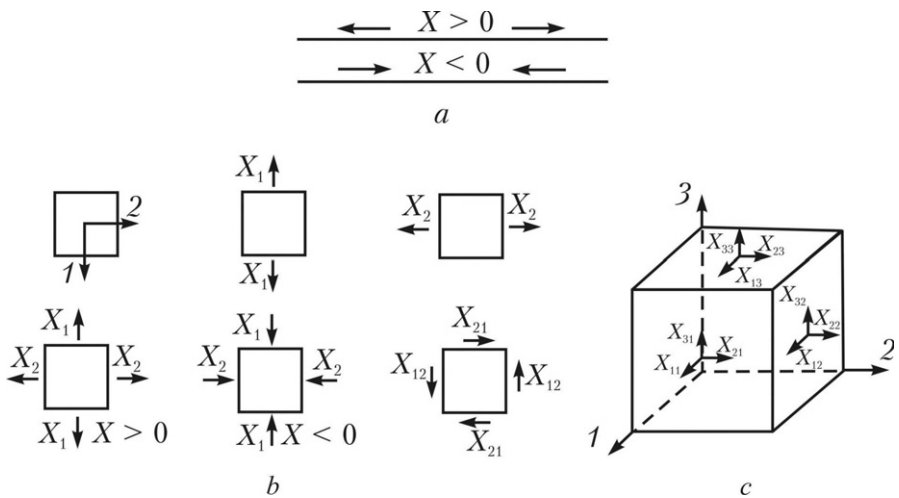

Fig. 3.3. Homogeneous mechanical stresses in the solids: *a* – one-dimensional model, *b* – two-dimensional model, *c* – three-dimensional model

For the two-dimensional crystal model the stretching-compression stresses are shown in Fig. 3.3 (*b*) along two perpendicular axes (X_1 and X_2). In addition, the shear stress, X_{12} and X_{21}, can be applied to the crystal. From the equilibrium conditions (assuming no displacement and rotation of the crystal) it is necessary that $X_{12} = X_{21}$.

In the three-dimensional crystals, Fig. 3.3 (*c*), mechanical stress is defined as the force applied to a unit area, and therefore it has the dimension $[X] = \mathrm{N/m^2} = \mathrm{Pa}$ (Pascal). The components of stresses (forces acting on the opposite faces of the cube) compensate each other. The normal components of the mechanical stress are denoted by the indexes: X_{11}, X_{22}, X_{33}, indicating the forces acting along the directions orthogonal to the surface faces of the cube. It is obvious that the opposite faces are under the influence of the forces of same magnitude and opposite directions, though this is not explicitly reflected in Fig. 3.3 (*c*). In addition to normal stresses directed along the normal to the edge, the shear stresses may also exist, directed tangentially to the faces of the cube under consideration. They are X_{13} and X_{23} on the top face of the cube, Fig. 3.3 (*c*), while X_{31} and X_{21} components correspond to the front face, and X_{12} and X_{32} to the right face of the cube. These tensions are also balanced to avoid any torque moment.

The above components of the mechanical stress form a second rank tensor. Since the shear stress does not create mechanical moment ($X_{ij} = X_{ji}$), the matrix of the stress tensor is symmetric

$$Xij = \begin{bmatrix} X_{11} & X_{12} & X_{13} \\ X_{21} & X_{22} & X_{23} \\ X_{31} & X_{32} & X_{33} \end{bmatrix}.$$

This tensor is characterized by a surface of the second order:

$$X_{11}\, x^2 + X_{22}\, y^2 + X_{33}\, z^2 = 1,$$

where X_{11}, X_{22} and X_{33} are matrix components reduced to a diagonal form. However, depending on the sign of X_{ij} this surface can be not only an ellipsoid, but also imaginary ellipsoid or hyperboloid, while the characteristic surface of permittivity material tensors (ε_{ij}) is always ellipsoid.

Strain tensor. Mechanical deformation (strain) appears in the crystal under the influence of mechanical stress. First consider as an example the one- dimensional model (Fig. 3.4). On the elastic rod the segment OA with the length a should be selected, as well as a small segment AB of length Δa. When the rod is subjected to the stretching, it is uniformly extended, and segment OA becomes longer: $a + u$, while the length of segment AB increases by Δu. Relative deformation at any part of the rod is defined as the limit:

$$x = \lim\left(\frac{\Delta u}{\Delta a}\right) = \frac{du}{da}; \Delta a \to 0.$$

Thus, the strain is a dimensionless parameter. In some crystals the strain under the large stress (up to mechanical destruction of the crystal) can reach the values $x \sim 10^{-2}$. In polar crystals under applied high electrical field (which grows up to electrical breakdown) the deformation can reach values of $x \sim 10^{-3}\ldots10^{-4}$.

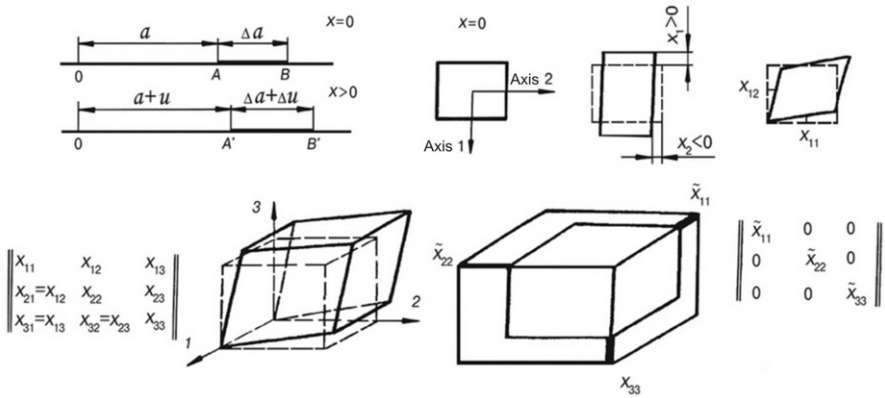

Fig. 3.4. Homogeneous mechanical deformation in a solid: one-dimensional, two-dimensional and three-dimensional models

In the one-dimensional model of a linear deformation the strain can be either of stretching type ($x > 0$) or compression type ($x < 0$). In the two-dimensional model it is assumed that the deformation of the film is uniform across its plane. This means that after deformation straight lines remain straight (not bent), and parallel lines remain parallel: they are equally lengthened (or shortened). In the 2D (planar) model, in addition to the linear strain (x_1 and x_2) it is possible to get angular deformation: x_{12} and x_{21}. It can be shown that the components of strain tensor form a second rank tensort x_{ij}, where $i, j = 1, 2$. The matrix of this tensor

$$x_{ij} = \begin{bmatrix} x_{11} & x_{12} \\ x_{21} & x_{22} \end{bmatrix}$$

is symmetrical relatively to the main diagonal: $x_{12} = x_{21}$. The symmetric matrix components determine the shear strain, while the components x_{11} and x_{22} are the strains of stretching-compression type.

In the general 3D case the deformation is three-dimensional (Fig. 3.4). The strain tensor x_{ij}, as well as mechanical stress tensor, is symmetric with respect to the

main diagonal of the corresponding matrix. The diagonal components of this tensor x_{ij} ($i = j$) have the meaning of tension-compression strains, while the non-diagonal components characterize the different shear strains. Similarly to the stress tensor, strain tensor can be represented by the surface of the second order:

$$x_{11}x^2 + x_{22}y^2 + x_{33}z^2 = 1,$$

that for positive coefficients x_{mm} is ellipsoid.

Elastic stiffness and elastic compliance. The applied external mechanical stresses X inversely change the size and the shape of the crystal, i.e. produce crystal strains. In the case of relatively small deformation a linear relationship holds:

$$x = sX,$$

where s is elastic compliance. This relationship is called the Hooke's law: deformation x increases (or decreases) in the direct proportion to the applied mechanical stress X. The changes in strain and stress are mutually conditioned, so the Hooke's law can be written as

$$X = cx,$$

where c is elastic stiffness, also known as Young's modulus. Since the strain is dimensionless and the unit of mechanical stress measurement is N/m^2, the same unit is assigned to the elastic stiffness: $[c] = N/m^2 = Pa$ (Pascal). The unit of the elastic compliance is determined as $[s] = Pa^{-1}$. Because of the practical smallness of the unit "Pascal", often “gigapascal”, that is 10^9 Pa, is used.

As x_{ij} and X_{ij} are the tensors of the second rank, in the anisotropic crystals it can be expected that each of the nine components of strain x_{ij} can be induced by nine stress tensor components X_{kp}:

$$X_{ij} = s_{ijkp}X_{kp}.$$

This short tensor representation implies nine equations in which the right hand side has nine elements. Obviously, the elastic compliance and the elastic stiffness are fourth rank tensors, each of them might have $3^4 = 81$ components. In fact, the number of independent components of these tensors is much smaller, because stress tensor and strain tensor are symmetrical ones. So they can contain (even in the most general case) not nine but six independent components. Accordingly, the tensor s_{ijkp} and the tensor c_{ijkp} are symmetrical ones for the first two and last two indices:

$$s_{ijkp} = s_{kpij} = s_{ijpk} = s_{ijpk}$$

Consequently, these tensors contain no more than 36 independent components. In turn, these 36 tensor components are also symmetric with respect to the diagonal of

the corresponding matrix. Thus, each crystal, including those that have the lowest category of symmetry, can not contain more than 21 independent tensor components of elastic compliance or elastic stiffness.

To reduce the number of indexes, the stiffness tensor (as well as the compliance tensor) is expressed not as a 4-th rank tensor s_{ijkp} (where $i, j, k, p = 1, 2, 3$) but as a matrix s_{mn}, where $m, n = 1, 2, ..., 6$.

Knowing all components of a tensor, such as the elastic stiffness tensor, it is possible to calculate the inverse tensor components, in a given case, the compliance tensor components from the elastic tensor components:

$$s_{mn} = \frac{(-1)^{m+n} \Delta c_{mn}}{|c_{mn}|},$$

where $|c_{mn}|$ is matrix determinant, Δc_{mn} is a minor of the matrix with n-row and m-column.

The density of elastic energy W of the strained crystal can be determined from the expression for the amount of mechanical work done by stress X for the deformation x: $dW = Xdx$. By integrating of this expression, it is possible to obtain:

$$W = -\frac{1}{2} xX.$$

Depending on the task and using the Hooke's law in two forms: $x = sX$ or $X = cx$, two equitable equations exist for the density of mechanical energy:

$$W_M = \frac{1}{2} cx^2 = \frac{1}{2} sX^2.$$

3.3. Electromechanical coupling in the polar crystals

Piezoelectric is a converter of energy: during the direct effect the mechanical (elastic) energy is converted into the electrical energy, and during the reverse effect the electrical energy is converted into the mechanical one. Therefore, the elastic and electrical properties of piezoelectric should be considered together, because any change in polar crystal electrical condition leads to changes in its mechanical condition, and vice versa.

The relationship of electrical and mechanical properties of the non-centrally symmetric crystals and textures (that exhibit piezoelectricity) is characterized by the electromechanical coupling coefficient K_{coup}. This is one of the most important parameters not only for piezoelectric materials, but also for piezoelectric devices.

Electromechanical coupling coefficient is defined in different ways. Essentially, the square of electromechanical coupling factor shows the proportion of the energy that is brought to the piezoelectric (W_{br}) that is converted into another type of energy (W_{conv}):

$$K_{coup}^2 = \frac{W_{conv}}{W_{br}}.$$

Definition of the K_{coup} resembles the definition of the efficiency coefficient; however, the energy loss in this expression is not included: electrical conductivity, mechanical damping and dielectric losses are neglected when determining of K_{coup}.

In the case of direct piezoelectric effect the crystal receives the mechanical energy that is spent not only on the elastic deformation (leading to the accumulation of the elastic energy W_{elas}) but also on the creation of electrical polarization, which causes the accumulation of the electrical energy W_{elec}:

$$K_{coup}^2 = \frac{W_{elec}}{W_{br}} = \frac{W_{elec}}{W_{elas} + W_{elec}}.$$

In the case of inverse piezoelectric elect (as well as for electrostriction) the formula for the coupling coefficient is different:

$$K_{coup}^2 = \frac{W_{elas}}{W_{br}} = \frac{W_{elas}}{W_{elas} + W_{elec}}.$$

In this case the electrical energy given to the crystal is spent not only on the electrical polarization, but also on the elastic deformation of piezoelectric. Difference between above coerced relations does not mean that K^2_{coup} for the direct and reverse piezoelectric effects add to one, as during the calculation of the energies different boundary conditions should be taken into account (the crystal can be free or clamped, short-circuited or disconnected).

Elastic energy can be defined as a quadratic form of the strain x or mechanical stress X – according to various choices of the parameters characterizing the elastic process:

$$W_{elas} = \frac{1}{2} xX = \frac{1}{2} cx^2 = \frac{1}{2} sX^2,$$

where c is elastic stiffness, s is elastic compliance (tensor inverse to c).

Similarly, the energy of the electrical polarization in the field E is expressed through the induction D and the dielectric constant ε, or via inverse to the ε tensor β:

$$W_{\text{elec}} = \frac{1}{2} ED = \frac{1}{2} \varepsilon_0 \varepsilon E^2 = \frac{1}{2} \left(\frac{\varepsilon_0}{\beta} \right) D^2.$$

For mixed elastic-to-electrical processes the contribution to energies W_{elas} and W_{elec} can also be expressed in other relationships. In addition to these relations, the electromechanical coupling coefficient is defined as the ratio of the density of electromechanical energy to the geometric mean of the density of the elastic and electrical energy:

$$K_{\text{coup}}^2 = \frac{W_{\text{em}}^2}{W_{\text{elas}} W_{\text{elec}}}.$$

In the case of the mechanically clamped (not deformed) piezoelectric, the density of electromechanical energy is $W_{\text{em}} = d \cdot X \cdot E$, and for the mechanically free piezoelectric $W_{\text{em}} = e \cdot h \cdot E$, where d and e are correspondent modules: $d = P/X$ and $e = P/x$. (Tensorial indices at the components of modules are neglected here to simplify the record of relationships).

Developers and researchers of piezoelectric and electrostrictive materials as well as designers of piezoelectric devices (surface acoustic wave devices, delay lines, filters, convolver-type signal converters etc.) sometimes, to determine K_{coup} use the change in the velocity of elastic waves in the piezoelectric:

$$K_{\text{coup}}^2 = \frac{2\Delta\upsilon}{\upsilon_0} + \left(\frac{\Delta\upsilon}{\upsilon_0} \right)^2,$$

where υ_0 is elastic waves velocity without piezoelectric effect, and $\Delta\upsilon$ is a change of speed obtained due to the electromechanical coupling.

Although K_{coup} is a scalar parameter, this coefficient depends on the direction of external influences and other causes. For example, polarized ferroelectric ceramics (that is a texture of $\infty \cdot m$ symmetry) can be identified by 12 different coupling coefficients depending on system boundary conditions (for many forms of piezoelectric sample), as well as on the manner of clamping and fixing. Numerical values of K_{coup} are determined by piezoelectric material properties. Most crystals and textures used in practice have $K_{\text{coup}} = 0.1 \ldots 0.5$, although in some crystals and for particular orientation the parameter K_{coup} reaches value of 0.8 ... 0.95.

It is possible to give some examples of K_{coup} depending on the orientation of piezoelectric sample. For polarized in the depth (anti-plane) direction piezoelectric plate shown in Fig. 1.1 (*a*) the transversal electromechanical coupling coefficient is

$$k_{31} = d_{31}(\varepsilon_{33} s_{11})^{-1/2}.$$

In the case of shear strain, Fig. 1.1 (*b*) for the same plate coupling coefficient is

$$k_{15} = d_{15}\left(\frac{\varepsilon_{11}}{s_{44}}\right)^{-1/2}.$$

Anti-plane polarized piezoelectric disk with radial deformations, shown in Fig. 1.1 (*c*) has coupling coefficient

$$k_p = k_{31}\left(\frac{2}{1-\sigma}\right)^{1/2},$$

where σ is Poisson's ratio: $\sigma = -s_{12}/s_{11}$. For the thickness vibrations of the same disk

$$k_t = h_{33}\left(\frac{\varepsilon_{33}}{c_{11}}\right)^{-1/2}.$$

3.4. Thermodynamic description of the piezoelectric effect

In thermodynamic theories (as opposed to microscopic theories) the atomic structure of material is not taken into account but the material is regarded as a continuum that has certain properties. In the case of piezoelectricity this continuum is anisotropic, as its electrical, thermal and elastic properties depend on the direction of the applied forces and fields.

***Thermodynamic potentials*.**

It is assumed that the thermal, elastic and electrical properties of piezoelectricity can be described by the six parameters: two thermal properties (T – temperature, S – entropy), two mechanical properties (X – stress, x – strain) and two electrical properties (E – electrical field, D – electrical induction).

If the dielectric gets a small amount of heat dQ, the change in its internal energy dU, according to the first principle of thermodynamics, is described by the expression:

$$dU = dQ + dW = dQ + Xdx + EdD, \qquad (3.1)$$

where dW is the work carried out by electrical (EdD) and mechanical (Xdx) forces. As the only reversible processes are considered (this includes both electrical polarization and mechanical strain), we have that $dQ = TdS$ – in accordance with the second principle of thermodynamics. As a result, the change in the internal energy (3.1) can be represented as a function of the six basic parameters of the dielectric:

$$dU = TdS + Xdx + EdD, \qquad (3.2)$$

where selected basic parameters are S, x and D. The remaining parameters (T, X and E) are defined as derivatives of the internal energy U on the entropy S, strain x and electrical induction D. During the differentiation, one parameter is assumed independent of the other two parameters denoted by the corresponding indexes:

$$\begin{aligned} T &= (\partial U/\partial S)_{x,D}; \\ X_n &= (\partial U/\partial x_n)_{S,D}; \\ E_i &= (\partial U/\partial D_i)_{S,x}. \end{aligned} \tag{3.3}$$

These ratios in the brief form are three equations of condition: thermal, elastic and dielectric. In Section 1.3 a variety of boundary conditions were discussed: electrical, mechanical and thermal. Correspondingly, of the three pairs of related parameters: $T - S$, $X - x$ and $D - E$ three independent parameters can be chosen, obviously, in eight different ways. The objectives of different boundary conditions describing thermal, elastic and electrical properties of polar crystals determine the choice of eight different thermodynamic functions (potentials), which can be used to express the basic equation of piezoelectricity. Equation (3.3), given earlier, is just one of them:

$$\begin{aligned} dU &= TdS + Xdx + EdD; \\ dH &= TdS - xdX - DdE; \\ dH_1 &= TdS - xdX + EdD; \\ dH_2 &= TdS + Xdx - DdE; \\ dA &= -SdT + Xdx + EdD; \\ dG &= -SdT - xdX - DdE; \\ dG_1 &= -SdT - xdX + EdD; \\ dG_2 &= -SdT + Xdx - DdE, \end{aligned} \tag{3.4}$$

where H – enthalpy, H_1 – elastic enthalpy, H_2 – electrical enthalpy, A – Helmholtz free energy; G – Gibbs free energy, G_1 – elastic Gibbs energy, G_2 – electrical Gibbs energy. The indexes of the vector and tensor parameters are omitted for simplicity.

From the equation (3.2) three equations were obtained (3.3). After increasing the number of thermodynamic functions to eight, the number of equations also increases. For example, suppose that the independent variables are selected to be the electrical induction D, strain x and temperature T; then as the thermodynamic potential one should select the Helmholtz free energy, and the equation of condition of the dielectric differs from the equations (3.3):

$$-S = (\partial A/\partial T)_{x,D};$$
$$X_m = (\partial A/\partial x_m)_{T,D};$$
$$E_i = (\partial A/\partial D_i)_{T,x}.$$

The equation of condition can be written as linear differentials of the independent variables:

$$\begin{aligned} dS &= (\partial S/\partial T)_{D,x}\, dT + (\partial S/\partial x_m)_{D,T}\, dx_m + (\partial S/\partial D_i)_{x,T}\, dD_i; \\ dX_n &= (\partial X_n/\partial T)_{D,x}\, dT + (\partial X_n/\partial x_m)_{D,T}\, dx_m + (\partial X_n/\partial D_i)_{x,T}\, dD_i; \\ dE_j &= (dE_j/\partial T)_{D,x}\, dT + (dE_j/\partial x_m)_{D,T}\, dx_m + (dE_j/\partial D_i)_{x,T}\, dD_i. \end{aligned} \qquad (3.5)$$

As the number of potentials is eight, then the total number of such equations is 24. The coefficients in these equations are the generalized condition of compliance – they define relationships between the various fields (electrical, mechanical and thermal). The most important coefficients are mentioned earlier, where we give a generic description of piezoelectrics, those are second rank tensors (ε_{ij}, α_{ij}), tensors of the third rank (d_{in}, e_{im}, h_{jn}, g_{jn}, the fourth rank tensors (c_{mn} and s_{mn}). Here the indices are $i, j, k = 1, 2, 3$; $m, n = 1, 2, ..., 6$, and they are used for matrix presentation of the parameters.

Thermodynamics of piezoelectricity.

The thermodynamic potentials (3.4), including the Helmholtz free energy, can be involved to describe not only the piezoelectric effect, but also the pyroelectric effect (discussed further in Section 3.5), ferroelectricity, and other phenomena. To restrict the description to the piezoelectric event only, we have to assume that the primary four potentials are adiabatic ($dS = 0$), and the following four potentials are isothermal ($dT = 0$).

Specifically for piezoelectric the Helmholtz free energy (based on $dT = 0$) is available :

$$dX_n = c^D{}_{mn}\, dx_m - h_{in}\, dD_i;$$
$$dE_j = -h_{jm}\, dx_m + (\beta^x{}_{ij}/\varepsilon_0)\, dD_i,$$

where the coefficients are: $c^D{}_{mn} = (\partial X_n/\partial x_m)_D = (\partial^2 A/\partial x_n \partial x_m)_D$ – elastic stiffness that is determined at the constant induction, while parameter $(\beta^x{}_{ij}/\varepsilon_0) = (\partial E_i/\partial D_j)_x = (\partial^2 A/\partial D_i \partial D_j)_x$ is the inverse permittivity of the clamped crystal. Parameter h_{jm} is one of four piezoelectric coefficients that also refer to one of the generalized compliances:

$$h_{jm} = -(\partial X_n/\partial D_j)_x = -(\partial E_i/\partial x_n)_D = -(\partial^2 A/\partial x_n \partial D_i).$$

Thus, one of four piezoelectric coefficients (*d, e, g, h*) is known.

The same pair of equations can be obtained from the expression for free energy and from the other thermodynamic potentials, whose number, given that $dS = 0$ and $dT = 0$, is reduced to four. As a result of the thermodynamic relations, four pairs of basic equations of piezoelectric effect follow as:

$$D_i = d_{in} X_n + \varepsilon_0 \varepsilon_{ij} E_j ;$$
$$x_m = s^E{}_{mn} X_n + d_{jm} E_j ;$$

$$D_i = \varepsilon_0 \varepsilon^x{}_{ij} E_j + e_{im} x_m ;$$
$$X_n = c^E{}_{nm} x_m - e_{jn} E_j ;$$

$$E_j = (\beta^x{}_{ji}/\varepsilon_0)\, D_i - h_{jm} x_m ;$$
$$X_n = c^D{}_{nm} x_m - h_{in} D_i ;$$

$$E_j = (\beta^x{}_{ji}/\varepsilon_0)\, D_i - g_{jn} x_n ;$$
$$x_m = s^D{}_{mn} X_n - g_{im} D_i .$$

Therefore, it is possible to find all four piezoelectric coefficients.

From thermodynamics it is also possible to find several expressions for the *electromechanical coupling coefficient*:

$$K^2{}_{\text{coup}} = d^2{}_{jm}/(\varepsilon_0 \varepsilon^x{}_{ij}\, s^E{}_{mn}) = e^2{}_{jm}/(\varepsilon_0 \varepsilon^x{}_{ij}\, c^E{}_{mn}),$$

$$K^2{}_{\text{coup}} = \varepsilon_0\, h^2{}_{jm}/(\beta^x{}_{ij}\, c^D{}_{mn}) = \varepsilon_0\, g^2{}_{im}(\beta^X{}_{ij}\, s^D{}_{mn}).$$

Two pairs of these equations were obtained and examined in the previous section. From the remaining piezoelectric equations another two expressions for $K^2{}_{\text{coup}}$ can be derived.

If thermal effects are neglected, the internal energy of piezoelectric is the sum of elastic and electrical energies:

$$U = \frac{1}{2} x_m X_n + \frac{1}{2} D_j E_i .$$

Using the first pair of piezoelectric equations, this formula can be transformed as:

$$U = \frac{1}{2} X_n s^E_{mn} X_n + \frac{1}{2} X_n d_{in} E_i + \frac{1}{2} E_i d_{in} X_n + \frac{1}{2} \varepsilon_0 \varepsilon_{ij} E_j E_i =$$

$$= W_{\text{elec}} + 2W_{\text{em}} = W_{\text{elas}}.$$

Thus, the electromechanical coupling factor can be found as

$$\frac{W_{em}^2}{W_{elas}^2} = K_{coup}^2, \qquad (3.6)$$

where $2W_{em} = d \cdot X \cdot E$ – mutual energy, $W_{elas} = ½\ sX^2$ – mechanical (elastic) energy; $W_{elec} = ½\varepsilon_0\varepsilon E^2$ – electrical energy.

This concusion holds true also for the third pair of the piezoelectric equations. However, the second and fourth pairs of equations are just other expressions:

$$\frac{W_{em}^2}{W_{elas} \cdot W_{elec}} = \frac{K_{coup}^2}{1 - K_{coup}^2}. \qquad (3.7)$$

Only for small values of coupling coefficients ($K_{coup} < 0.3$) it is possible to assume that the formulas (3.6) and (3.7) are approximately the same (this question was discussed in the Section 2.2, where the corresponding expressions have been obtained by other methods).

Thus, thermodynamic (phenomenological) theory allows, without clarifying the molecular mechanisms, to get all the basic equations that describe the direct and inverse piezoelectric effect at the macroscopic level. These equations are used in engineering calculations, and the parameters of these equations can serve as a basis for comparing the properties of various piezoelectric materials.

Mechanical (elastic), electrical and thermal properties of crystals can be described by six parameters: two mechanical, two electrical and two thermal parameters. Thermal parameters must be considered for further thermodynamic analysis of the pyroelectric effect and for explaining the conditions enabling the pyroelectric effect in a piezoelectric crystal.

Consequently, different boundary conditions need to describe elastic, electrical and thermal properties of polar crystals determine. The choice of eight different thermodynamic functions (potentials) is essential, with which it is possible to express the basic equations of piezoelectricity. Most appropriate for the piezoelectricity analysis is to use the thermodynamic potential "Helmholtz free energy". From this analysis we obtained eight basic equations of the piezoelectric effect and the basic formulas for the coefficient of electromechanical coupling.

3.5. Pyroelectric effect thermodynamic description

Pyroelectric effect is defined as a change of spontaneous polarization P_S in the electrically and mechanically free crystal under the uniform alteration of crystal temperature T. This change is characterized by the pyroelectric coefficient

$\gamma^{X,E} = \dfrac{\partial P_S}{\partial T}$, where the upper indices indicate that $\gamma^{X,E}$ is determined for a given constant electrical field E_i and mechanical stress X_m. The simple model of pyroelectricity shown in Fig. 1.5 as well as the strictly thermodynamic analysis imply the phenomenological division of pyroelectric effect into the primary and the secondary ones, with the coefficients $\gamma^{(1)}$ и $\gamma^{(2)}$ correspondingly:

$$\gamma_i^{X,E} = \gamma_i^{(1)} + \gamma_i^{(2)} = \gamma_i^{x} + d_{im}^{T} c_{mn}^{X,E} a_n^{X,E}, \qquad (3.8)$$

i = 1, 2, 3; m, n = 1, 2, … 6.

The contribution of the primary pyroelectric effect can be found based on the clamped crystal study, when the strain is absent ($x_n = 0$), i.e. $\gamma^{(1)} = \gamma_i^{x}$. The contribution of the secondary effect corresponds to the difference in the pyroelectric coefficient between the free and the clamped crystal: $\gamma_i^{(2)} = \gamma_i^{X,E} - \gamma_i^{x}$, and it can be calculated by Equation (3.8) for the given components of piezoelectric modulus d_{im}^{T}, elastic stiffness $c_{mn}^{X,E}$, and thermal expansion coefficient $a_n^{X,E}$. In the linear pyroelectrics $\gamma = 10^{-7} \ldots 10^{-5}$ C·m^{-2}·K^{-1}, while in the ferroelectrics $\gamma = 10^{-5} \ldots 10^{-3}$ C·m^{-2}·K^{-1}.

The symmetry requirements permit both primary and secondary pyroelectric effects only in 10 of the 20 piezoelectric classes of crystals. In a pyroelectric there is a "special polar direction" along which the pyroelectric response is maximal. In the remaining 10 piezoelectric but non pyroelectric crystal classes any scalar (homogeneous) influence, including the temperature, cannot lead to a vectorial (electrical) response under homogeneous boundary conditions, i.e., if the crystal is completely free or fully mechanically clamped. To induce an electrical response in the piezoelectric by the thermal influence, the temperature gradient or inhomogeneous boundary conditions are required.

A pyroelectric is a transducer of thermal energy into electrical energy. When using the electro-calorific effect, which is the inverse effect to the pyroelectric one, electrical energy is converted into heat. The mark of efficiency of thermal into electrical and vice versa energy conversion is the coefficient of electro-thermal bonding $K_{TE} = K_{ET}$. The square of the thermoelectric conversion coefficient, K_{TE}^2, gives the fraction of thermal energy dW_T delivered to an energy converter element that is transformed into electrical energy dW_E:

$$K_{ET}^2 = \frac{dW_E}{dW_T}. \qquad (3.9)$$

In the view of the difficulties associated with determining K_{ET} in the dynamic elements, the thermoelectric conversion efficiency is usually estimated using the quasi-static thermodynamic relations derived based on the Gibbs thermodynamic or electrical potential (G or G_2 resp.), which describe the equilibrium properties of crystals.

There are eight thermodynamic potentials, corresponding to the eight combinations of conjugate thermodynamic variables D and E, X and x, S and T, three out of which are selected as the dependent and the remaining three as the independent variables. The independent variables of potential G are the stress (X), the electrical field (E), the temperature (T), while the dependent variables of G are the strain (x), the electrical displacement (D) and the entropy (S).

The independent variables of potential G_2 are the strain (x), the electrical field (E) and the temperature (T), while its dependent variables are the stress (X), the electrical displacement (D) and the entropy (S). Increment of thermodynamic potentials determined by the work done by the reformative element under certain boundary conditions on the functional specificity of the element:

$$dG = -x_i\,dX_i - D_n\,dE_n - S\,dT\,,$$
$$dG_2 = X_i\,dx_i - D_m dE_m - S\,dT,$$

where

$$x_j = -\partial G/\partial X_j\,;\ D_m = -\partial G/\partial E_m;\ S = -\partial G/\delta T,$$

and, correspondingly,

$$X_j = -\partial G_2/\delta x_j\,;\ D_m = -\partial G_2/\delta E_m;\ \ S = -\partial G_2/\delta T\,;$$

where: $i, j = 1,..3$ while $n, m = 1, 2,\ldots 6$.

The choice of a potential (out of eight possible) to estimate the work carried out by a thermodynamic system is determined by the mechanical, electrical and thermal boundary conditions under which the device works. The change of independent variables (X, E, T) corresponds to the equation of state for the dependent variables (x, D, S), where the superscripts X, E, T denote the so-called boundary conditions, which must be invariable while crystal parameters are measured:

$$dx_i = s_{ij}^{E,T} dX_j + d_{in}^{X,T} dE_n + a_i^{X,E} dT;$$
$$dD_n = d_{nj}^{E,T} dX_j + e_{nm}^{X,T} dE_m + \gamma_n^{X,E} dT; \qquad (3.10)$$
$$dS = \alpha_j^{X,E} dX_j + \gamma_n^{X,T} dE_n + C^{X,E} \frac{dT}{T}.$$

In the above expressions (3.10), the following notations are adopted:

$$s_{ij}^{E,T} = \frac{dx_i}{dX_j} = -\frac{\partial^2 G}{\partial X_i \partial X_j}$$

– which is the elastic stiffness, a fourth-rank tensor;

$$d_{nj}^{X,T} = d_{nj}^{T} = \frac{dx_j}{dE_n} = \frac{dD_n}{dX_j} = -\frac{\partial^2 G}{\partial X_j \partial E_n}$$

– which is the piezoelectric modulus, a third-rank tensor;

$$\varepsilon_{nm}^{X,T} = \frac{\partial D_n}{\partial E_m} = -\frac{\partial^2 G}{\partial E_n \partial E_m}$$

– which is the permittivity, a second-rank tensor;

$$\alpha_j^{X,E} = \alpha_j^{E} = \frac{dx_j}{dT} = -\frac{\partial^2 G}{\partial T \partial X_j}$$

– which is the free-crystal thermal expansion, a second rank tensor;

$$\gamma_n^{X,E} = \gamma_j^{E} = \frac{dD_n}{dT} = \frac{\partial S}{\partial E_n} = -\frac{\partial^2 G}{\partial T \partial E_n}$$

– which is the pyroelectric coefficient, a tensor of the first rank;

$$C^{X,E} = T \frac{dS}{\delta T} = -T \frac{d^2 G}{\partial T^2}$$

– which is the specific volumetric heat capacity, a scalar (i.e. a tensor of rank zero).

The piezoelectric strain tensor presentations are: $e_{nj}^{x,T} = e_{nj}^{E,T} = e_{nj}^{E}$.

Under the extra condition that the shape and the volume of crystal element do not change ($x = 0$, i.e. crystal is mechanically clamped), from the above equations in the case of $E = 0$ it is possible to obtain the contribution of the *primary* pyroelectric effect:

$$dP_n = \gamma_n^{x} dT, \qquad (3.11)$$

where $\gamma_n^{x} = \gamma^{(1)}$.

The above equations allow also to find the piezoelectric contribution to the pyroelectric coefficient, as well as the dielectric constant and the volumetric specific heat of the crystal. Pyroelectric measurements are usually carried out at the condition $E = 0$. By applying Eq. (3.10) it is possible to obtain the following relationship between pyroelectric coefficient of free ($X = 0$) and mechanically clamped ($x = 0$) crystal:

$$\gamma_n^X = \gamma_n^x + e_{mj}^T \alpha_j^E, \tag{3.12}$$

which means $\gamma = \gamma^{(1)} + \gamma^{(2)}$, because the expression $e_{mj}^T \alpha_j^E = \gamma^{(2)}$ describes the contribution of the secondary pyroelectric effect.

At constant temperature, the dielectric constants of mechanically free, $\varepsilon_{nm}^{X,T}$, and clamped crystal, $\varepsilon_{nm}^{x,T}$, are related as follows:

$$\varepsilon_{nm}^{X,T} = \varepsilon_{nm}^{x,T} + d_{nj}^T e_{mj}^T, \tag{3.13}$$

where $d_{nj}^T e_{mj}^T$ is the piezoelectric contribution to the permittivity. The corresponding experimental data were shown in Fig. 1.9.

For the heat capacity of electrically short-circuited ($E = 0$) and mechanically free pyroelectric crystal the following relation holds:

$$C^{E,X} = C^{E,x} + T\alpha_i^E c_{ij}^{E,T}.$$

Note that the difference between the $C^{E,X}$ and $C^{E,x}$ is small, so that in the notation of volume specific heat often only one superscript is kept: C^E.

From the above equations it follows that if the pyroelectric element is studied in the absence of mechanical stress ($X = 0$) as well as electrical field ($E = 0$) then the accumulation of electrical energy in the pyroelectric element dW_E is described by the potential G, which, under the given boundary conditions, corresponds to the expression:

$$dW_E = dD_n\, dE_n = \frac{(dP_s)^2}{\varepsilon_0 \varepsilon_{nm}^{X,T}} = \frac{\left(\gamma_n^{X,E}\right)^2 (dT)^2}{\varepsilon_0 \varepsilon_{nm}^{X,T}}, \tag{3.14}$$

where $dP_s = dD_n$ and dW_E is the desired quantity of electrical energy.

Thermal energy dW_T that is spent on energy storage in a crystal, by definition equals to $dSdT$; under the given boundary conditions it corresponds to the expression:

$$dSdT = \left(\alpha_j^{X,E} dX_j + \gamma_n^{X,T} dE_n + C^{X,E} \frac{dT}{T} \right) dT ,$$

where the increments dX_j and dE_n respectively represent the appearance of the spontaneous stress and coercive electrical field in the free crystal. The estimation of the amount

$$\alpha_j^{X,E} dX_j + \gamma_n^{X,T} dE_n$$

in the different pyroelectric crystals shows that it is just a small fraction of a percent of the value $\left(C^{X,E} \frac{dT}{T} \right)$, so

$$dW_T \approx C^{X,E} \frac{(dT)^2}{T_p}, \qquad (3.15)$$

where $T_p = T$ is the operating temperature of the element and dW_T is the desired quantity of thermal energy.

Thus, when the crystal element is mechanically free ($X = 0$), Eq. (3.9) after the substitution of Eq. (3.13) can be written as follows:

$$K_{\mathrm{ET}}^2 = \frac{\dfrac{\left(\gamma_n^{X,E}\right)^2 (dT)^2}{\varepsilon_0 \varepsilon_{nm}^{X,T}}}{\dfrac{C^{X,E} (dT)^2}{T_p}} = \frac{\left(\gamma_n^{X,E}\right)^2 T_p}{\varepsilon_0 \varepsilon_{nm}^{X,T} C^{X,E}} .$$

Similarly, the factor of electro-thermal conversion for mechanically clamped crystal element is:

$$K_{\mathrm{ET}}^2 = \frac{\dfrac{\left(\gamma_n^{x,E}\right)^2 (dT)^2}{\varepsilon_0 \varepsilon_{nm}^{x,T}}}{\dfrac{C^{x,E} (dT)^2}{T_p}} = \frac{\left(\gamma_n^{x,E}\right)^2 T_p}{\varepsilon_0 \varepsilon_{nm}^{x,T} C^{x,E}} .$$

A comparison of the key parameters relevant for thermo-electrical conversion is given in Table. 3.1 for different pyroelectrics.

Relatively low efficiency of the thermoelectric conversion is due to the physical nature of this phenomenon in dielectric crystals, which are "electrically hard" with respect to external influences. Note in this regard that the efficiency of

energy conversion is much higher in the case of the piezoelectric effect. The corresponding electromechanical coupling coefficient K_{EM} by far exceeds the pyroelectric K_{ET}. The value of K_{EM} sometimes reaches 95 %, and in the case of piezoelectric resonance in crystals with high electro-mechanical quality this coefficient increases to almost 1.

Table 3.1.

Pyroelectric coefficient γ_n specific heat C, permittivity ε and efficiency K_{ET}^2 for basic pyroelectric materials

Pyroelectric	γ_n^X, 10^{-4} C/(m^{2}K)	$C^{X,E}$, 10^6 J/(m^{3}K)	$\varepsilon_{nm}^{X,T}$	K_{ET}^2, %
Crystals:				
TGS	3.5	2.5	40	4
$LiTaO_3$	2.0	3.2	43	1
$LiNbO_3$	0.4	3.2	30	0.1
SBN	5.5	2.1	400	1.2
Ceramics:				
$BaTiO_3$	4.0	3.0	1000	0.2
PZT	4.2	2.7	1500	0.14
PKD	2.0	2.7	290	0.17
PVDF	0.4	2.3	12	0.2

In spite of the low efficiency, the pyroelectric effect is in practical use, primarily for the detection and measurement of heat flow, and, under certain conditions, for direct transition of thermal energy into electricity. The "direct" conversion of heat into electricity is used in thermal imaging and highly sensitive temperature sensors.

The effect that is inverse to the pyroelectric effect is the *electrocaloric effect*, has an influence upon the permittivity of a polar crystal. When thermal equilibrium has enough time to be established at the frequency of the applied electrical field, the crystal increases the electrical capacity, which is experienced like an increase in crystal permittivity ε_{nm}^T (isothermal permittivity). At higher frequencies, the electrical field has no time for thermal energy exchange (thermal equilibrium cannot be set). It is experienced as a decrease in the capacitance of pyroelectric element, so at the increased speed the adiabatic permittivity ε_{nm}^S is measured. The difference $\Delta\varepsilon_{EC} = \left(\varepsilon_{nm}^T - \varepsilon_{nm}^S\right)$ is the electrocaloric part of low-frequency permittivity; this

difference is possible only in pyroelectrics and it depends on the value of the specific heat and on the pyroelectric coefficient: $\Delta\varepsilon_{EC} = \frac{\gamma_n^2 T}{\varepsilon_0 C^{x,E}}$.

The electrocaloric effect, in which electrical energy is linearly converted into heat, enables crystal cooling due to the applied electrical field of a certain polarity. The "inverse" transformation in the form of solid body cooling is promising for a new type of refrigerators that do not have the environmentally harmful freon gas and electrical motors (machinery). Electrocaloric effect can be applied also to an electrically controlled decrease of temperature (for example, to achieve a better cooling in cryogenics).

3.6. Thermodynamic description of artificial pyroelectric effect

The concept of the artificial pyroelectric effect (APE) refers to the effect that is induced in a polar cut of non-central symmetric crystal by the homogeneous heating, whereby part of thermal strain is artificially restricted. We formulate the equations that allows to determine the APE-coefficient (that is similar to the pyroelectric coefficient) for various classes of non-central symmetric crystals using components of piezoelectric tensor, elastic compliance and thermal expansion coefficient.

As already mentioned, the normal pyroelectricity is defined as the change of spontaneous polarization P_S of electrically and mechanically free crystal with an uniform change in its temperature T. The pyroelectric effect consists of primary and secondary effects $\gamma_i^{X,E} = \gamma_i^{(1)} + \gamma_i^{(2)}$. The contribution of the primary effect is determined by the study of completely clamped crystal, which has no strain ($x_n = 0$), i.e. $\gamma^{(1)} = \gamma_i^x$. Contribution of the secondary effect corresponds to the difference of the coefficients $\gamma_i^{(2)} = \gamma_i^{X,E} - \gamma_i^x$.

In the piezoelectric materials the thermoelectric response can be obtained either under inhomogeneous influence (temperature gradient over the sample) or in the case of inhomogeneous boundary conditions. It is for a long time known that in piezoelectric a non-uniform thermal impact causes the polar response. In early studies this phenomenon was called as actinoelectricity. Later it was identified as a tertiary pyroelectricity. The tertiary effect can be also defined as the temperature variation of polarization of piezoelectric material that is induced by the thermal stress:

$$dP_i = d_{im}^T c_{mn}^{X,E} (x_n - \alpha_n^{X,E} dT).$$

Here it is shown that under the uniform thermal excitation of the piezoelectric (when grad $T = 0$) the polar response also can be obtained, if such conditions are created that partly inhibit the thermal strains. In this case, the permissible thermal strain induces piezoelectric polarization which is due to the *partial clamping* of the crystal, so it can not be compensated by the influence of other deformations. At the partial clamping conditions the crystal is the similar at all his parts, but it is uniformly stressed. In the experiment, the anisotropic thermal deformation limitation can be implemented in different ways, e.g., by artificially fixing a piezoelectric thin plate on a rigid substrate, or due to the natural limitation of the radial deformation of a thin disk above the frequency of electromechanical resonance, etc.

Thus, the artificial pyroelectric effect is defined as the one induced by the mechanical stress polarization in electrically free, but mechanically partially clamped piezoelectric under the uniform thermal exposition. Partial clamping is provided by the inhomogeneous boundary conditions that anisotropically limit the thermal strains of the non centrally symmetric crystal, so it is stressed homogeneously, yet anisotropically. Artificial pyroelectric effect manifests itself maximally in the direction of an arbitrary polar-neutral axis of the piezoelectric crystal. This axis, under the influence of stress, is transformed into a special polar axis in accordance with the Curie principle.

The effective pyroelectric coefficient characterizing the APE depends on the elastic and thermal properties of the crystal, as well as on the method of limiting the thermal deformations:

$$\gamma^{*}_{APE} = \gamma_k^{X_k,E} = d^{T}_{km}\lambda^{*}_{m},$$

where λ^{*}_{m} is the thermo-elastic coefficient of partially clamped crystal. Superscript index at the APE coefficient γ_k indicates that only some of elastic stress tensor components X_k are zero. For various piezoelectrics the coefficient $\gamma^{*}_{APE} = 10^{-6} \ldots 10^{-4}$ $C \cdot m^{-2} \cdot K^{-1}$, i.e, by magnitude the APE is comparable to the pyroelectric coefficient of usual pyroelectrics and ferroelectrics. The dimension of the APE coefficient corresponds to dimension of usual pyroelectric coefficient $\gamma_i^{X,E}$. The artificial effect could be classified as a "secondary" effect, in view of the similarity in the calculation methods. However, this definition is incorrect as the secondary pyroelectric effect is manifested in mechanically free crystals while the artificial pyroelectric effect is observed only in partially clamped crystals.

It is interesting to compare the artificial pyroelectric effect with the so-called "tertiary pyroelectric effect". In accordance with known definition, both the tertiary effect and the APE originate from thermal stresses in the piezoelectrics. However, in the case of the tertiary pyroelectric effect these stresses are caused by spatial heterogeneity in crystal temperature. At the same time the APE is a conventional pyroelectric effect that occurs due to uniform heating or cooling of the crystal. It appears under the restriction of certain strains of the crystal, i.e. it arises as a result of inhomogeneous boundary conditions (which in the traditional pyroelectric would, in the contrary, disable the secondary pyroelectric effect).

In all cases, the APE induced in a piezoelectric can be regarded as a consequence of the superposition of crystal symmetry and symmetry of the impact . The most accurate definition of the APE effect would be "the pyroelectricity in partially clamped piezoelectrics", but the preferred term “artificial pyroelectric effect” in a compact form indicates the physical mechanism of the phenomenon under discussion.

In the previous section Eq. (3.8) was obtained for pyroelectric coefficient of crystals using Gibbs thermodynamic potential by setting stress *X,* field *E* and temperature *T* as the independent variables and strain *x*, electrical displacement *D* and entropy *S* as the dependent ones. In this case, the equation of state of a pyroelectric can be written as follows:

$$\begin{aligned} dx_m &= s_{mn}^{X,E} dX_n + d_{mi}^{T} dE_i + \alpha_m^{X,E} dT, \\ dD_j &= d_{jm}^{T} dX_m + \varepsilon_{ij}^{X,T} dE_i + \gamma_j^{X} dT, \\ dS &= \alpha_m^{E} dX_m + \gamma_j^{X} dE_j + C^{E,T} \frac{dT}{T}, \end{aligned} \tag{3.16}$$

where $s_{mn}^{X,E}$ is the tensor of elastic compliance, γ is one of pyroelectric coefficients (see explanation to Fig. 1.9), and $C^{E,T}$ is the heat capacity. For piezoelectrics, in the simplest experimental situation, when the crystal is electrically free (i.e., short-circuited, $E = 0$ and $D = P$), and in the absence of spontaneous polarization $P_j^X = 0$, the equations get the form:

$$\begin{aligned} dx_m &= s_{mn}^{X,E} dX_n + \alpha_m^{X,E} dT, \\ dP_j &= d_{jn}^{T} dX_n, \\ dS &= \alpha_m^{X,E} dX_m + C^{E,T} \frac{dT}{T}, \end{aligned} \tag{3.17}$$

where S is entropy. Superscripts indicating the thermodynamic state of the crystal are omitted in further analysis. Since it is assumed that E and T are constant, in the partially clamped piezoelectrics the isothermal current pyroelectric coefficient $\gamma_{APE} = \frac{\partial P_i}{\partial T}$ might be calculated.

Equations (3.17) should be specified in accordance with boundary conditions. It is assumed that in experimental studies or practical applications the pyroelectric device constitutes an "endless" thin piezoelectric plate that is "ideally" fixed on a thick rigid substrate that has zero thermal expansion coefficient ($\alpha_n = 0$). The thickness of this plate h must be substantially less than the penetration depth of the temperature wave with length $l = \sqrt{\frac{2a}{\omega}}$, where a is temperature conductivity and ω is heat flow modulation frequency. At these conditions, the temperature gradient in the piezoelectric can be neglected, and the substrate under the influence of the temperature wave will not flex (because $\alpha_n = 0$).

As a result, the tangential deformation of the piezoelectric is completely suppressed, and the deformation is permitted only in the direction perpendicular to of the surface. Shear deformations under the uniform heat flux are not excited, while the "infinitely large" area of the plate allows neglect by the boundary effects in this model. The normal to the plate is oriented accordingly to one of the polar directions of the piezoelectric crystal, which, because of the limitations in planar strains, becomes a special polar axis, in accordance with the Curie principle of superposition.

The solutions of the Equations (3.17) depend on the crystal symmetry.

Quartz crystal (first example)

As the simplest case, consider crystal class 32, which includes the well-studied piezoelectric quartz. In the basic setting, the crystals of class 32 are characterized by longitudinal piezoelectric module d_{11}, transverse module $d_{12} = -d_{11}$ and shear modules d_{14}, d_{25} и d_{26}. A thin quartz plate is cut perpendicular to axis *1* (this is an *X*-cut, or Curie slice, Fig. 1.5). A rigid substrate prevents deformation in the cutting plane: $dx_2 = dx_3 = 0$, so that the only deformation allowed is dx_1 (the shear deformations, according to the conditions, are not induced). The electrodes cover the surface (100), so $E_1 = 0$, moreover, $X_1 = 0$, because the strain x_1 is permitted; the elastic compliances satisfy $s_{11} = s_{12}$, $s_{13} = s_{33}$, the thermal expansion coefficients satisfy $\alpha_1 = \alpha_2 \neq \alpha_3$. Under these conditions, Equations (3.17) get the form:

$$dx_1 = s_{11}dX_2 + s_{12}dX_3 + \alpha_1 dT,$$
$$dx_2 = s_{22}dX_2 + s_{23}dX_3 + \alpha_2 dT = 0,$$
$$dx_3 = s_{32}dX_2 + s_{33}dX_3 + \alpha_3 dT,$$
$$dP = d_{12}dX_2. \qquad (3.18)$$

From Equations (3.18) the expression for the pyroelectric coefficient of the partially clamped crystal can be obtained as

$$\gamma_{1\,APE} = \frac{dP}{dT} = \frac{d_{11}(\alpha_1 s_{33} - \alpha_3 s_{13})}{s_{11}s_{33} - s_{13}^2}. \qquad (3.19)$$

For an *X*-cut of the quartz (SiO_2) crystal at the temperature of 300 K the APE coefficient is $\gamma_{1\,APE}$ = 2.5 $\mu C \cdot m^{-2} \cdot K^{-1}$. For other crystals of the 32 symmetry class the calculations show the following results: in berlinite crystal ($AlPO_4$) $\gamma_{1\,APE}$ = 5.7 $\mu C \cdot m^{-2} \cdot K^{-1}$, in calomel crystal ($Hg_2Cl_2$) $\gamma_{1\,APE}$ = 8.7 $\mu C \cdot m^{-2} \cdot K^{-1}$, and tellurium crystal (Te) shows $\gamma_{1\,APE}$ = 10 $\mu C \cdot m^{-2} \cdot K^{-1}$.

Gallium arsenide (second example)

In practical applications the artificial pyroelectricity is the most promising for wide-gap semi-insulated (*s/i*) semiconductors of GaAs group, as they can be simultaneously used as thermo-electrical converters and as semiconductors with high electron mobility. These crystals have sphalerite structure with polar-neutral symmetry. In the specially oriented plates using restriction of some thermal deformations the APE becomes apparent. The voltage sensitivity for artificial pyroelectric in *s/i*-GaAs, for instance, is the same as in the natural one in the pyroelectric ceramics. The GaAs plate with a thickness of 100 microns at temperature change about 1 K shows “pyroelectrical” potential 2 V. This can be of interest for the implementation in the multi-element planar integral thermal IR detectors. It is conjectured that semi-insulating layers or micro-regions embedded in the gallium arsenide integrated circuit together with amplifiers and switching devices and oriented in a special way, may form a mosaic microstructure of non-selective and highly sensitive infrared detectors.

The electrical polarity of piezoelectric-active wtde-gap semiconductors of $A^{III}B^{V}$ type, with a sphalerite structure, is directed along each of third-order axes of the cubic crystal. The own polarity of crystal’s unit cell is completely compensated; therefore, any scalar influence on the crystal, including a uniform temperature

change, cannot produce an electrical response. However, this compensation of electrical polarity can be broken in specially oriented plates (layers) in which thermal deformations are anisotropically limited, Fig. 2.11. Along one of the three-fold polar axes an electrical response appears, and that is the artificial pyroelectric effect.

The high symmetry of cubic crystals class 43m is characterized by the isotropy of thermal expansion coefficient: $\alpha_{ij} = \alpha$ (for GaAs $\alpha = 5.8 \cdot 10^{-6}$ K^{-1} at 300 K). For the same reason, the tensor of elastic compliance $s_{mn}^{E,T}$ is reduced to just three independent components: in GaAs $s_{11}^{E,T} = 12 \cdot 10^{-11}$, $s_{12}^{E,T} = -3.6 \cdot 10^{-11}$ and $s_{33}^{E,T} = 17 \cdot 10^{-11}$ m^2/N. Piezoelectric properties is characterized by a matrix:

$$d_{im} = \begin{bmatrix} 0 & 0 & 0 & d_{14} & 0 & 0 \\ 0 & 0 & 0 & 0 & d_{25} & 0 \\ 0 & 0 & 0 & 0 & 0 & d_{36} \end{bmatrix}, \qquad (3.20)$$

In the case of $A^{III}B^{V}$ crystals, due to their cubic symmetry, in standard installation of crystal the piezoelectric components are equal: $d_{14} = d_{25} = d_{36}$, and, therefore, they can be denoted as d. In gallium arsenide $d = 2.7 \cdot 10^{-12}$ C/N, i.e., it surpasses the quartz piezoelectric module ($d_{11} = 2.3 \cdot 10^{-12}$ C/N). From Equation (3.20) one cannot see any opportunity of APE effect in the GaAs, since matrix (3.20) contains only shear piezoelectric components, which cannot be excited by the heat exposure. As it was shown in the previous section, the APE generally occurs due to the de-compensation of contributions from longitudinal and transverse piezoelectric effects, described by the left half of the matrix (3.20). But in this case (i.e., in the *standard installation* of $A^{III}B^{V}$ crystal) all the components of the longitudinal and transverse piezoelectric module are zero.

But for other orientations of crystallographic axes, the standard matrix (3.20) can be transformed, and both the longitudinal and transverse components of piezoelectric module can appear. These components are maximal in the slice of the crystal that is oriented perpendicularly to the axis of the third order (which is a spatial diagonal of a cube), since the internal polarity of the $A^{III}B^{V}$ crystal coincides with these directions. This polarity is due to the partially ionic character of the chemical bond A¬B, and to the anisotropy in the electronic density distribution, which is increased in the vicinity of the B-ion.

The maximum of the artificial pyroelectric effect in the 43m class of symmetry can be achieved in such a special installation, in which one of the axes (new axis *3'*) coincides with one of the polar crystal axes such as [111]. The new axis *1'* should be

directed normally to the axis passing through the *3′* plane of symmetry of the cube, while orientation of the new axis *2′* is predetermined by the Decart coordinate system. When the above procedure is applied, the matrix of piezoelectric module for 43m crystal in a new installation is:

$$d_{i'm'} = \begin{bmatrix} 0 & 0 & 0 & 0 & -\frac{d}{\sqrt{3}} & \frac{2d}{\sqrt{6}} \\ \frac{d}{\sqrt{6}} & -\frac{d}{\sqrt{6}} & 0 & -\frac{d}{\sqrt{3}} & 0 & 0 \\ -\frac{d}{2\sqrt{3}} & -\frac{d}{2\sqrt{3}} & \frac{d}{\sqrt{3}} & 0 & 0 & 0 \end{bmatrix}. \qquad (3.21)$$

All components of this new matrix are expressed in terms of the shear module *d*, taken from the basic installation of the crystal (3.20). The third row of the matrix (3.21) characterizes the piezoelectric properties of the crystal plate that is cut perpendicularly to the axis *3′* = [111], which is characterized by the longitudinal piezoelectric module $d_{3'3'} = \frac{d}{\sqrt{3}}$ and by the transverse effects $d_{3'1'} = d_{3'2'} = -\frac{d}{2\sqrt{3}}$. The shear components in the third row of the matrix are absent.

Under the uniform change in temperature and the resulting thermal deformations of GaAs plate the piezoelectric response from the longitudinal and transverse effects completely compensate each other (due to isotropic thermal expansion coefficient). This was shown in Fig. 2.7 (*b*). But if one type of thermal deformation (normal or tangential) is prohibited or limited, the uniform heating leads to polarization, which is experienced as the APE.

One possible way of the tangential and normal thermal strains de-compensation was shown in Fig. 2.11 (b), where it is done by rigid connection of a GaAs plate on substrate that differs from the GaAs crystal by the value of thermal expansion coefficient. In microelectronic practical devices, it is advisable to form pyroelectric-active *s/i* (dielectric) layer of Ga(As,P) or (GaAl)As directly onto the substrate of GaAs crystal.

The calculation of artificial pyroelectric coefficient $\gamma_{APE} = \frac{dP_i}{dT}$, where P_i is polarization and *T* is temperature at the ideal conditions at which polarization from the tangential thermal strains is completely suppressed by the rigid substrate: $dx_1 = dx_2 = 0$. Therefore, at the uniform temperature change the only allowed strain is dx_3 (here and in sequel we skip the apostophe in the underscore indices for simplicity).

Since the "polar" direction "*3*" deformation is allowed, the corresponding component of the mechanical stress tensor X_3 is zero. Another boundary condition is the $E_3 = 0$, i.e. crystal is assumed electrically free (open-circuited), as it is usually supposed in thermodynamic analysis of piezoelectric and pyroelectric effects. Corresponding equations are presented below:

$$dx_n = s_{mn}^{E,T} dX_m + \alpha_n^E dT,$$

$$dP_i = d_{in}^T dX_n. \qquad (3.22)$$

Here x_n and X_m are strain and stress tensor components, the parameters $s_{mn}^{E,T}$, d_{in}^T and α_n^E are, respectively, the tensor components of elastic compliance, the piezoelectric module and the thermal expansion. Indices *E* and *T*, as usual, indicate persistence of the tensor components at crystal determination. For the crystals group 43*m* at the chosen boundary conditions Equations (3.22) can be written as:

$$dx_1 = s_{11}^{E,T} dX_1 + s_{12}^{E,T} dX_2 + \alpha dT = 0,$$

$$dx_2 = s_{12}^{E,T} dX_1 + s_{22}^{E,T} dX_2 + \alpha dT = 0,$$

$$dx_3 = s_{31}^{E,T} dX_1 + s_{32}^{E,T} dX_2 + \alpha dT,$$

$$dD_3 = dP_3 = d_{31}^T dX_1 + d_{32}^T dX_2. \qquad (3.23)$$

Taking into consideration that in the cubic crystals $s_{11}^{E,T} = s_{22}^{E,T}$ and $X_1 = X_2$, for the APE coefficient in the new installation of the crystal (returning back to the indexes with apostrophe) it is possible to obtain

$$\gamma_{3'} = \frac{dP_{3'}}{dT} = \frac{2d_{3'1'}\alpha}{s_{1'1'}^{E,T} + s_{1'2'}^{E,T}}.$$

We invert the transformation from standard to new installation described previously, as it is required to represent all tensor components in the standard installation of the crystal (which is usually listed in the reference books), and we obtain:

$$\gamma_{111} = \frac{2\sqrt{3}d_{14}\alpha}{4s_{11}^{E,T} + 8s_{12}^{E,T} + s_{44}^{E,T}}. \qquad (3.24)$$

For gallium arsenide the APE coefficient is $\gamma_{111} = 1.5\ \mu C \cdot m^{-2} \cdot K^{-1}$. Recall that similar calculation of the APE coefficient for quartz shows $\gamma_{100} = 2.6\ \mu C \cdot m^{-2} \cdot K^{-1}$, whereas in the well-known pyroelectric tourmaline the pyroelectric coefficient is $4\ \mu C \cdot m^{-2} \cdot K^{-1}$.

In gallium arsenide the artificial pyroelectric effect in the directions of basic axes [100], [010] and [001] is impossible. The APE maximum in the $A^{III}B^{V}$ crystals corresponds to [111]-type cut plates, whereas the APE is possible in other slanting sections of the GaAs crystal. Spatial distribution of artificial pyroelectric coefficient in the 43m symmetry crystals is shown in Fig. 3.5, and it reminds the piezoelectric module distribution shown previously.

$$\gamma(\theta,\varphi) = \gamma_{111} \cdot \sin\theta \cdot \sin 2\theta \cdot \cos 2\varphi$$

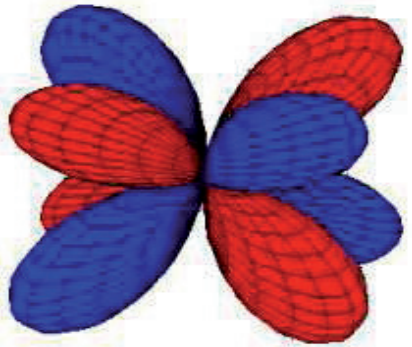

Fig. 3.5. Spatial distribution of the APE for gallium arsenide type crystals: along any of the basic directions of the cube [100], [010] and [001] the artificial pyroelectric effect is absent, but it is maximal along any of the four axes of the order *3* ([111] type)

The indicatory surface of the APE for polar cubic crystals consists of eight identical teardrop surfaces that radiate from the centre of the cube to its vertices at the angle of 109.5°. It is possible to estimate the APE in any direction for the crystal of gallium arsenide group. The magnitude of the APE coefficient is determined as a radius-vector emanating from the centre of the cube to the intersection with the pointing surface. Compared with quartz, Fig. 2.2 (b), the indicative surface of gallium arsenide crystals group is more complicated because it characterizes the APE along the four polar-neutral axes (and each has two directions).

APE in other non centrally symmetric crystals

In the trigonal crystals of polar class 3*m,* in addition to usual pyroelectric effect along the polar axis [001], the artificial pyroelectric response is observed as well, but this holds for the [010]-direction, which is perpendicular to the [001] axis. The equation for APE calculation is similar to (3.19), but with another parameters:

$$\gamma_{2\,APE} = \frac{dP}{dT} = \frac{d_{22}\left(\alpha_1 \cdot s_{33} - \alpha_3 \cdot s_{13}\right)}{s_{11} \cdot s_{33} - s_{13}^2}.$$

Let us give the APE values for some crystals of the polar class 3*m*: in the proustite crystal (Ag_3AsS_3) $\gamma_{2\,APE} = 10\ \mu C \cdot m^{-2} \cdot K^{-1}$; in the pyrargyrite crystal (Ag_3SbS_3) $\gamma_{2\,APE} = 15\ \mu C \cdot m^{-2} \cdot K^{-1}$; in lithium tantalate ($LiTaO_3$) $\gamma_2 = 20\ \mu C \cdot m^{-2} \cdot K^{-1}$, and in lithium niobate ($LiNbO_3$) $\gamma_2 = 40\ \mu C \cdot m^{-2} \cdot K^{-1}$. Note that the order of magnitude for the APE response is comparable to the conventional pyroelectric response of the last mentioned crystals: in lithium niobate, for example, $\gamma_3 = 50\ \mu C \cdot m^{-2} \cdot K^{-1}$.

In the case of anisotropic restriction of thermal deformations the artificial pyroelectric response can be observed in any piezoelectric, but the analysis of this effect very often needs to use a non-standard installation of the crystal. For example, in the cubic piezoelectric class 23, to which the prevalent crystal bismuth germanate ($Bi_{12}GeO_{20}$) belongs, the polar direction is the [111]-type axis, and the maximum of the APE is observed just in this direction:

$$\gamma_{[111]\,APE} = \frac{2\sqrt{3}\alpha d_{14}}{4s_{11} + 8s_{12} + s_{44}}. \qquad (3.25)$$

At the temperature near 300 K in the piezoelectric $Bi_{12}GeO_{20}$ this parameter exceeds many times the APE in quartz as well as in GaAs, and equals $\gamma_{[111]\,APE} = 20\ \mu C \cdot m^{-2} \cdot K^{-1}$.

In the 42*m* symmetry class which include the well-known piezoelectrics of KDP and ADP types, piezoelectric module matrix in the standard installation of these crystals (in their paraelectric phase) also shows no longitudinal and no transverse effects. As in the above mentioned cases, to express the artificial pyroelectricity one need to change the standard setting of crystal, for example, by turning the axes *1* and *2* around the axis *3* at an angle of $\pi/4$. In these crystals it is advisable to select the piezoelectric element not in a form of thin plate, but as a long rectangular rod, extending along one of the new axes of *1′* or *2′* while the electrodes should be deposited on the surface of piezoelectric element perpendicularly to the axis *3′* = *3*.

Clamping in longitudinal deformation of the rod allows to obtain the expression for APE coefficient

$$\gamma_{3\,APE} = \frac{2d_{36}\alpha_1}{2s_{11} + 2s_{12} + s_{66}}. \qquad (3.26)$$

At the temperature of 300 K the artificial pyroelectric coefficient for the ADP crystal is $\gamma_{3\,APE} = 17\ \mu C \cdot m^{-2} \cdot K^{-1}$ and for the KDP crystal $\gamma_{3\,APE} = 17\ \mu C \cdot m^{-2} \cdot K^{-1}$.

Table 3.2

Artificial pyroelectric effect for 10 classes of actual piezoelectric crystals

Symmetry classes, axes orientation (x, y, z)	Sample and its orientation as to basic axes	Calculation expressions for APE coefficient $\gamma_{n\,APE}$	Piezoelectric, γ_{nAPE} [$\mu C/m^2 \cdot K$)] found at 300 K
32 (for basic coordinate system)	Rectangular rod with length l along y and thickness along x	$\gamma_1 = \dfrac{d_{11}^T \cdot \alpha_1^E}{s_{11}^{E,T}}$	SiO_2, $\gamma_1 = 2.6$
	Disk with normal d directed along x	$\gamma_1 = \dfrac{d_{11}^T \left(\alpha_1^E \cdot s_{33}^{E,T} - \alpha_3^E \cdot s_{13}^{E,T} \right)}{s_{11}^{E,T} \cdot s_{33}^{E,T} - \left(s_{13}^{E,T} \right)^2}$	SiO_2, $\gamma_1 = 2.7$
$\bar{4}2m$ (axes x and y are rotated around axis z at the angle of 45°)	Rectangular rod with length l and normal d directed along axis z *а*) l is directed on x, *б*) l is directed on y	$\gamma_3 = \dfrac{\pm 2 \cdot d_{36}^T \cdot \alpha_1^E}{2 \cdot s_{11}^{E,T} + 2 \cdot s_{12}^{E,T} + s_{66}^{E,T}}$	KDP, *а*) $\gamma_3 = -6$ *б*) $\gamma_3 = +6$ ADP, *а*) $\gamma_3 = -17$ *б*) $\gamma_3 = +17$
$\bar{4}3m$ and 23 (axis z is directed on the third fold axis)	Disk, d directed along z	$\gamma_3 = \dfrac{-2\sqrt{3} \cdot d_{14}^T \cdot \alpha^E}{4 \cdot s_{11}^{E,T} + 8 \cdot s_{12}^{E,T} + s_{44}^{E,T}}$	Tl_3TaSe_4, $\gamma_3 = -23.5$; $Bi_{12}GeO_{20}$, $\gamma_3 = -20$
222 (axes x and y are turned around axis z at the angle of 45°)	Rectangular rod with normal d directed along axis z and length l directed *а*) l along axis x, *б*) l along axis y	$\gamma_3 = \dfrac{\pm d_{36}^T \left(\alpha_1^E + \alpha_2^E \right)}{s_{11}^{E,T} + s_{22}^{E,T} + 2 \cdot s_{12}^{E,T} + s_{66}^{E,T}}$ *а*) corresponds to sign «+» *б*) corresponds to sign «–»	
622 and 422 (axes y and z are turned around axis x at the angle of 45°)	Rectangular rod with normal d directed along axis x and length l directed *а*) l along axis y, *б*) l along axis z	$\gamma_3 = \dfrac{\pm d_{14}^T \left(\alpha_1^E + \alpha_3^E \right)}{s_{11}^{E,T} + s_{33}^{E,T} + s_{44}^{E,T} + 2 \cdot s_{13}^{E,T}}$ *а*) corresponds to sign «+» *б*) corresponds to sign «–»	
$\bar{4}$ (standard)	Rectangular rod with normal d directed along axis z and length l directed *а*) l along axis x, *б*) l along axis y	*а*) $\gamma_1 = \dfrac{-d_{31}^T \cdot \alpha_1^E}{s_{11}^{E,T}} = R$ *б*) $\gamma_1 = -R$	
$\bar{6}m2$ and $\bar{6}$ (standard)	Disk, normal d is oriented along axis y	$\gamma_1 = \dfrac{d_{22}^T \left(\alpha_1^E \cdot s_{33}^{E,T} - \alpha_3^E \cdot s_{13}^{E,T} \right)}{s_{11}^{E,T} \cdot s_{33}^{E,T} - \left(s_{13}^{E,T} \right)^2}$	

The magnitude of the pyroelectric response in the partially clamped piezoelectrics depends not only on the orientation of piezoelectric element, but also on its shape. For example, for a long rectangular rod of quartz crystal (symmetry class 32), the APE coefficient can be determined from the a simpler equality: $\gamma_1' = \frac{d_{11}\alpha_1}{s_{11}}$. It is assumed that the rod extends along the axis *2*, and the electrodes coated the surface perpendicularly to the axis *1*, for this orientation and sample shape we have: $\gamma_{1\,APE}' = 2.4\ \mu C \cdot m^{-2} \cdot K^{-1}$. The expressions for APE calculation for all 10 classes of the actual piezoelectrics (those which do not possess the conventional pyroelectric effect) are shown in Table 3.2.

It should be emphasized that dielectric sensors have much lower noise coefficients because they use the change of polarization (semiconductor sensor has the shot noise). External electrical field, as a rule, is not applied to the crystalline dielectric sensor element, and its polarization is a spontaneous one. That is why, for the temperature (δT) or pressure (δp) measurement, the dielectric sensors must use the corresponding change in spontaneous polarization (δP_S). However, in ceramics, this polarization should be induced and supported by the electrical bias field as well.

The change of the P_S with temperature results in the polar crystals in the pyroelectric effect ($\delta P_i = \gamma_i \delta T$) or the volumetric piezoelectric effect ($\delta P_i = \xi_i \delta p$). As indexing indicates, δP_i a vectorial value. Thus, the pyroelectric coefficient γ_i as well as the volumetric piezoelectric coefficient ξ_i also vectors, inherent only to pyroelectrics. These parameters being vectors indicates that a pyroelectric can transferee scalar influences, δT or δp, into the vector type of responses, which are electrical voltage or electrical current.

Conclusions

Pure ionic, as well as pure covalent crystals are defined by the centrally-symmetric structure and do not show piezoelectric effect. Therefore, non centrally-symmetric crystalline structure is the only manifestation of a mixed ionic-covalent bonding of its atoms. This bonding is directional, and therefore it leads to the different manifestations of the asymmetry and complexity of polar crystal structure. When originating polar crystal formation from the charged ions (from initially liquid or fumes state of material) a polar structure of non-centrally symmetric crystals is formed spontaneously. In this book latent polarity is simplistically described by a combination of imaginary dipoles, which leads to the electrical moments describable by tensors of different ranks.

We discuss a conception that any piezoelectric possesses an intra-crystalline polar moment, even though this crystal does not belong to the classes of pyroelectric symmetries. In line with this assumption, the internal polarity of piezoelectric crystals is described by multiple high-rank moments of different types. Octopole–sextuple–dipole moments correspond to three–two–one dimension arrangement of the intra-crystalline polarity. Dipole (1D) polarity is the pyroelectric spontaneous polarization that is a vector (first rank tensor). The 2D sextuple moment is located in a plane of a non-centrally symmetric configuration of three dipoles, and it is described by the second rank polar tensor. The octopole moment is the non-centerally symmetric spatial (3D) conformation of four dipoles that is described by the third rank tensor.

Temperature dependence of intra-crystalline polar moment components show a critical law $P \sim (\theta - T)^n$ and vanishes at the phase transition temperature θ. The critical parameter equals to $n = 1$ if all components of intrinsic polarity have a flat arrangement (two-dimensional case, 2D). For the spatial (3D) arrangement of the latent polarity components this exponent is $n = 2$. These differ essentially from 1D ferroelectric spontaneous polarization that shows $P_S(T)$ critical law with $n = 0.5$.

For technical applications, it means that under the anisotropy of boundary conditions any high-gap $A^{III}B^{V}$ large-gap semiconductor-piezoelectric shows behaviour of pyroelectric crystal. It is important that such a crystal can be used as a far infrared sensor or as a volumetric piezoelectric effect sensor integrated with amplifier in one $A^{III}B^{V}$ crystal. On the other hand, any device based on $A^{III}B^{V}$ semiconductor that has erroneous orientations of a crystal can generate polarization noises due to vibrations or thermal fluctuations.

References

Books:

1. W.O. Cady. *Piezoelectricity*. New York, 1946, 717 pages.
2. J.F. Nye. *Physical properties of crystals*. Oxford press. Bristol, 1957, 385 pages.
3. W. Mason. *Physical acoustic.* Academic Press. New York, 1964, 592 pages.
4. F. Jona and G. Shirane. *Ferroelectric crystals*. Pergamon Press, Oxford, 1962, 555 pages.
5. J.C. Burfoot and G,W. Taylor. *Polar dielectrics and their application*. Macmillan Press, New Jersey, 1979, 466 pages.
6. M.E. Lines and A.M. Glass. *Principles and application of ferroelectrics and related materials*. Clareton Press. Oxford, 1977, 736 pages.
7. Y.I. Sirotin and M.I. Shaskolskaya. *Basic of crystal physics* (in Russion). Moscow, 1975, 677 p.
8. I.S. Jeludev. Physics of crystalline dielectrics (in Russion). Moscow, 1968, 472 pages.
9. I.S. Jeludev. Basic of ferroelectricity (in Russion) Moscow, 1973, 471 pages.
10. Y.M. Poplavko. *Physics of Dielectrics* (text book, in Russian*)*. Ed. "Vischa Skola", Ukraine, Kiev, 1980, 400 pages.
11. I.S. Rez and Y.M. Poplavko. *Dielectrics. Main properties an electronics applications* (in Russian). Moscow, Ed. "Radio e Svjaz", 1989, 290 pages.
12. Y.M. Poplavko and Y.I. Yakimenko. *Physical basis of piezoelectricity.* (Text book, in Russian*)*. Ed. "Avers"Ukraine, Kiev, 1988, 100 pages.
13. Y.M. Poplavko. L.P Pereverzeva, A.S. Voronov, Y.I. Yakimenko, *Material Sciences, part II DILELECTRICS* (in Ukrainian), Ed. "Polytechnik", Ukraine, Kiev, 2007, 390 pages.
14. Y.M. Poplavko. L.P Pereverzeva, I.P. Raevskiy. *Physics of Active dielectrics.* (Text book, in Russian) Ed. "Souse Federal University of Russia", Postov-na-Donu, 2009, 478 pages.
15. Y.M. Poplavko and Y.I. Yakimenko. *Piezoelectrics.* (in Ukrainian), Ed. "Polytechnik", Ukraine, Kiev, 2013, 333 pages.
16. W. Martienssen and H. Warlimant. Condensed matter an materials data. Spinger Handbook, New York, 2007, 1120 pages.

Articles:

1. E.N. Dimarova and Y.M. Poplavko. *Temperature dependence of thermal conductivity of TGS crystals*. Physika Tverdogo Tela, 1964, Vol.6, N^{o} 10, p.2828.
2. Y.M. Poplavko, E.N. Dimarova. *Thermoconductivity of ceramic $BaTiO_3$ and its solid solutions.* Izvestia AN SSSR, Serial Phys., 1965, Vol.29, N^{o}6, p.987.
3. Y.M. Poplavko. *Microwave dielectric dispersion mechanisms in ferroelectrics of $BaTiO_3$ type.* Izvestia AN SSSR, Serial Phys., 1965, Vol.29, N^{o}11, p.2020.
4. Y.M. Poplavko, L.P. Solomonova. *Dielectric relaxation in TGS crystals.* Physika Tverdogo Tela, 1966, Vol.8, N^{o} 8, p.2456.
6. E.N. Dimarova and Y.M.Poplavko. *Electrical bias field influence on ferroelectrics thermal-conductivity.* Izvestia AN SSSR, Serial Phys., 1967, Vol.31, N^{o}11, p.1842.
7. Y.M. Poplavko and L.P. Solomonova. *Frequency characteristics of TGS and Rochelle Salt crystals.* Izvestia AN SSSR, Serial Phys., 1967, Vol.31, N^{o}11, p.1771.
8. Y.M. Poplavko. *Dielectric dispersion in ferroelectrics.* In the book "Relaxation in solids" (in Russian), Moscow, 1968, p.600.
9. E.N. Dimarova, N.V. Gorbokon, Y.M. Poplavko. *Thermoelastic properties of KDP crystals near high-temperature phase transitions.* Kristalographija, 1972, Vol.17, N^{o}3, p.680.

10. E.N. Dimarova, N.V. Gorbokon, Y.M. Poplavko. *Deiterium influence on thermal and elastic properties of TGS ferroelectrics.* Ukrainsky Fizichesky Jurnal, 1972, Vol.17, N°7, p.1189.
11. Y.M. Poplavko, L.P. Pereverzeva et al. *Dielectric permittivity dispersion in KDP type crystals.* Kristallographija, 1973, Vol.18, N°3, p.645.
12. L.P. Pereverzeva, Y.M. Poplavko. *Dielectric constant dispersion in TGS near phase transition temperature.* Kristallographija, 1973, Vol.18, N°4, p.784.
13. Y.M. Poplavko et al. *Rochelle salt dielectric spectrum in the frequency range 1 Hz - 300 GHz.* Physika Tverdogo Tela, 1973, Vol.15, N°8, p.2515.
14. Y.M. Poplavko. *Dielectric relaxation mechanisms in ferroelectrics of order-disorder type.* In book: "Relaxation in solids", Lithuania, Kaunas, 1974, p.280.
15. Y.M. Poplavko et al. *Low temperature phase transition in Rochelle Salt.* Pisma v JETF,Vol.19, N°9, p.557.
16. Y.M. Poplavko et al. *Temperature dependence of soft mode frequency and damping in various ferroelectrics*. Ferroelectrics (USA) 1978, Vol. 21, No 1-2, p.399.
17. E.N. Dimarova, Y.M. Poplavko et al. *Domain structure and heat capacity anomalies in ferroelectrics.* Izvestia AN SSSR, Serial Phys. 1984, Vol.48, p.1155.
18. Y.M. Poplavko, V.M. Pashkov et al. *Microwave study of sillinite type crystals.* Physika Tverdogo Tela, 1984, Vol.26, p.844.
19. V.F. Zavorotnii, Y.M. Poplavko. *Planar temperature waves method for termoconductivity study.* Pribori e Technika Experimenta, 1984, N°5, p.189.
20. N.V. Slesarenko, L.A. Pasechnik, Y.M. Poplavko et al. *Rochlle Salt heat capacity near phase transitions.* Physika Tverdogo Tela, 1985, Vol.27, p.1248.
21. Y.M. Poplavko, L.P.Pereverzeva and Y.V.Prokopenko. *Thermomechanically induced pyroelectricity and its possible applications*. Ferroelectrics (USA), 1994, 153, 353-358.
22. Y.M.. Poplavko *Artificial Pyroelectricity in GaAs and its application*. Proceed. Intern. Symp. "GAAS`94", Italy, Torino, 1994, p.101-104.
23. Y.M. Poplavko, V.A. Moskaljuk et al. *Pyrotransistor - GaAs FET with a pyroelectric wafer-gate.* Proc. of 9th Int. Symp. on Appl.of ferroel., PennState University, USA, 1994, 698-701.
24. Y.M. Poplavko et al. *Thermomechanically induced electric field in.GaAs and application of this new effect*. Proceed. 1994 Asia-Pacific Microwave Conf. Tokyo, Vol.**II**, p.701-704.
25. L.P.Pereverzeva and Y.M. Poplavko *Polar properties of non-isotropic clamped piezoelectrics.* Ukrainskii fizich. zhurnal, 1993, **38**, 1383-1388.
26. V.F. Zavorotny, Poplavko Y.M. et al. *Diffusion of heat in KDP-type ferro- and antiferroelectrics*. Phys. Solid State, 1993, **35**(10), 1402-1402 {Fiz.Tverd.Tela (St.Peterburg) **35**, 2832-2834}.
27. L.P. Pereverzeva, Y.M. Poplavko et al. *Pyroelectricity in non-central crystals*. Acta Physica Polonica A, 1993, 84, No **2**, 287-291.
28. L.P. Pereverzeva, Y.M. Poplavko et al. *Thermopiezoelectricity in non-central crystals*. Sov.Phys.Solid State, 1992, **34**(1), 147- 151 [Fiz. Tverd. Tela (St.Petersburg), 1992, **34**, 281-287].
29. Y.M. Poplavko and L.P. Pereverzeva *Pyroelectricity of partially clamped piezoelectrics.* Ferroelectrics (USA), 1992, **130**, 361-366.
30. Y.M. Poplavko and L.P. Pereverzeva *Artificial pyroelectricity in gallium arsenide.* Sov.Phys.Tech.Phys. 1992, **37**(2), 163-165 [Zh. Tekh. Fiz., 1992, **62**, 93-97].
31. Y.M. Poplavko, M.E. Ilchenko and L.P. Pereverzeva *Pyroelectric response of piezoelectrics*. Ferroelectrics (USA), 1992, **134**, 207-212.
32. Y.M. Poplavko et al.*Termopiezoelectric transducers*. Ferroelectrics (USA), 1992, **131**, 331.
33. M.E. Ilchenko, Y.M. Poplavko et al. *Volume piezoeffect in partially clamped piezoelectrics*. Electron. Technic, Part Radiodetails and radiocomponets. 1992, No.2-3 (87-88) pp. 70-73.
34. Y.M. Poplavko and L.P. Pereverzeva *Pyroelectricity in clamped piezoelectrics.* Pis`ma v zhurnal tekhnicheskoi fiziki, 1991, **17**, No.18, 84-87.

35. L.P. Pereverzeva, Y.M. Poplavko et al. *Dynamics secondary pyroelectric effect in lithium niobate*. Pis`ma v zhurnal eksperimentalnoi i teoreticheskoi fiziki, 1990, **52**, 820-822.
36. L.P. Pereverzeva, Y.N. Bondarenko and Y.M. Poplavko *Microwave signal convertion using thermoelastic and pyroelectric properties of crystals*. Izvestiya vysshikh uchebnykh zavedenii, serija radioelectronika, 1990, **33**, vipusk 10, 19-24.
37. A.I. Otko, Y.M. Poplavko, L.A. Shuvalov, *Thermo- and mechano-electret effect in lithium tantalate crystals.* Ferroelectric letters, Vol.**18**, 1995, pp.127-132.
38. Y.M.Poplavko, L.P.Pereverzeva. *Volumetric piezoelectric effect and artificial pyroelectricity in GaAs.* Proc. of Europ. GaAs and related III-V compounds application Symposium, Paris, 1996, pp.4A2.
39. Y.M. Poplavko et al. *Quartz temperature and pressure sensors*. Proc. Int. Symp. Appl. Ferroelectrics, USA, 1996, East Brunswick, pp. 639-643.
40. L.P. Pereverzeva, Y. M. Poplavko. *Partial clamping effect on ferroelectric integrated films electrical properties.* 9-th Intern. Symp. Integrated Ferroelectrics. USA, 1997, pp.98-99.
41. L.P. Pereverzeva, Y.M. Poplavko, *Partial clamping influence on electrical properties of ferroelectric and paraelectric integrated films.* Proc. Int. Conf. MicroMaterials`97, Berlin.
42. Y.M. Poplavko, L. Pereverzeva, N.-I. Cho, Y.S.You and H. Nam. *Feasibility of microelectronic quartz temperature and pressure sensors.* Jpn. J. Appl. Phys., Vol. 37, 1998, pp. 4041-4048.
43. Y. Poplavko, M. Ilchenko, L. Pereverzeva, Y. Prokopenko. *Pyroelectric-like response in semi-Insulating III-V crystal*. Proc. GAAS`99. Munich, October 1999, pp.203-209.
45. Y. Poplavko and L. Pereverzeva. *Connection between pyroelectric and piezoelectric properties of non-central crystal*s. Electronics and Communications, Kiev, 2000, #8, pp.63 – 66.
46. Y.M. Poplavko and N.-I. Cho. *Clamping influence on ferroelectric integrated film microwave properties.* Semiconductor Science and Technology, 1999, Vol. 14, pp.961-966.
47. Y. Poplavko, M. Ilchenko, L. Pereverzeva, Y. Prokopenko. *Pyroelectric-like response in semi-insulating III-V crystal*. Proc. Conf. GAAS`99. Munich, October 1999, pp.203-209.
48. Y.M. Poplavko, L.P. Pereverzeva. *Connections between pyroelectric and piezoelectric properties of non-central crystals*. Electronics and Commun., Kiev, 2000, N^0 8, pp. 63 – 66.
49. L. Pereverzeva, Y. Poplavko. *Hihg rank electric polar moments and piezoelectrocity.* Abstracts of 10^{th} Int. Meeting on Ferroelectricity, Sept. 2001, Madrid, p.200.
50. Y. Poplavko, L. Pereverzeva, S. Voronov. *Artificial pyroelectric effect in quartz and its application in pyroelectric sensors.* Electronics and Communications, Kiev, 2001, N^0 11.
51. L. Pereverzeva, Y. Poplavko, S. Voronov. *Pyroelectricity in semi-insulating III – V crystals*. Electronics and Communications, Kiev, 2002, N^0 14, pp. 122 – 116.
52. L. Pereverzeva, Y. Poplavko, S. Voronov et. al. *The efficiency of thermal-to-electric energy conversion in pyroelectric materials*. Electron. and Commun., Kiev, 2002, N^0 16, pp. 29- 33.
53. Y.V. Prokopenko,Y.M. Poplavko. *Uncooling GaAs "Pyroelectric" Sensor*. Abstr. of 7-th Int. Symp. on Integrated Ferroelectrics (ISIF) 1995, Colorado Springs, USA, p.117-118.
54. Y.M. Poplavko, L.P. Pereverzeva and V.V. Meriakri. *Clamping influence on ferroelectric film.* Proc. of 9-th Int. Conf. "DIELECTRICS-2000", St.-Peterburg, Vol. 2. pp. 154-155.
55. Y.M. Poplavko, Y.I. Yakimenko. *Pyroelectric Response of Strain Limited III-V Semiconductor*. J. Electronics and Communications, Kiev, 2014, Vol. 6 (77). pp. 9-15.
56. Y.M. Poplavko and Y.I. Yakimenko. *Physical Nature of Piezoelectricity (Part 1 – Latent Polarity, Part 2 – Temperature dependencies)* IEEE 34-th Intern. Conf. ELNANO–2014, pp. 22-26.